School of Doctoral Studies in Biological Sciences

University of South Bohemia in České Budějovice

Faculty of Science

Role of adenosine pathway on cell growth and stress response in *Drosophila*

Ph.D. Thesis

MSc. Houda Ouns Maaroufi

Supervisor: Prof. RNDr. Michal Žurovec, CSc.

Faculty of Science, University of South Bohemia

Biology Centre of the Czech Academy of Sciences, Institute of Entomology

České Budějovice 2022

This thesis should be cited as:

Maaroufi, H.O., 2022: Role of adenosine pathway on cell growth and stress response in *Drosophila*.

Ph.D. Thesis. University of South Bohemia, Faculty of Science, School of Doctoral Studies in Biological Sciences, České Budějovice, Czech Republic, 106 pp.

Annotation

The thesis surveyed the effects of the adenosine pathway on cell growth and stress response. We described the effects of mutation of the concentrative nucleoside transporter cnt1 on male fertility, particularly spermatogenesis, using a *Drosophila melanogaster* model. We also described the effects of the adenosine pathway on the cytotoxicity of mHTT.

Declaration

I declare that I am the author of this graduation thesis and that I used only sources and literature displayed in the list of references in its preparation.

Place and Date:

Student's signature:

This thesis originated from a partnership of Faculty of Science, University of South Bohemia, and the Institute of Entomology, Biology Centre of the CAS, both supporting doctoral studies in the Physiology and Developmental Biology study programme.

Financial support

This work was supported by the European fund for regional development "Interreg Austria/Czech Republic" (REGGEN-ATCZ207) and the junior grant project GACR (19-13784Y to LK).

Acknowledgements

First and foremost, I would like to thank my thesis advisor, Prof. Michal Zurovec, for his continuous support, motivation, and encouragement throughout my doctoral studies. His guidance helped me throughout the research and inspired me to become an independent student, learn different experimental techniques, expand my knowledge, and achieve many goals. I would also like to thank all my lab mates for their encouragement, help and friendly lab environment.

A heartfelt gratitude to my family, especially my mother Mounira Eddous for her endless love, patience, and support ♥.

Last but not least, I would like to acknowledge all my international friends who brought a special touch and excitement to my life and shared their struggles and successes related to our studies.

No attempt at any level can be satisfactorily completed without the support of each of them.

List of papers and author's contribution

I. **Houda Ouns Maaroufi**, Lucie Pauchova, Yu-Hsien Lin, Bulah Chia-hsiang Wu, Lenka Rouhova, Lucie Kucerova, Ligia Cota Vieira, Marek Renner, Hana Sehadova, Miluse Hradilova, Michal Zurovec (2022). Mutation in *Drosophila* concentrative nucleoside transporter 1 alters spermatid maturation and mating behavior. Front. Cell Dev. Biol. DOI: 10.3389/fcell.2022.945572

Student's share: 90%

Houda Ouns Maaroufi was responsible for planning and conducting the experiments, analyzing the data, and writing the manuscript.

Impact factor of the journal: 6.081

II. Yu-Hsien Lin, **Houda Ouns Maaroufi**, Lucie Kucerova, Lenka Rouhova, Tomas Filip, Michal Zurovec (2021). Adenosine signaling and its downstream target mod(mdg4) modify the pathogenic effects of polyglutamine in a *Drosophila* model of Huntington's disease. Front. Cell Dev. Biol. DOI: doi.org/10.3389/fcell.2021.651367

Student's share: 20%

Houda Ouns Maaroufi assisted in recording the adult lifespan and eye phenotypes, and performed the brain dissection, immunochemistry, and confocal microscopy imaging.

Impact factor of the journal: 6.081

III. Yu-Hsien Lin, **Houda Ouns Maaroufi**, Emad Ibrahim, Lucie Kucerova, Michal Zurovec (2019). Expression of human mutant huntingtin protein in *Drosophila* hemocytes impairs immune responses. Frontiers in immunology. DOI: 10.3389/fimmu.2019.02405

Student's share: 25%

Houda Ouns Maaroufi performed the hemocyte counting, imaging and made the summary illustration.

Impact factor of the journal: 8.786

List of papers not included in the thesis

I. Yun-Heng Lu1, Carol-P Wu, Cheng-Kang Tang, Yu-Hsien Lin, **Houda Ouns Maaroufi**, Yi-Chi Chuang, Yueh-Lung Wu (2020). Identification of Immune Regulatory Genes in Apis mellifera through Caffeine Treatment. *Insects* DOI: 10.3390/insects11080516

II. Lucie Kucerova, Vaclav Broz, Badrul Arefin, **Houda Ouns Maaroufi**, Jana Hurychova, Hynek Strnad and Michal Zurovec, Ulrich Theopold (2016). The *Drosophila* Chitinase-Like Protein IDGF3 Is Involved in Protection against Nematodes and in Wound Healing. J. Innate Immun. 8:199–210, DOI: 10.1159/000442351

Co-author agreement

Michal Žurovec, the supervisor of this Ph.D. thesis and co-author of papers I, II, and III fully acknowledges the stated contribution of “Houda Ouns Maaroufi” to these manuscripts.

……

Prof. Michal Žurovec

Contents

List of abbreviations

Ado	Adenosine
AdoR	Adenosine receptor
A1	Adenosine 1 receptor
A2A	Adenosine 2A receptor
A2B	Adenosine 2B receptor
A3	Adenosine 3 receptor
CNT	Concentrative nucleoside transporter
ENT	Equilibrative nucleoside transporter
SLC29A3	Solute Carrier Family 29 Member 3
AMP	Adenosine monophosphate
ADP	Adenosine diphosphate
ATP	Adenosine triphosphate
dATP	Deoxyadenosine triphosphate
cAMP	Cyclic AMP
ADK	Adenosine kinase
ADA	Adenosine deaminase
Adgf-A	Adenosine deaminase-related growth factor A
GSC	Germline stem cell
CySC	Somatic cyst stem cell
IC	Individualization complex
CB	Cystic bulge
WB	Waste bag

TE	Terminal epithelium
SV	Seminal vesicle
DNA	Deoxyribonucleic acid

Introduction

1. Introduction to adenosine metabolic and signaling pathways

Adenosine (Ado) is an endogenous ubiquitous metabolite and a signaling molecule generated and released in cells (Sun and Huang, 2016; Franco et al., 2021). It is a purine nucleoside which regulates several fundamental cellular functions through the activation of Ado signaling and metabolic pathways that are well conserved among phyla (Lin et al., 2021; Maaroufi et al., 2022). Under certain circumstances, Ado may regulate both cell proliferation and apoptosis, which could affect cell survival (Merighi et al., 2002). It has been found to be increased in hypoxia and tissue damage. The prolonged Ado level may cause chronic inflammation, fibrosis and organ damage (Borea et al., 2017). Ado is produced intracellularly by the hydrolysis of adenosine monophosphate (AMP) using 5‘-nucleotidase and extracellularly by degradationof extracellular adenosine triphosphate (ATP) (Camici et al., 2018).

1.1. Adenosine metabolic pathway

The uptake and release of Ado requires specific cell membrane transporters due to its hydrophilic nature (Young, 2016). These transporters are classified into two protein families: equilibrative nucleoside transporters (Ents) and concentrative nucleoside transporters (Cnts) (Figure. 1). Ents are bidirectional carriers that mediate the efflux and influx of substrates by passive diffusion (Figure. 2A). However, Cnts are unidirectional carriers that mediate the energy-consuming influx of substrates driven by the transmembrane sodium gradient (Figure. 2B) (Gray et al., 2004). The efficiency of Cnt influx depends on coupling ratio of cation to nucleoside; the higher the ratio, the lower the efficiency of Cnt influx (Young, 2016). In humans, four *ent* and three *cnt* genes have been characterized. Ents are ubiquitously expressed transporters, whereas Cnts have limited tissue distribution in bloodtestis barrier and specialized epithelial cells, such as intestinal epithelia, liver, as well as in macrophages and leukemic cells (Masino and Boison, 2013). Most of the nucleoside transporter studies were mainly based on the cell culture experiments and focused on the affinity of the nucleoside transport, as well as the transmission efficiency of nucleoside-derived antiviral or anticancer drugs (Zhang et al., 2007). There are only few reports describing the possible association between nucleoside transporters and human diseases. A rare mutation in human *SLC29A3* gene encoding Ent3

has been associated to H syndrome, pigmented hypertrichosis and insulin-dependent diabetes mellitus syndrome (PHID) (Kang et al., 2010). The reported *ent3* mutation in mice resulted in lysosomal nucleoside accumulation, leading to impaired lysosome function and macrophage homeostasis (Hsu et al., 2012). However, some microarray data indicated that the expression of *cnts* is decreased in oxygen deprivation conditions (hypoxia) both humans and rat tumor tissues of the rats (Dragan et al., 2000; Wojtal et al., 2014; Mukhopadhya et al., 2016). In addition, deficiency of human Cnt1 has been associated with congenital dysfunction of pyrimidine metabolism and organ failure in infants (Pérez-Torras et al., 2019).

Ents and Cnts are highly conserved in other living organisms including *Drosophila melanogaster*. This latter has proven to be a valuable research tool because of its lower genetic complexity and greater genetic tractability than mammalian models. In *Drosophila*, mutation of ent2 has been found to be lethal and essential for development.. In addition, the hypomorphs have reduced associative learning and impaired synaptic function (Knight et al., 2010). However, unlike Ents, the physiological functions of Cnts have not been examined yet. Two types of Cnts have been identified in *Drosophila*; *cnt1* and *cnt2*, which share 40% and 43% sequence identity with human *cnt2*, respectively (Sayers et al., 2012; Benson et al., 2013).

Ado is required for the biosynthesis of ATP. This process occurs via a phosphorylation cascade of Ado, ultimately forming ATP in the mitochondrial matrix. Synthesis of AMP to ADP is by adenylate kinase, while ATP is synthesised from ADP by ATP synthase (Richani et al., 2019). ATP synthesis has been found to be necessary for, among other things, the motility of some cells, such as sperm. (Xie et al., 2006; Yu et al., 2019).

Ado levels are well regulated in the body. In case of Ado excess, its metabolism is adjusted extracellularly by adenosine deaminases, which catalyze the deamination of adenosine to inosine. Thus, adenosine deaminases, in addition to nucleoside transporters, play a key role in stabilizing adenosine concentrations (Cristalli et al., 2001). Deficiency of adenosine deaminase (ADA) can lead to immunodeficiency in humans (Sanchez et al., 2007). It has been reported that deficiency of ADA induces apoptosis in immature immune cells (thymocytes). Deficiency of ADA has also been associated with high levels of deoxyadenosine triphosphate (dATP), which inhibits the enzyme ribonucleotide reductase,

important for DNA replication and repair (Lee et al., 1984; Sanchez et al., 2007). Furthermore, the high content of deoxyadenosine inhibits transmethylation reactions essential for lymphocyte activation (Sanchez et al., 2007). In *Drosophila*, a mutation in *Adenosine deaminase-related growth factor A* (*adgf-a*) caused a dramatic increase of Ado level in the hemolymph. This phenotype was accompanied by fatbody disintegration and formation of melanotic aggregates in the late third instar larvae (Dolezal et al., 2005). These data suggest that maintaining a constant level of Ado is important for a functioning immune system. Along with adenosine deaminase, adenosine kinase (ADK) is one of the most important enzymes that can lower Ado levels. While ADA converts Ado to inosine, ADK phosphorylates Ado to AMP. (Maier et al., 2005; Stenesen et al., 2013) The deficiency in AdenoK was reported to be connected to liver disease, dysmorphic features, epilepsy and developmental delay since it disrupts the adenosine/AMP cycle (Becker et al., 2021).

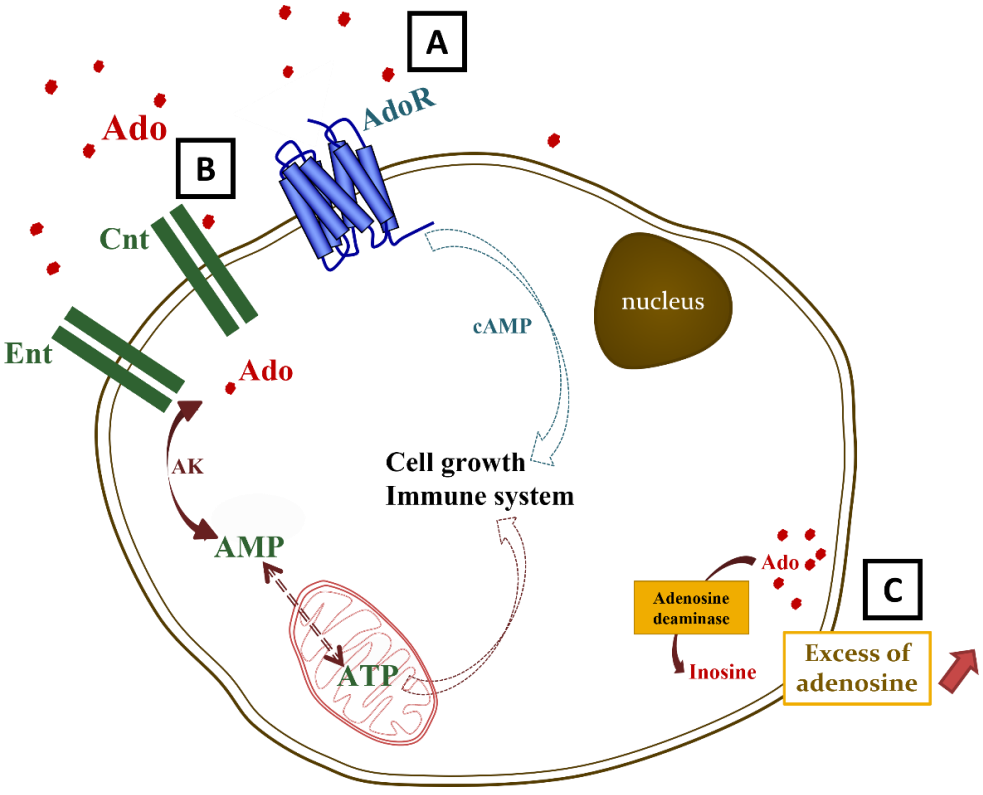

Figure 1. Ado signaling and metabolic pathways. **A)** Extracellular Ado generates a signal through AdoR that eventually modulates cell growth and immune system

pathways. **B)** Extracellular Ado concentration is controlled by ENTs and CNTs. Intracellularly it undergoes a phosphorylation cascade for the biosynthesis of ATP. **C)** Ado excess is deaminated to inosine.

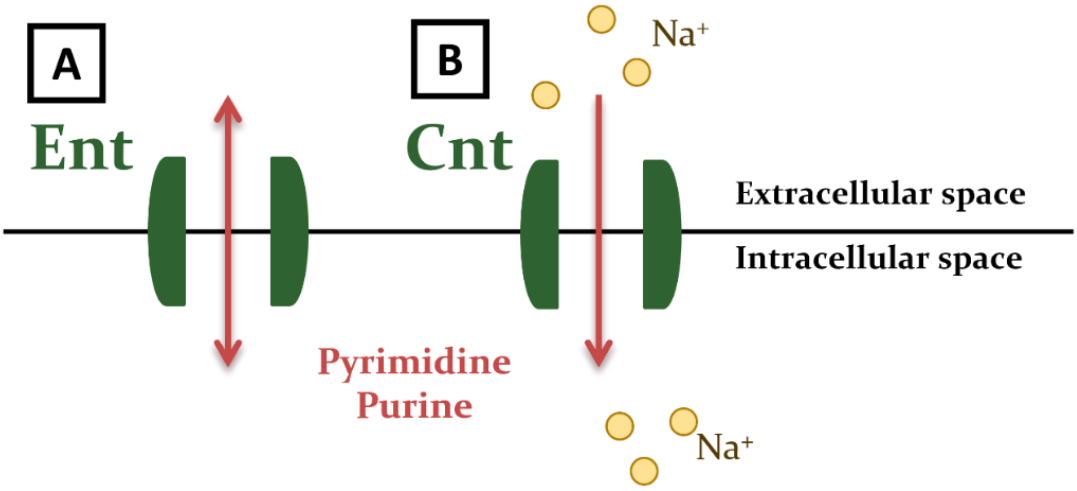

Figure 2. Profiles of the Ent and Cnt nucleoside transporters. **A)** Ents are bidirectional transporters that mediate the outflow and inflow of substrates via passive diffusion. **B**) Cnt are unidirectional transporters that mediate energy-consuming influx of substrates driven by the transmembrane sodium gradient.

1.2. Adenosine signaling pathway

As a signalling molecule, Ado binds to the adenosine receptor (AdoR) whose signal is transduced intracellularly by the second messenger, cyclic AMP (cAMP). The increased level of cAMP stimulates cAMP-dependent protein kinases that regulate the transcription of genes associated with cell growth and the immune system (Figure. 1) (Borea et al., 2017). In mammals, there are four distinct AdoRs; A1, A2A, A2B and A3 receptors, which are G protein-coupled cell membrane receptors. It has been reported that A2A and A2B receptors stimulate the adenylate cyclase, while A1 and A3 receptors inhibit it. The adenylate cyclase is important to catalyse the conversion of ATP to cAMP (Fredholm et al., 1994; Linden, 1994; Gemignani and Abbott, 2010).

2. Role of adenosine pathway in cell growth

The growth of organs during animal development occurs mainly by cell proliferation, which is often followed by an increase in cell mass (cell growth) (Enesco and Leblond, 1962; Mandaravally Madhavan and Schneiderman, 1977; Falconer et al., 1978). In most developing animals, each organ has its own growth and cell proliferation pattern and size. In addition, the different parts of a developing organ have characteristic initial sizes, growth rates, and final sizes (Dobbing and Sands, 1973; Summerbell, 1976). Therefore, cell proliferation must be controlled at the local level to provide an appropriate final number of cells for each organ and each part of it. Several studies have shown that, in addition to mechanisms occurring within the developing organ, an adequate supply of nutrients and hormones is essential for normal growth (Bryant and Simpson, 1984). For example, Ado is one of the nutrients that have been shown to play an important role in the metabolic pathways of cell growth, such as in testis (Merighi et al., 2002). In humans and mammals, adenosine has been reported to be essential for sperm development and mechanical movement (Bellezza and Minelli, 2017). Some studies suggest that Ado induces proliferation of male germ cell through AdoR, which is present in the cells of the testicular tubules of mammals and fish. It has also been suggested that high levels of ATP are maintained in Sertoli cells (cells that provide essential nutrients during spermatogenesis), in which AdoR serves as a sensor for energy balance (Bellezza and Minelli, 2017). In addition, nucleoside transporters are also important for sperm development. Ents and Cnts are found in the blood-testis barrier and especially in Sertoli cells to transport essential nucleosides during sperm development. Blockade of nucleoside transporters in Sertoli cells impaired spermatid maturation, suggesting that extracellular Ado in epididymal plasma must be regulated by nucleoside transporters (Leung et al., 2001; Klein et al., 2017). However, only pharmacological studies showed the relationship betweennucleoside transporters to spermatogenesis, but no detailed study have been published about how spermatogenesis is affected after the blockade of the nucleoside transporters.

Numerous model organisms have been used to study spermatogenesis, both *in vivo* and *in vitro*, including insects such as *Drosophila melanogaster*. For 100 years, *Drosophila* has been one of the best model organisms for studying development and growth. The small size of the flies, their larvae, and well-sequenced genome make it easy to manipulate and

breed these animals and perform numerous experiments. In addition, the fruit fly is a complex multicellular organism in which many aspects of development and behavior are compatible with those of mammals. In *Drosophila*, Ado has been reported to be a key regulator of gut cell proliferation, hemocyte differentiation, and brain synaptic plasticity (Knight et al., 2010; Mondal et al., 2011; Bajgar et al., 2015; Xu et al., 2020). Furthermore, one of the common organs to study cell growth is testis. The transition from a stem cell to a mature sperm is quite similar in both *Drosphila* and mammals, which makes it interesting to investigate the interaction between Ado pathway and spermatogenesis of the major components of the Ado pathway, *cnt1* is highly expressed in *Drosophila* male testis (Clark et al., 2016; Maaroufi et al., 2022), Suggesting that Ado pathway might interact with sperm development and mating behavior. The study in our published article I summarises our findings on the association of *cnt1* with spermatogenesis and mating behavior (Maaroufi et al., 2022) (Figure 3).

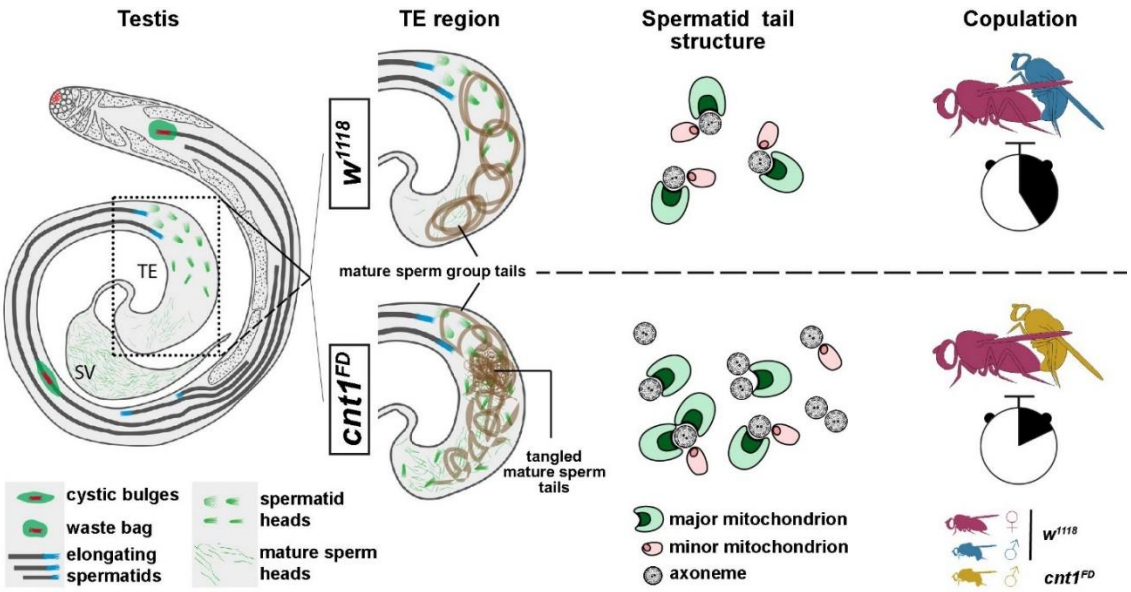

Figure 3. Summary of the pleiotropic effects of the *cnt1* mutation on mating behavior, spermatid maturation, and mitochondrial morphology in *Drosophila*.

2.1. *Drosophila* spermatogenesis

Drosophila melanogaster testes develop from larval gonads with defined apical and basal poles containing stem cells and primary spermatocytes, respectively. During *Drosophila* morphogenesis, the gonads undergo elongation, and the basal end of the testis is coiled. Through its basal end, the testis is connected to the seminal vesicle which serves for storing sperms prior ejaculation. The first mature spermatids appear at the basal end of the testis, indicating that spermatogenesis is complete. (Coutelis et al., 2008)

In adult flies, the stem cell niche is located at the apical end of the testis, where germline stem cells (GSCs) divide asymmetrically to generate a stem cell and a goniolblast that begins differentiation along with somatic cyst stem cells (CySCs). Each gonioalblast undergoes four mitotic divisions to generate a cluster of 16 spermatogonia, followed by cell growth that forms spermatocytes. The latter undergo two meiotic divisions to produce a syncytial group of 64 round haploid spermatids. (Steinhauer, 2015) Simultaneously, the spermatids undergo elongation in which the tail extends toward the apical end of the testis and the nuclei of the round spermatids become long and thin (Tokuyasu, 1975; Noguchi and Miller, 2003). Morphogenesis of the spermatid head is accompanied by chromatin condensation. The round-shaped nucleus passes through the leaf and early canoe stages under the influence of histone modifications. Subsequently, the nucleus changes from the early canoe to the late canoe stage, where histones are replaced by transition proteins. Finally, under the influence of protamine, the nucleus makes the transition from the late canoe stage to the acicular stages. (Fabian and Brill, 2012). The fully elongated spermatids start the individualization process in the region of the terminal epithelium (TE), which is located at the basal end of the testis. Actin-based individualization complexes (ICs) form around the elongated nuclei and then move to the end of the tails, taking up redundant organelles and additional cytoplasm. During this process, a cystic bulge (CB) forms and increases in volume as it migrates along the spermatid tails. Once the CB reaches the tip of the tails, it detaches and forms a waste bag (WB) that decomposes so that each mature sperm enclosed in its own membrane (Bader et al., 2010; Fabian and Brill, 2012). The individualization process is accompanied by apoptosis, which is well controlled in the testis by the activation of testis-specific caspases using triggers such as *cytochrome c* (Steller, 2008). Any alteration in the apoptosis process can lead to malformation of CB and WB and

failure of individualization (Huh et al., 2004). After successful individualization, each mature sperm group coils in the TE region and single motile sperm are released into the testicular lumen, from where they migrate to the seminal vesicle (SV) prior ejaculation (Fabian and Brill, 2012; Demarco et al., 2014). (Figure 4)

Complete spermatogenesis is necessary for successful transfer of healthy sperm into the female genitalia followed by a proper mating behavior (Baptissart et al., 2013; Lotti and Maggi, 2018). *Drosophila* mating behavior is a complex ritualized behavior. itially, the male attracts the female by orienting toward her,, tapping her abdomen with his forelegs, and extending a wing to produce a mating sound. Later, the male touches the female‘s genitalia with his mouthparts and attempts to start copulation by curving his abdomen toward the female‘s abdomen. Finally, the female either accepts the copulation attempts by slowing her movement or rejects them by legskicking the male with her hind legs. (Pavlou and Goodwin, 2013; Ziegler et al., 2013) Sperm transfer to the female genitalia is well controlled by the male, with copulation duration related to the amount of sperm ejaculated (MacBean and Parsons, 1967; Gilchrist and Partridge, 2000; Lee and Hall, 2001; Acebes et al., 2004; Crickmore and Vosshall, 2013).

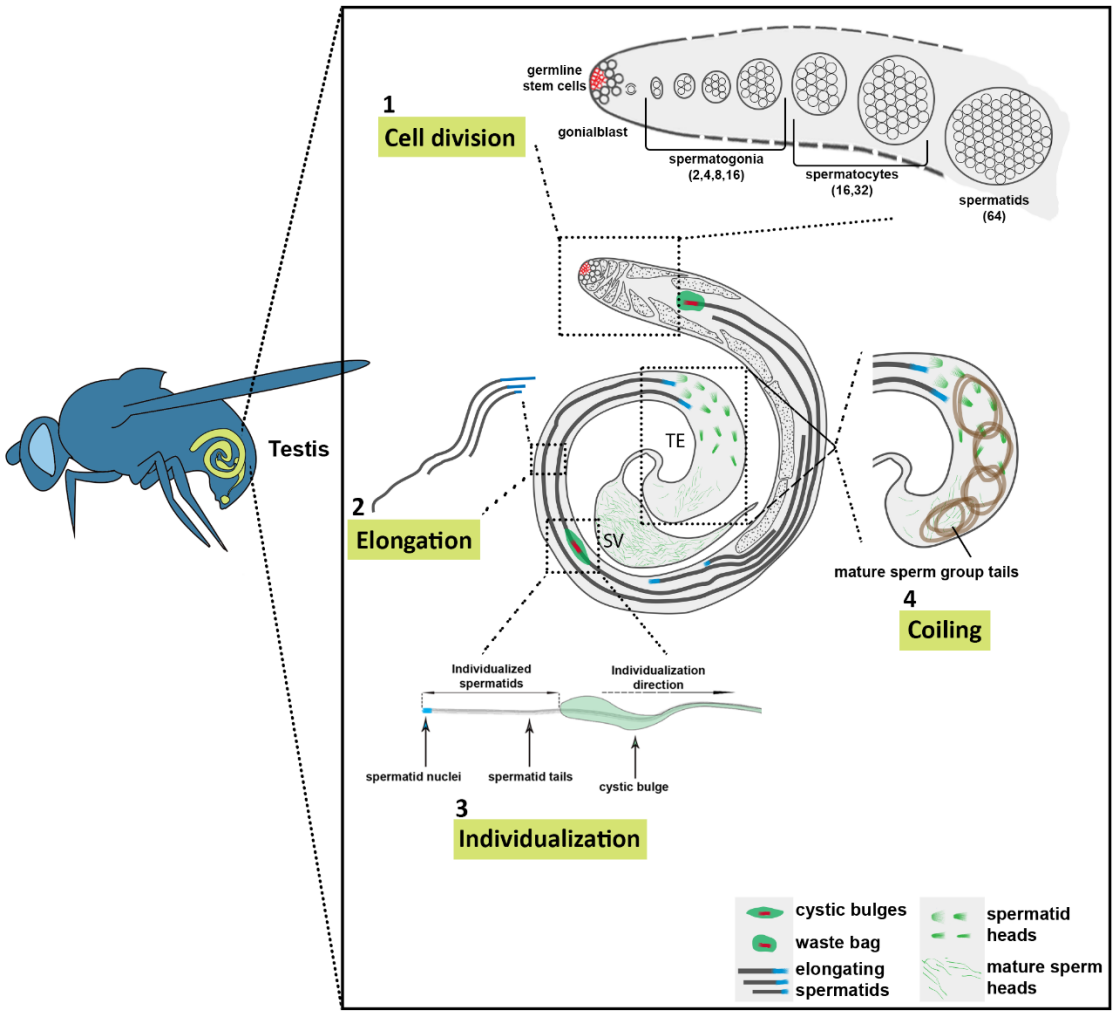

Figure 4. *Drosophila* spermatogenesis. The figure illustrates the main steps of spermatogenesis and their position in *Drosophila melanogaster* testis. **1)** Cell division is located at the apical region of the testis. **2)** Elongation occurs along the testis. **3)** Individualization occurs in the TE region. **4)** Coiling occurs in the TE region of the testis. Terminal epithelium (TE), seminal vesicle (SV). (Maaroufi et al., 2022)

3. Role of adenosine pathway on stress response

Ado is one of the key molecules with a cytoprotective effect, but the response to Ado signaling may vary depending on the cell type (Fleischmannova et al., 2012). Under inflammatory and hypoxic conditions, Ado levels increase to act as an anti-inflammatory molecule, restore the balance between oxygen supply and demand, and stimulate

angiogenesis to prevent tissue damage (Borea et al., 2016). Dephosphorylation of ATP is the main mechanism for the increase in extracellular Ado concentration (Borea et al., 2016). However, persistent Ado signaling can exacerbate stress and promote chronic tissue injury (Lin et al., 2021). A mutation in the huntingtin protein (mHTT), which is essential for neuronal development, promotes cytotoxic stress in *Drosophila*. This cytotoxicity triggered a decrease in hemolymph Ado levels and an increase in the production of heat shock proteins (Hsp70), which are known to prevent the cytotoxicity of mHTT (Lin et al., 2021). mHTT has also been described as a stressor for the immune system (Lin et al., 2019). Under such stress conditions, blockade of Ado signaling appears to be beneficial.

The study in our published article II and III summarizes our findings on Ado signaling pathway under stress conditions (Lin et al., 2019, 2021) (Figure 5).

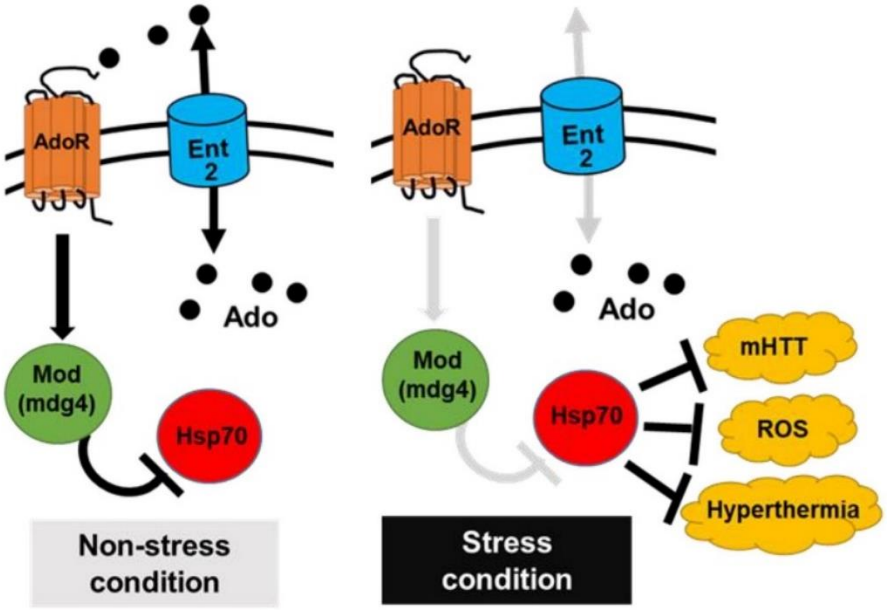

Figure 5. Effect of Ado signaling on stress response. Under nonstress conditions, Ado activates AdoR, leading to a decrease in Hsp70 production controlled by Mod (mdg4). Under stress conditions, decreased Ado signaling leads to an increase in Hsp70 production, which increases stress tolerance. (Lin et al., 2021)

4. Aim of my studies

Although the adenosine signaling and metabolism pathways in *Drosophila* has been studied in context of cell growth and stress response, information on some protein components of these pathways has been lacking. In my first publication, I characterized the function of one of the major proteins of the Ado metabolic pathway, *cnt1*. Functional characterization of *cnt1* was done using *Drosophila* as a model organism to study the effects of Ado on cell growth and differentiation in the testis.

I also collaborated on a study of the cytotoxic effect of mHTT on the immune system and the Ado pathway. It is well known that the Ado pathway plays a role under stress conditions, such as in the presence of mHTT. Its pathogenic effect on neurodegeneration and the immune system of mice has been reported previously. Therefore, in the second and third publications, we thus characterized the effect of mHTT on the immune system and investigated its effects on Ado metabolic and signaling pathways in *Drosophila*; and identified novel downstream proteins in the Ado pathway.

Summary of results

Publication I

Houda Ouns Maaroufi, Lucie Pauchova, Yu-Hsien Lin, Bulah Chia-hsiang Wu, Lenka Rouhova, Lucie Kucerova, Ligia Cota Vieira, Marek Renner, Hana Sehadova, Miluse Hradilova, Michal Zurovec (2022). Mutation in *Drosophila* concentrative nucleoside transporter 1 alters spermatid maturation and mating behavior. *Front. Cell Dev. Biol.* DOI: 10.3389/fcell.2022.945572

In the first publication, we show the importance of the Ado metabolic pathway in the regulation of cell growth in the testis. We specifically investigated the physiological role of one of the major transmembrane proteins, *concentrative nucleoside transporter 1* (*cnt1*), in *Drosophila melanogaster*. We found that Cnt1 is highly expressed in *Drosophila* testes, particularly in the head and tail of spermatids. Therefore, we checked whether cnt1 plays a role in modulating *Drosophila* fertility. We used the CRISPR/Cas9 system to create a mutation in the *cnt1* gene. The *cnt1* mutants exhibited partial sterility associated with a defect in mating behavior. The mutants had reduced duration of copulation compared to controls. The cnt1 mutation also impaired spermatid maturation. Although the mutant males exhibited a defect in mating behavior, we found that they also released high numbers of mature spermatids released in the TE region, but a lower number in the SV, indicating impaired movement of mature spermatids, compared with controls. We found that the tails of the mature sperm were not properly coiled and became tangled in the TE region, which correlates with the lack of sperm migration toward SV. We also observed by electron microscope that the tails of spermatids had an abnormal number of mitochondrial subunits. This defect explains that the mature spermatids have a mechanical problem with the mitochondrial defect caused by the cnt1 mutation. Analysis of our RNAseq data using RT -qPCR screening revealed impaired expression of a *sperm-specific dynein intermediate chain 4* (*sdic4*), which is essential for sperm tail motorization. We also found that ATP synthesis was also impaired. The latter is essential for sperm dynein motorization. Overall, our results demonstrate the importance of *cnt1* in male fertility and suggest that the

observed defects in mating behavior and spermatogenesis are due to alterations in nucleoside transport and related metabolic pathways.

frontiers | Frontiers in Cell and Developmental Biology

TYPE Original Research
PUBLISHED 23 August 2022
DOI 10.3389/fcell.2022.945572

OPEN ACCESS

EDITED BY
Sung Min Han,
University of Florida, United States

REVIEWED BY
Paul Lasko,
McGill University, Canada
Patrizia Morciano,
Gran Sasso National Laboratory (INFN), Italy

*CORRESPONDENCE
Michal Zurovec,
zurovec@entu.cas.cz

SPECIALTY SECTION
This article was submitted to Stem Cell Research, a section of the journal Frontiers in Cell and Developmental Biology

RECEIVED 16 May 2022
ACCEPTED 27 July 2022
PUBLISHED 23 August 2022

CITATION
Maaroufi HO, Pauchova L, Lin Y-H, Wu BC-H, Rouhova L, Kucerova L, Vieira LC, Renner M, Sehadova H, Hradilova M and Zurovec M (2022), Mutation in Drosophila concentrative nucleoside transporter 1 alters spermatid maturation and mating behavior.
Front. Cell Dev. Biol. 10:945572.
doi: 10.3389/fcell.2022.945572

Mutation in *Drosophila concentrative nucleoside transporter 1* alters spermatid maturation and mating behavior

Houda Ouns Maaroufi[1,2], Lucie Pauchova[1,2], Yu-Hsien Lin[1,2], Bulah Chia-Hsiang Wu[1,2], Lenka Rouhova[1,2], Lucie Kucerova[1], Ligia Cota Vieira[1], Marek Renner[2], Hana Sehadova[1,2], Miluse Hradilova[3] and Michal Zurovec[1,2]*

[1]Biology Centre of the Czech Academy of Sciences, Institute of Entomology, Ceske Budejovice, Czechia, [2]Faculty of Science, University of South Bohemia, Ceske Budejovice, Czechia, [3]Institute of Molecular Genetics, Czech Academy of Sciences, Prague, Czechia

Concentrative nucleoside transporters (Cnts) are unidirectional carriers that mediate the energy-costly influx of nucleosides driven by the transmembrane sodium gradient. Cnts are transmembrane proteins that share a common structural organization and are found in all phyla. Although there have been studies on Cnts from a biochemical perspective, no deep research has examined their role at the organismal level. Here, we investigated the role of the *Drosophila melanogaster cnt1* gene, which is specifically expressed in the testes. We used the CRISPR/Cas9 system to generate a mutation in the *cnt1* gene. The *cnt1* mutants exhibited defects in the duration of copulation and spermatid maturation, which significantly impaired male fertility. The most striking effect of the *cnt1* mutation in spermatid maturation was an abnormal structure of the sperm tail, in which the formation of major and minor mitochondrial derivatives was disrupted. Our results demonstrate the importance of *cnt1* in male fertility and suggest that the observed defects in mating behavior and spermatogenesis are due to alterations in nucleoside transport and associated metabolic pathways.

KEYWORDS

cnt1, gamete, spermatogenesis, testis, adenosine, copulation, mitochondria, male fertility

Introduction

Male fertility in *Drosophila* depends on a number of traits, including appropriate mating behavior and proper progression of spermatogenesis (Baptissart et al., 2013; Lotti and Maggi, 2018). Mating is a complex process that is essential for reproductive success. The male pursues the female while vibrating his wings to produce a courtship song, tapping the female's abdomen with his forelegs, touching the female's genitals with his mouthparts, and curving his abdomen for copulation (Pavlou and Goodwin, 2013; Ziegler

et al., 2013). The transfer of mature and healthy sperm to the female genitalia also depends on proper spermatogenesis, which involves the proliferation and differentiation of spermatogonial stem cells (Wakimoto et al., 2004; Yuan et al., 2019).

Spermatogenesis in *Drosophila* begins with stem cell proliferation, wherein the stem cell undergoes four mitotic divisions with incomplete cytokinesis, forming a cyst with 16 interconnected spermatogonia. This is followed by cell growth and meiosis to produce a syncytial group of 64 spherical haploid spermatids (Steinhauer, 2015). Subsequently, these spermatids undergo elongation and individualization (Tokuyasu, 1975; Noguchi and Miller, 2003), a process known as *Drosophila* spermiogenesis, in which the spermatids are remodeled into spermatozoa (Alzyoud et al., 2021). Spermatogonia develop in an enclosure formed by two cyst cells of somatic origin that undergo extensive morphogenesis and eventually differentiate into the head and tail cysts during spermatid elongation (Lindsley and Tokuyasu, 1980; White-Cooper, 2004). During this process, the round-shaped spermatid nuclei become long and thin (needle-shaped nuclei), accompanied by chromatin condensation. The fully elongated spermatids begin the individualization process at the basal end of the testis in the region of the terminal epithelium (TE), where actin-based individualization complexes (ICs) form around the nuclei then migrate from the heads to the tip of the tails. As ICs move along the elongated spermatid, unnecessary organelles and additional cytoplasm are stripped off and form a cystic bulge (CB). Once the cyst detaches from the tail, it forms a rounder waste bag (WB), which is eventually degraded, leaving each mature spermatozoon enclosed in its own tight membrane (Bader et al., 2010; Fabian and Brill, 2012). At the end of spermatogenesis, each mature sperm group coils in the TE region and is released in the testis lumen before migrating from the TE region to the seminal vesicle (SV), where it is prepared for ejaculation (Fabian and Brill, 2012; Demarco et al., 2014).

More than 2000 mutations affecting male fertility have been discovered in *Drosophila* (Wakimoto et al., 2004), but most of these mutations are not well characterized. Moreover, a number of genes with specific expression in the testis have not been well studied (Wakimoto et al., 2004; Zhao et al., 2010; Vedelek et al., 2018; Witt et al., 2019). Previous studies have shown that some of the mutations that affect mating behavior are connected to *Drosophila* morphology (*white* and *yellow* (Zhang and Odenwald, 1995)), learning and memory (*dunce* and *amnesiac* (Siegel and Hall, 1979)), sex determination (*fruitless* (*fru*) (Baker et al., 2001; Rideout et al., 2007)), or copulation (*Phosphodiesterase 1c* (*pde1*) (Morton et al., 2010)). Most of the spermatogenesis-related mutations affect germline cells (e.g., *zn finger homeodomain 1* and *delta* (Leatherman and Dinardo, 2008; Ng et al., 2019)), spermatocytes (e.g., *cannonball* (Chen et al., 2005)) and spermatids (e.g., *driceless* and *dynein intermediate chain at 61B* (*dic61B*)) (Huh et al., 2004; Fatima, 2011)). Other mutations may regulate the number (e.g., *headcase* (Resende et al., 2013)), morphology (e.g., *salto* (Augière et al., 2019)), or motility (e.g., *hemingway* (Soulavie et al., 2014)) at different cell stages.

We studied a gene encoding the *Drosophila concentrative nucleoside transporter 1* (*cnt1*), which is expressed in a testis-specific manner (Larkin et al., 2021). Cnt1 is a unidirectional carrier that mediates the energy-costly influx of nucleosides driven by the transmembrane sodium gradient (Gray et al., 2004; Chintapalli et al., 2007; Larkin et al., 2021). Nucleoside transporters and the enzymatic activities of adenosine metabolism affect many physiological processes by influencing the adenosine levels as a signaling molecule, especially the role of the adenosine signal terminator at the respective receptor (Knight et al., 2010). Cnts are found in most organisms, including mammals and insects, and are fairly conserved among phyla. For example, Cnts in humans and *Drosophila* have 24–33% sequence similarity (Machado et al., 2007). The involvement of *Drosophila* Cnt1 and Cnt2 in adenosine transport was examined in a previous study that showed that knocking down their expression rescues Cl.8 + tissue culture cells from the cytotoxic effect of a high concentration of extracellular adenosine (Fleischmannova et al., 2012). The Cnt protein structure is characterized by 13 transmembrane domains (Young et al., 2013; Dos Santos-Rodrigues et al., 2015), and they seem to have limited tissue distribution within organisms. For example, in mammals, Cnts have been detected in specialized cells, particularly intestinal and hepatic epithelial cells and testis (Kato et al., 2005; Masino and Boison, 2013). Cnts have been identified in rat epididymis and shown to play a role in sperm maturation (Leung et al., 2001; Klein et al., 2017). In addition, in a recent study, the deficiency of human Cnt1 has been associated with a newly discovered inborn error of pyrimidine metabolism and organ failure in an infant (Pérez-Torras et al., 2019).

In the present study, we identified the *cnt1* gene as an important component in mediating the crosstalk between fertility and systemic metabolism in *Drosophila*. We showed that Cnt1 is highly expressed in testes. To determine the role of *cnt1* in *Drosophila*, we created a mutation in this gene using the CRISPR/Cas9 system and named the obtained allele *cnt1{fertility defect}* (*cnt1*^{FD}). The mutation in *cnt1* caused a defect in mating behavior (copulation duration) and spermatid maturation that significantly impaired male fertility. The prominent effect of the *cnt1*^{FD} mutation in spermatid maturation involved an abnormal structure of the spermatid tail and low sperm count.

Materials and methods

Fly stocks

Fly strains were reared on a standard cornmeal medium at 25°C with 12/12 h light/dark cycle and 60% relative humidity.

Cnt1^{FD} mutant and *cnt1::GFP* were used and generated as described below. *W*^{1118} was used as a wild-type control. Flies containing *protA::GFP* were provided by Dr. R. Renkawitz-Pohl and Dr. Ch. Rathke (Jayaramaiah Raja and Renkawitz-Pohl, 2005), while the *dj::GFP* (BL 5417, USA) and *Df(2R)BSC271* (BL 23167, USA) were obtained from Bloomington (BL5417, USA).

Generation of the *cnt1* gene mutation

The mutation in the *Drosophila cnt1* gene was generated through the CRISPR/cas9 gene editing approach (Kondo and Ueda, 2013). Two guide RNA (gRNA) [GGCAAAGCGAAT CACCTATCTGG and GTGCCGCAATGACGCATACAAGG] were used to create a deletion. The first was located in the first coding exon and the second in the third coding exon. The double-strand break was corrected by non-homologous end-joining, which led to an open reading frame deletion of 477 bp and substitution of one amino acid at the break site (the entire *cnt1* deletion comprises 752 bp, including coding exon 1, complete exon 2, part of coding exon 3, and two complete introns.). The *cnt1*^{FD} mutants were generated by injecting the described construct into the embryos of nanos-cas9 expressing flies and examined through polymerase chain reaction (PCR). The flies were isogenized to the background of *w*^{1118} flies. Both male and female flies were homozygous viable for this deletion. We confirmed the mutation in *cnt1* (*cnt1*^{FD}) with the primers at the deletion site (Supplementary Table S1).

Generation of *cnt1*-tagged GFP

We generated flies containing a genomic sequence of *cnt1* tagged with *GFP* (*cnt1::GFP*) (Ejsmont et al., 2011). We cloned the GFP sequence into a fosmid vector containing the *cnt1* gene as a pre-tagging vector (Ejsmont et al., 2011; Sarov et al., 2016). The tagged clone was later injected into *Drosophila* embryos using GenetiVision services (Groth et al., 2004). The mutation in the flies was verified via PCR according to manufacturer protocol (Thermo Scientific Phusion High-Fidelity PCR Master Mix). The transgenic flies, *cnt1::GFP*, were used to trace the expression pattern of *cnt1* through the integrated *GFP* and used as a rescuers by combining it with the *cnt1*^{FD} mutant fly.

Real-time quantitative reverse transcription-PCR

The RT-qPCR was performed as previously described (Lin et al., 2019). Total RNA was extracted from adult flies using TRIzol reagent (#1559026, Invitrogen, USA). Thereafter, the isolated RNAs were treated with DNase using the Promega RQ1 RNase-free DNase kit to prevent genomic DNA contamination. The DNase-treated RNAs were used for cDNA synthesis from 2 μg total RNA using a RevertAid H Minus First Strand cDNA Synthesis Kit (Thermo Fisher Scientific, Vilnius, Lithuania). The cDNA was amplified by RT-qPCR using the 5 × Hot FirePol EvaGreen qPCR Mix Plus with ROX (Solis BioDyne, Tartu, Estonia) and Rotor Gene Q Instrument (QIAGEN, Hilden, Germany). The primers used for *cnt1* quantification are presented in Supplementary Table S1. *αTub84B* (FBgn0003884) and *act5C* (FBgn0000042) were used as reference housekeeping genes. The expression level was calculated using the $2^{-\Delta\Delta Ct}$ method after normalizing the ct values of the target genes to the reference gene.

Fertility test

Virgin male and female flies were collected and separated for 3 days. Then, each of the adult male flies was placed in a vial along with 10 *w*^{1118} virgin female flies (3 days old) at 25°C. After 24 and 48 h, the females were placed in individual vials and examined for the appearance of offspring. The number of fertilized females per male was recorded.

Copulation assay

For the copulation length assay, virgin male and female flies were collected and separated for 3 days. Thereafter, the flies were sedated, placed in individual vials, and left to recover for 1 h. Then, a single male and a female were placed in a common vial, and video recording was undertaken.

For the copulation frequency assay, virgin male and female flies were collected and separated for 3 days. Then, a single male and 10 female flies were placed in a vial. Afterwards, the number of copulations was recorded.

Histology: Immunohistochemical staining

Immunohistochemical staining was performed as described previously with a few modifications (Lin et al., 2021). *Drosophila* adult testes were dissected in 1 × phosphate buffer saline (PBS) and fixed in 4% paraformaldehyde for 20 min. After washing with PBST (0.3% Triton in 1× PBS) three times, the testes were incubated in a blocking buffer (5% goat serum in 0.1% PBST) for 1 h. Next, the blocking buffer was replaced by primary antibodies mixed in PAT (1% BSA, 0.1% Triton and 0.01% sodium azide in 1× PBS) and the incubation lasted for overnight. Then, the testes were washed three times with 0.1% PBST and incubated in secondary antibodies mixed in 0.1% PBST for 1 h. After washing with 0.1% PBST three times, the tissues were stained with DAPI for 10 min and washed three times before mounting

with Fluoromount-G. DAPI (#MBD0015, Sigma-Aldrich, Germany), DCP1 (#9578S, Cell signaling, USA).

Image analysis

Images of the stained testes were taken using a laser scanning confocal microscope FluoView™ FV1000 (Olympus, Tokyo, Japan). To quantify the canoe-stage spermatids, sperms, and waste bags, the area of the TE region was obtained using ImageJ software (Schneider et al., 2012).

Ultrathin section of *Drosophila* testis specimens

The testes dissected in PBS were fixed in 2.5% glutaraldehyde for at least 4 h at room temperature (RT) or overnight at 4°C. The specimens were placed in a wash solution containing PBS with 4% glucose (three times for 15 min at RT) and then treated with a 1: 1 mixture of PBS and 4% OsO4 solution (for 2 h at RT). After application of the wash solution (three times for 15 min at RT), the tissues were dehydrated in an acetone series (30, 50, 70, 80, 90, 95, and 100% for 15 min each). The dehydrated samples were embedded in Epon resin by gradually increasing the volume ratio of resin to acetone (1:2, 1:1, and 2:1 for 1 h each at RT). The specimens were left in the resin for 24 h (RT), and then the resin was polymerized at 62°C for 48 h. The ultrathin sections were cut with a diamond knife and stretched with chloroform. The sections were placed on copper meshes and contrasted with uranyl acetate and lead citrate, after which they were coated with carbon. The samples were imaged under the JEOL JSM-7401F transmission electron microscope (JEOL, Akishima, Japan).

Statistical analysis

Graphs were produced in GraphPad Prism 5 software. Statistical analysis of the data was executed using Statistica software (StarSoft CR) and Microsoft Excel. Significance was established using parametric tests: Student's t-test (N.S., not significant, $*p < 0.05$, $**p < 0.01$, $***p < 0.001$) and one-way ANOVA (combined with Tukey post-hoc test), or non-parametric test: Kruskal–Wallis (combined with comparisons of mean ranks of all pairs of groups post-hoc test). Statistical analysis of the RT-qPCR was done using log2 value (Supplementary Table S2).

RNAseq

The *Drosophila* testes were dissected and frozen in liquid nitrogen. Biological triplicates were prepared, and 40 individuals were dissected for each replicate. TRIzol (#1559026 Invitrogen, USA) was applied to each sample, and RNA was isolated according to manufacturer protocol. The isolated RNA was further purified and treated by cDNAse using a NucleoSpin RNA kit (#740955.250 Macherey-Nagel, Germany). The quality of total RNA was controlled using an RNA 6000 Nano Kit on an Agilent Bioanalyzer 2,100 and the quantity using an RNA BR Assay Kit on a Qubit 2.0 Fluorometer (Life Technologies, USA). The sequencing library was prepared from a 1,000 ng input of high-quality (RIN >7) total RNA using a KAPA mRNA HyperPrep Kit for Illumina Platforms (Roche, KK8580, Switzerland) according to manufacturer protocol, with fragmentation conditions set at 94°C and 7 min. The final library PCR amplification was set at nine cycles. Library length profiles and concentrations were monitored using an Agilent Bioanalyzer (High-Sensitivity DNA chip) and a Qubit 2.0 Fluorometer (dsDNA HS Assay Kit), respectively. A pool of libraries in equimolar ratio was generated and sequenced in single-end mode on the NextSeq 500 Illumina platform using the NextSeq 500/550 High Output Kit v2.5 (75 Cycles) with a loading molarity of 1,8 p.m. including 1% PhiX control. Data analysis was performed using Galaxy online software and its associated tutorial (Batut et al., 2018). Our SRA database has been released on NCBI under the accession: PRJNA838856.

Phylogeny tree

Representative protein sequences of Cnt homologs, namely Sodium/Nucleoside Cotransporters or Solute Carrier Family 28 Members-3, covering the phylogeny of the genus *Drosophila* and the phylogeny of insects were identified using the Basic Local Alignment Search Tool (BLAST) in the GenBank database (Clark et al., 2016). Amino acid sequences were then aligned using the software MUSCLE (Edgar, 2004). Smart Model Selection, an online software (Lefort et al., 2017), was used to pick the best model according to the lowest Bayesian Information Criterion (BIC) score. Phylogenetic analyses were conducted through the Maximum Likelihood approach in PhyML 3.0 (Guindon et al., 2010). For each branch, statistical support was calculated as aBayes values. Trees were finalized with the aid of MEGA version X (Kumar et al., 2018).

Results

Phylogeny of Cnts in insects and drosophilidae family

The *cnt* genes are present in most living organisms, including eubacteria, suggesting that they are evolutionarily ancient (Young et al., 2013). Different taxonomic groups may differ in the number of *cnt* isoforms. For example, insects have one to

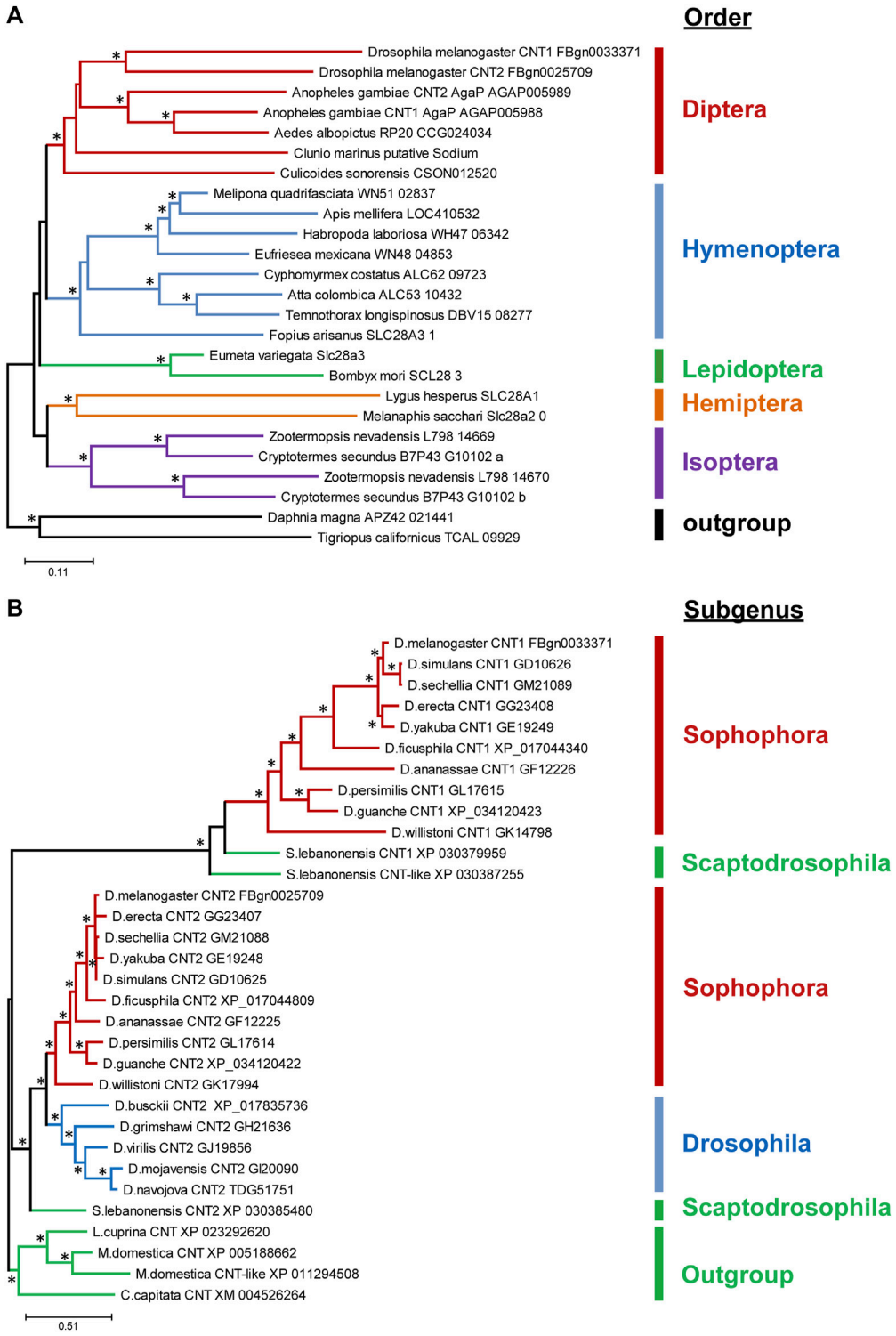

FIGURE 1
Distribution of Cnts in insects and family drosophilidae. **(A)** Simplified phylogenetic tree of Cnts among insects. Each color represents a particular order of insects. **(B)** Simplified phylogenetic tree of Cnt in *Drosophila*. Each color represents a subgenus of *Drosophila*. Branches with statistical support (aBayes values) greater than 70 are marked with asterisks.

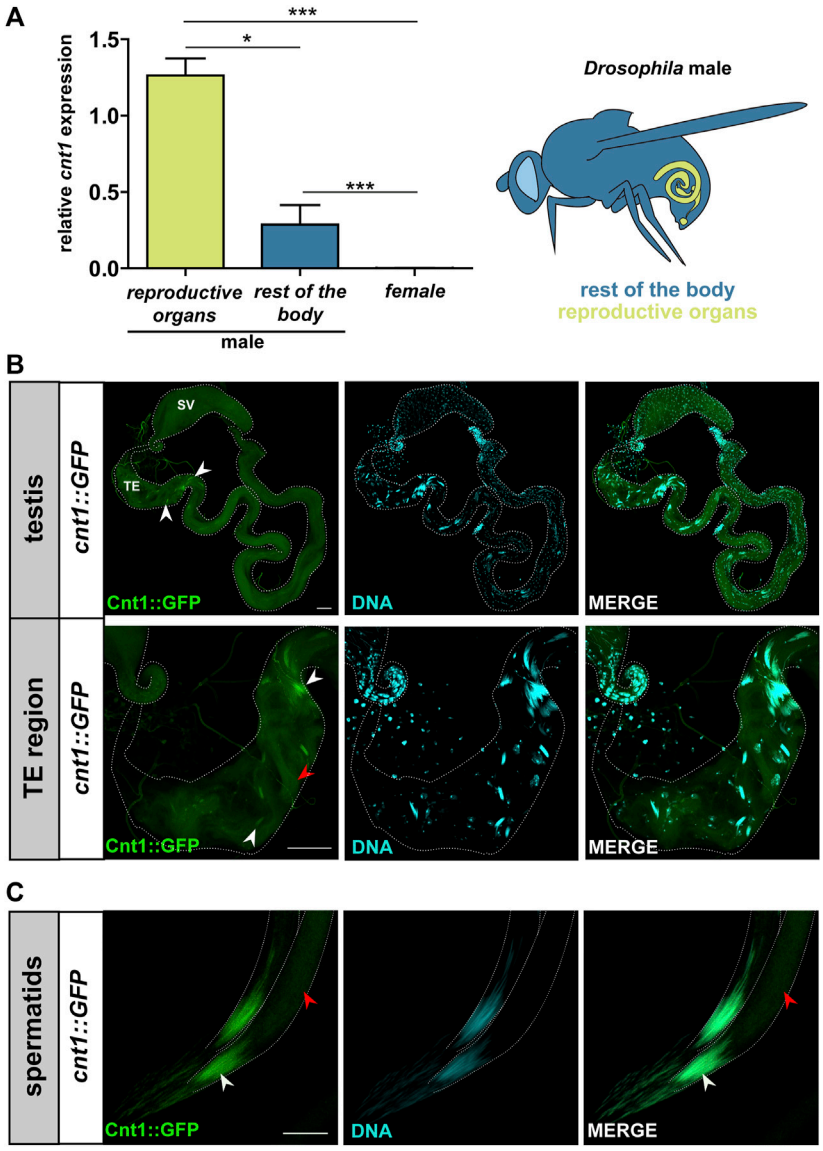

FIGURE 2
Cnt1 expression in the head and tail of spermatids. **(A)** The results of RT-qPCR analysis show a relative expression of *cnt1* in the reproductive organs and the rest of the body of the w^{1118} male and female flies (see the illustration). Expressions were normalized to *αTub84B* and *act5C* transcripts (ΔΔCT). Significance was analyzed by one-way analysis of variance (ANOVA) and labeled as follows: *$p < 0.05$, ***$p < 0.001$; n = 5. Error bars are given as mean ± SEM. **(B)** Cnt1::GFP localization in *Drosophila* testes and its TE region. Scale bar: 40 μm. **(C)** A closer look at the localization of Cnt1::GFP in spermatid heads (needle-stage spermatids). Scale bar: 10 μm. Cnt1::GFP staining in green and DNA staining (DAPI) in cyan. Head of spermatids (white arrowhead), tail of spermatids (red arrowhead), terminal epithelium (TE), seminal vesicle (SV).

three *cnt* isoforms, whereas mammals have three different *cnt* genes (Molina-Arcas and Pastor-Anglada, 2013; Young et al., 2013; Young, 2016). Moreover, among insects, Isoptera and Diptera seem to be the only insect orders where duplication events occur (Figure 1A). The duplication within the Isoptera appears to be a single origin event, whereas in Diptera, there seem to be multiple duplications and gene loss events. A closer look at the distribution of *cnts* within the genus *Drosophila* reveals a recent duplication of *cnt* in the common ancestor of *Drosophila* and *Scaptodrosophila*, with a secondary loss of *cnt1* in the subgenus *Drosophila* (Figure 1B). Based on the alignments among insects, the Cnts differ mainly by the first 20 amino acids, while the rest of the sequences are well conserved (Supplementary Figure S1).

The presence of Cnts in all species indicates that they perform important functions in organisms. The presence of

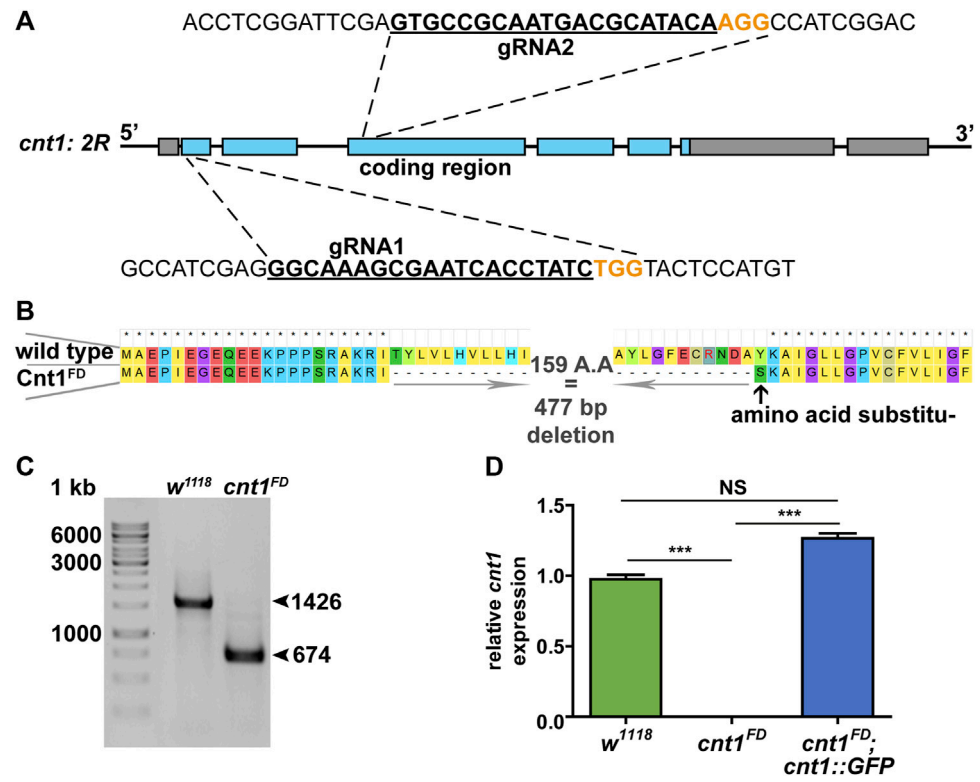

FIGURE 3
Generation of mutation in *Drosophila cnt1*. **(A)** Schematic representation of the *cnt1* mutation using two guide RNAs (gRNA); the target of the first gRNA is located in the first coding exon and the second in the third coding exon. **(B)** Protein sequence alignment of Cnt1 in control w^{1118} and $cnt1^{FD}$. The mutation caused a deletion of 477 bp (159 A.A) in the coding region of *cnt1* gene (a total of 752 bp including introns) and a substitution of the tyrosine residue for serine. **(C)** The PCR products of the *cnt1* mutant compared with its control. **(D)** Results of RT-qPCR analysis showing a relative expression of *cnt1* in control flies, $cnt1^{FD}$ mutant flies, and rescue flies $cnt1^{FD}$;*cnt1::GFP*. Expressions were normalized to *αTub84B* and *act5C* transcripts (ΔΔCT). Significance was analyzed by one-way analysis of variance (ANOVA) and labeled as follows: ***$p < 0.001$, NS > 0.05; n = 4. Error bars are shown as mean ± SEM.

multiple isoforms in some *Drosophila* species suggests that they may also be required in a tissue-specific manner.

cnt1 is associated with male fertility

According to FlyBase, *cnt1* is highly expressed in the male testes (Larkin et al., 2021). To confirm this expression profile, we performed RT-qPCR using *cnt1* gene-specific primers on the extracted reproductive organs and the rest of the body of w^{1118} male flies and females (Supplementary Table S1). Data analysis showed a high expression of *cnt1* in males and especially in the testes rather than the rest of the body organs in males (Figure 2A). We also used the fosmid *FlyFos* transgene (Ejsmont et al., 2009) and analyzed the expression of *GFP*-tag (Sarov et al., 2016) (*cnt1::GFP*) in w^{1118} background. A well-defined GFP signal was found in the TE region of the testis in flies carrying the *cnt1::GFP* transgene but not in the control w^{1118} (Figure 2B and Supplementary Figure S2). This signal was located in the head of the canoe- and needle stage-spermatids and overlapped with the DNA staining. In addition, a weak GFP signal was detected in the spermatid tail (Figures 2B,C). Detailed analysis showed that Cnt1 expression begins during spermiogenesis when late canoe-stage spermatids start to form, and that the signal persists until the formation of needle-stage spermatids (Figure 2C). These results confirm the tissue specificity of Cnt1 expression.

Using CRISPR-Cas9 technology (Kondo and Ueda, 2013), we deleted the internal part of the *cnt1* gene using two guide RNAs (gRNA) targeting the first and third coding exons (Figure 3A). The double-strand breaks resulted in a deletion of 477 bp and the substitution of an amino acid at the break site (Figures 3B,C). The deletion did not affect the reading frame of the gene but removed three transmembrane domains out of 13. We confirmed the *cnt1* mutation by sequencing and RT-qPCR (Figure 3D).

The male and female mutants showed normal viability. Given that *cnt1* expression is high in *Drosophila* testes, we investigated whether *cnt1* mutation affects male fertility. Individual naive

10.3389/fcell.2022.945572

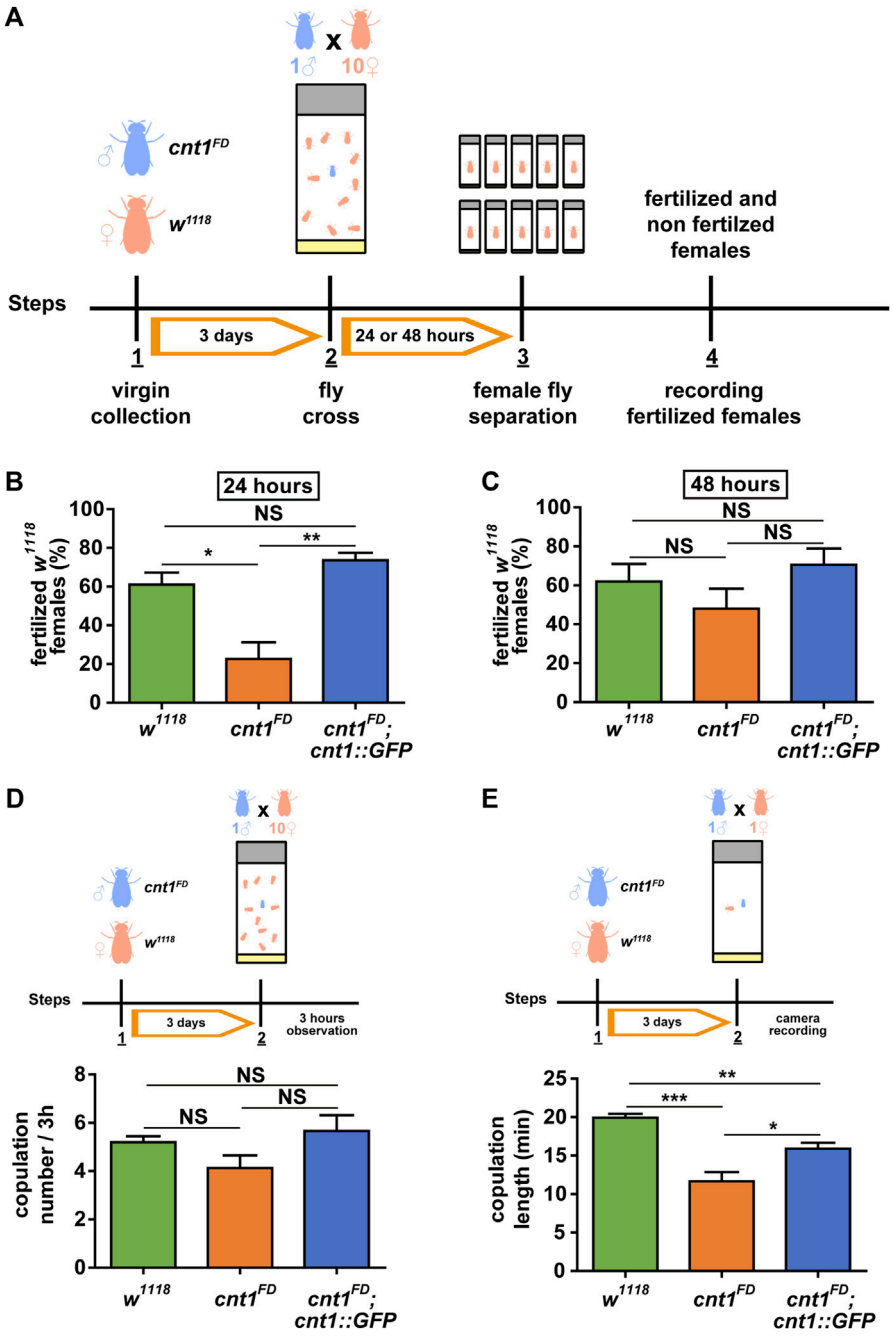

FIGURE 4
The *cnt1* mutation causes partial sterility in *Drosophila* males. **(A)** Experimental procedure of the fertility assay. Virgin mutant males ($cnt1^{FD}$) and control females (w^{1118}) were collected. After 3 days, one male was placed in a vial with 10 females for 24 or 48 h. Subsequently, each female was placed separately in a single vial, and the presence or absence of larvae was recorded. **(B)** Percentage of fertilized females after 24 h of mating with $cnt1^{FD}$ males; n ≥ 10. **(C)** Percentage of fertilized females after 48 h of mating with $cnt1^{FD}$ males; n ≥ 10. **(D)** Number of copulations within 3 h of observation. Virgin males ($cnt1^{FD}$) and females (w^{1118}) were collected. After 3 days, one male was placed in a vial with 10 females, and their mating was observed; n = 15. Error bars are presented as mean ± SEM. **(E)** Duration of copulation and experimental procedure. Virgin males ($cnt1^{FD}$) and females (w^{1118}) were collected. After 3 days, a male was placed in a vial with a female, and mating was recorded with a camera. The calculated times of copulations are in minutes; n = 15. Significance was analyzed by one-way ANOVA **(C)** and Kruskal–Wallis **(B,D,E)**; and labeled as follows: *$p < 0.05$, **$p < 0.01$, ***$p < 0.001$, NS > 0.05. Error bars are presented as mean ± SEM.

males of w^{1118} and $cnt1^{FD}$ were confined with 10 virgin w^{1118} females for 24 or 48 h (Figure 4A). The $cnt1^{FD}$ males were able to fertilize three times fewer females within 24 h than the control male flies (Figure 4B). Notably, extending the mating to 48 h showed no significant difference in fertility between the $cnt1^{FD}$ and w^{1118} males (Figure 4C), suggesting that $cnt1^{FD}$ males are less fertile and may require more time to inseminate all females.

Previous experiments have shown that 75% of the proteins tagged with GFP are functional *in vivo* (Nagarkar-Jaiswal et al., 2015). To determine whether the tagged *cnt1* was functional and test whether the observed $cnt1^{FD}$ phenotype was specific to $cnt1^{FD}$ mutation, we crossed the $cnt1^{FD}$ flies with flies carrying the *cnt1::GFP* transgene. As shown in Figures 4B,C, males of the rescue line $cnt1^{FD}$;*cnt1::GFP* were as fertile as the control line. We also used hetero-allelic flies carrying a genomic deletion including *cnt1* and the results show that after 24 h of mating the hetero-allelic male $cnt1^{FD}/Df(2R)BSC271$ flies were able to fertilize a similar percentage of females as the homozygous male $cnt1^{FD}$ mutants but not as many as the control male w^{1118} flies (Supplementary Figure S3). These data confirm that the observed phenotypes are caused by the loss of *cnt1* function.

cnt1 affects mating behavior

Based on the above results, we tested whether the fertility disorder was related to abnormal mating behavior. To test whether mating frequency is affected by the *cnt1* mutation, we performed a test in which a male was placed in a vial with 10 virgin females and mating was recorded for 3 h. The observations showed no significant difference in mating frequency among the $cnt1^{FD}$ flies, w^{1118} control flies, and $cnt1^{FD}$;*cnt1::GFP* rescue flies (Figure 4D).

In the next experiment, single 3-day-old naïve males were paired with single virgin females, and their copulation time was recorded. Again, we observed that all $cnt1^{FD}$ males mated with the females at the same frequency, but the copulation time was shorter compared with the controls (Figure 4E). Thus, we conclude that the changes in copulation duration in *cnt1* mutants likely contribute to the observed phenotype of lower fecundity.

cnt1 mutation affects spermatogenesis

The maximum *cnt1* expression is detected in canoe- and needle-stage spermatids. We tested whether their numbers are affected by the *cnt1* mutation. To test whether the reduced fertility of mutant males was caused by a defect in spermatid production, we used the *protamine A* (*protA*) fluorescent marker (*protA::GFP*) (Jayaramaiah Raja and Renkawitz-Pohl, 2005) to determine spermatid and sperm counts. *ProtA* is known to be expressed in the sperm heads from the end of spermiogenesis. We also used another marker, *don Juan* (*dj*) tagged with *GFP* (*dj::GFP*) (Santel et al., 1997; Santel et al., 1998), which is present in spermatids and sperm tails, to monitor possible defects in sperm flagella. Both *protA::GFP* and *dj::GFP* were used in the background of $cnt1^{FD}$ mutants, as well as in its control w^{1118}. Analysis showed that, in contrast to the control, $cnt1^{FD}$ had a higher number of spermatid groups, including the needle-stage spermatid groups, which were scattered throughout the TE region (Figures 5A–C). The volume in this region was also increased (Figure 5D). Moreover, we counted the number of mature sperms released in the TE region and found it to be higher in $cnt1^{FD}$ mutants compared with the control (Figure 5E). The higher number of spermatid groups and mature sperms in the TE region of $cnt1^{FD}$ mutants could be due to their higher production or slow mature sperm displacement toward the SV.

To distinguish whether the increased number of mature sperms is the result of their higher production or accumulation, we investigated whether the defect of the spermatid group number occurs in newly emerged males. The microscopic analysis of the TE regions from 24-hour-old males shows that $cnt1^{FD}$ already produces a high number of spermatid groups (Supplementary Figure S4). Thus, the effect of *cnt1* on spermatid groups starts at an early age in adult males, possibly due to their higher production.

The alteration in spermatid group production was followed by the disorganization of the tails of the mature sperm groups in the TE region, which sometimes showed tangled tails. This phenomenon, most likely occurred during coiling (Figure 5F). In wild-type flies, the coiling process of mature sperm groups occurs with a well-defined circular pattern of flagella, whereas mature sperm groups from $cnt1^{FD}$ flies do not show a similar circular shape (Figures 5F,G). We also show that $cnt1^{FD}$ flies have a high proportion of miscoiled tails (87.8%) compared with w^{1118} (11.76%) and $cnt1^{FD}$;*cnt1::GFP* (19.44%) (Supplementary Figure S5). This could be due to insufficient space in the TE region for new ICs to proceed with the remaining steps of spermatogenesis or because the tail of the *Drosophila* mature sperm has a defect in coiling due to the *cnt1* mutation.

We also counted the number of spermatozoa in the SV to verify whether the observed tail defect in the TE region affected sperm migration. The results showed that sperm count was lower in the $cnt1^{FD}$ SV compared with the control. This may indicate that the fertility defect in $cnt1^{FD}$ males is partly due to insufficient sperm count in the SV (Supplementary Figure S6).

cnt1 mutation affects the apoptotic machinery during spermatid individualization

To further examine the reason for the accumulation of spermatids and the disorganization of mature sperms during coiling in the TE region of the *cnt1* mutant, we tested whether the

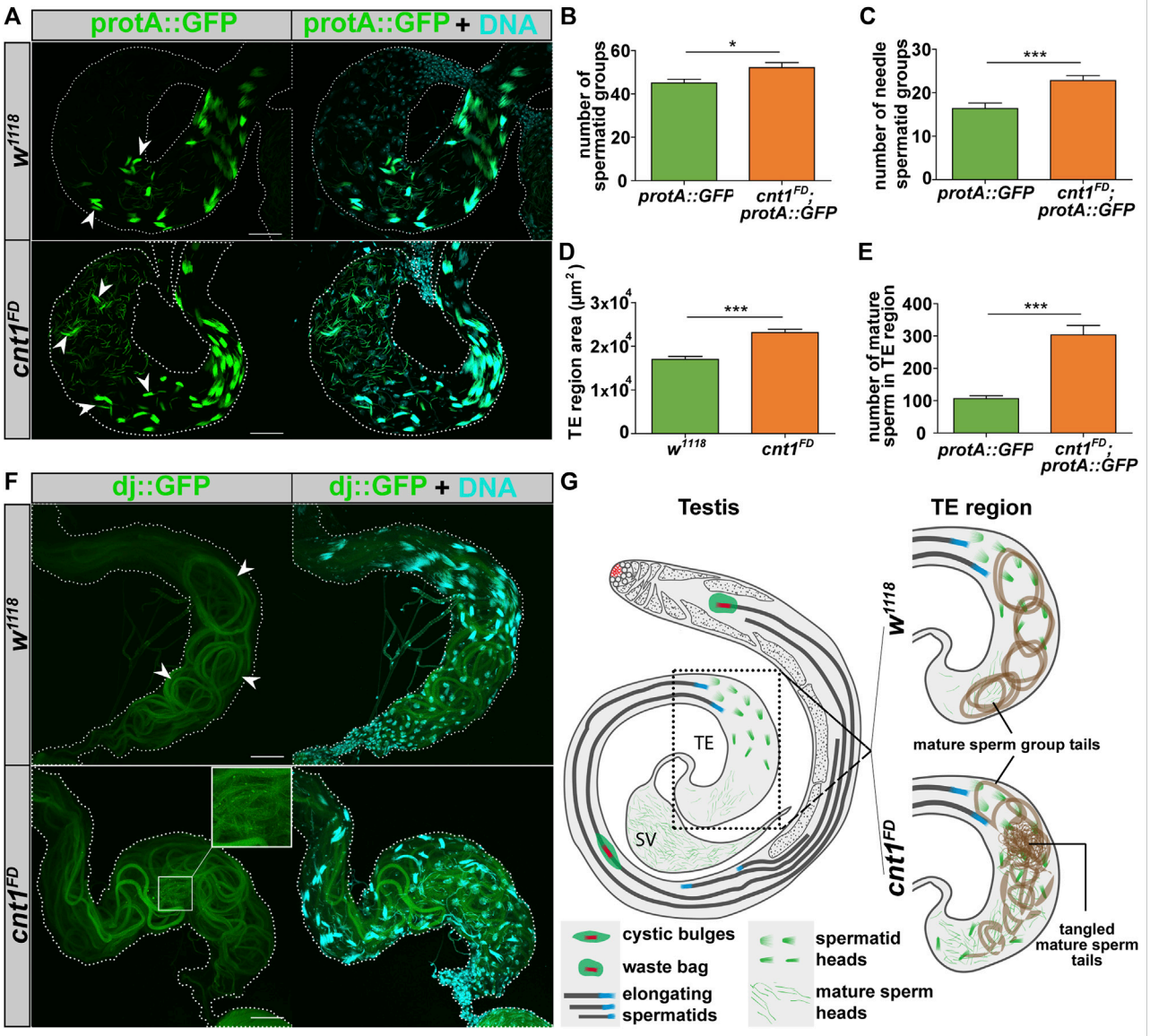

FIGURE 5
The *cnt1* mutation increases the number of spermatid groups and spermatozoa in the TE region and causes tail miscoiling. **(A)** Microscopic observation of spermatids expressing protamine A signals in the region of the terminal epithelium of the testis. The arrowheads show examples of the needle spermatid groups. W^{1118} is used as a control. In w^{1118}, spermatid groups expressing protamine A are observed in the first half of the TE region, whereas the spermatid groups are scattered throughout the TE region in the $cnt1^{FD}$ mutants. Protamine A (green), DNA (cyan). Scale bar: 40 µm. **(B)** Number of spermatid groups; n ≥ 10. **(C)** Number of needle-stage spermatid groups; n ≥ 10. **(D)** Size of the TE region; n ≥ 28. **(E)** Number of mature sperm in the TE region; n ≥ 10. Significance was analyzed with a one-tailed Student's t-test and labeled as follows: $*p < 0.05$, $***p < 0.001$. Error bars are shown as mean ± SEM. **(F)** Microscopic observation of coiled tails of mature sperm groups expressing a "dj" signal in the region of the terminal epithelium of the testis. W^{1118} is used as a control. In w^{1118}, the tails of the mature sperm group were well organized and coiled (white arrowhead). In $cnt1^{FD}$, the tails of mature sperm were poorly organized. Upon closer inspection, the tails were tangled in the region of the TE. Dj (green), DNA (cyan). Scale bar: 40 µm. **(G)** Summarized representation of protamine A and dj organization in mature sperm in w^{1118} and $cnt1^{FD}$.

individualization process was affected. We used the *death caspase-1 (dcp1)* antibody, which stains CB and WB. In *Drosophila*, CB and WB are formed during the individualization of elongated spermatids. They are important for the removal of redundant cytoplasm and organelles that are degraded in the bag once they reach the end of the spermatid tail (Fabian and Brill, 2012). As shown in Figure 6A, $cnt1^{FD}$ has more WB than the control group. In addition, most of the CB did not have an oval shape but were irregular and left a trail as they moved toward the tail end of the spermatid (Figures 6B,C). This indicates that caspase signaling remained active in the individualized portion of the spermatids (Huh et al., 2004),

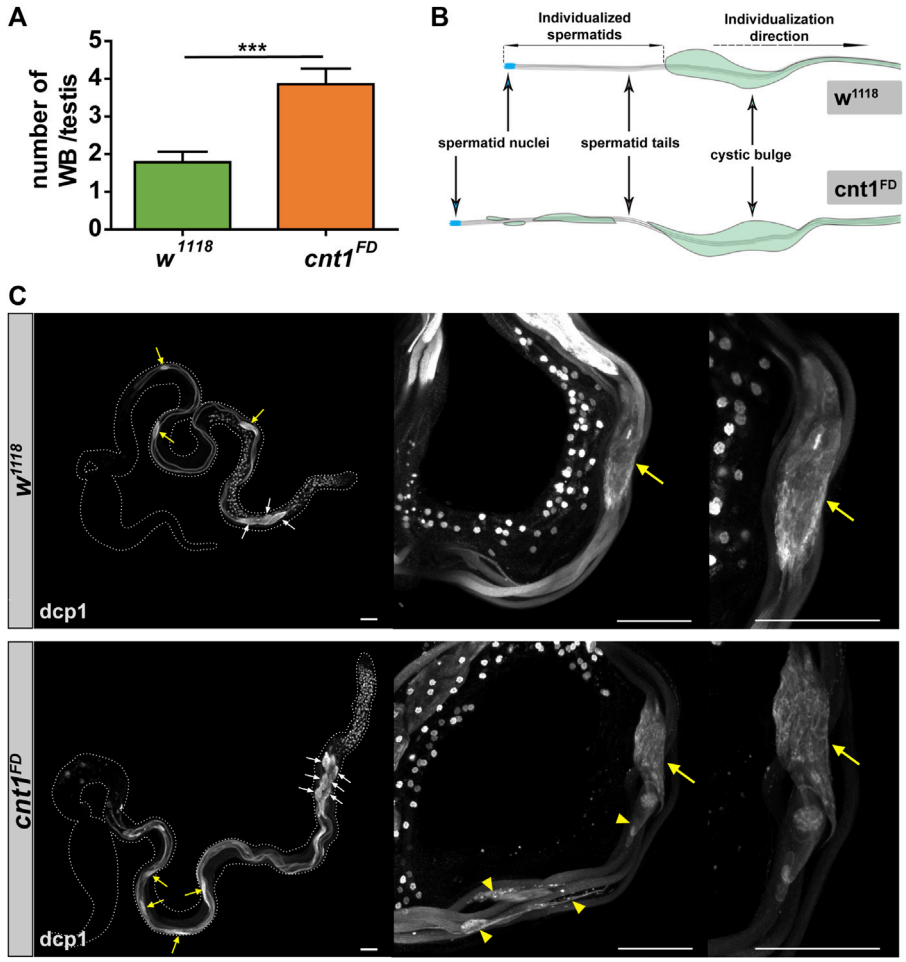

FIGURE 6
Cnt1 mutation impairs spermatid maturation during the spermatid individualization process. **(A)** Number of waste bags in w^{1118} and $cnt1^{FD}$ strains. Significance was analyzed using one-tailed Student's t-test and labeled as follows: ***$p < 0.001$; $n \geq 10$. Error bars are shown as mean ± SEM. **(B)** Illustration of the distorted shape of the cystic bulge in $cnt1^{FD}$ compared with w^{1118}. **(C)** Testis staining with death caspase-1 antibody (white). Dcp1 signal is absent in the individualized part of the cyst in w^{1118}, whereas it is present in *cnt1* mutants (yellow arrowhead). The yellow arrows point to the cystic bulges, while the white arrows point to the waste bags. Scale bar: 50 μm.

and that the apoptotic-like process required for the elimination of excess organelles is impaired in $cnt1^{FD}$ mutants. This may be related to the disorganization of the tail of spermatids observed in $cnt1^{FD}$ in the TE region.

cnt1 is required to maintain mitochondrial morphology

To further explore the cause of the increased number of spermatids and the disorganization of their tails in the TE region, we checked the number of spermatids within their cyst group and the elongated spermatid shape under a transmission electron microscope in both control and mutant testes. This allowed us to examine the major spermatid structures, including the major and minor mitochondria and the axoneme. These components serve as structural support for the sustained elongation of the sperm tail and sperm motility in *Drosophila* (Porter, 1996; Noguchi et al., 2011). In the cross-section of the w^{1118} testis, the spermatid cysts revealed a group of 64 spermatids. Moreover, the structure of the elongated spermatids in the w^{1118} had all the components required to generate a healthy sperm (Figures 7A,B). By contrast, $cnt1^{FD}$ had a lower number of spermatids within a cyst, ranging from 47 to 64, compared to the controls (Figure 7A and Supplementary Figures S7A,B). Some of these cysts contained unusual shapes of elongated spermatids (Figures 7A,B and Supplementary Figure S7).

The male $cnt1^{FD}$ mutant, in contrast to w^{1118} and $cnt1^{FD}$;*cnt1::GFP*, exhibited spermatids with abnormal numbers of major and minor mitochondria (Figures 7B,C and Supplementary Figures

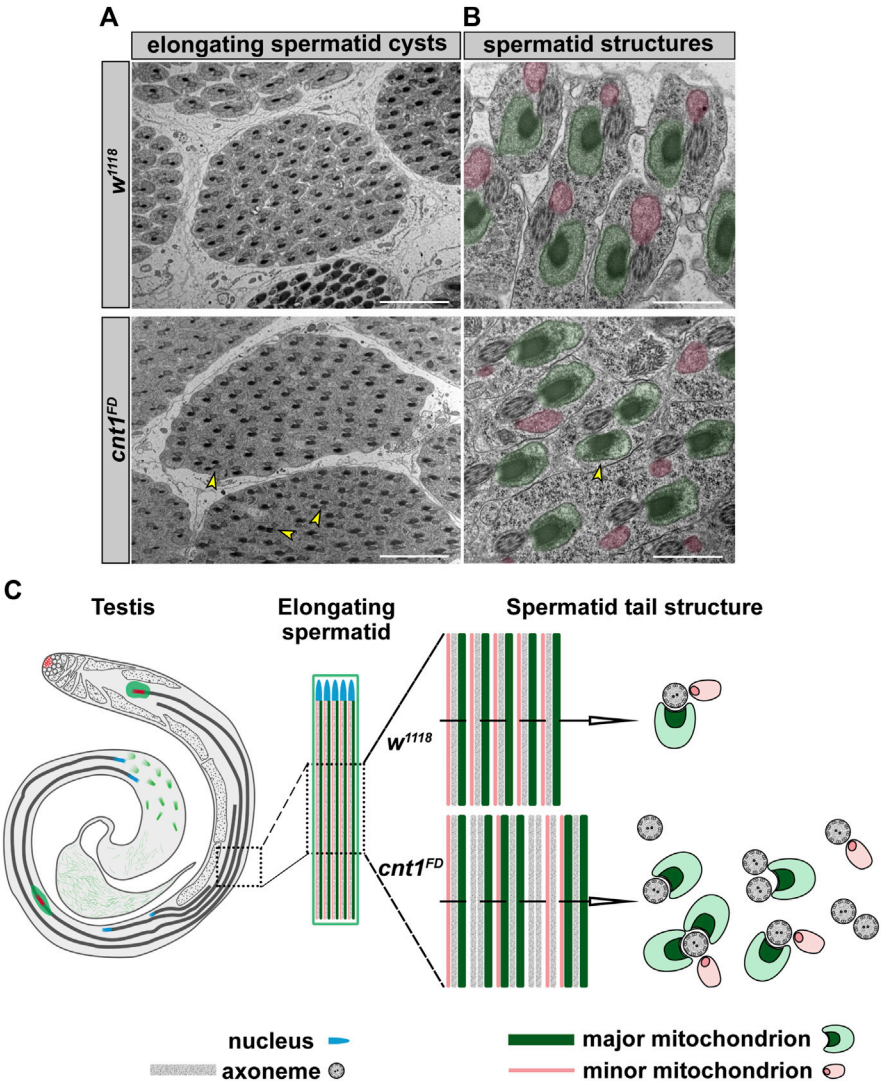

FIGURE 7
The *cnt1* mutants exhibit mitochondrial defects. **(A)** Transversal section of w^{1118} and $cnt1^{FD}$ mutant testes showing a cyst of elongating spermatids. Scale bar: 5 µm. **(B)** W^{1118} shows a normal structure of an elongated spermatid tail with one axoneme, two major mitochondria, and one minor mitochondrion. $cnt1^{FD}$ shows an abnormal structure of an elongated spermatid tail with one or two axonemes and an abnormal number of mitochondrial subunits. Major mitochondria (highlighted in green), minor mitochondria (highlighted in pink). Scale bar: 1 µm. **(C)** Summary of observed mitochondrial phenotypes in the $cnt1^{FD}$ mutant compared with w^{1118}.

S7A,C). In several cysts, some of the spermatid structures were in a common cytoplasm, indicating that they could not be separated from each other (Supplementary Figure S7A) (Huh et al., 2004). Fused spermatids and spermatids with altered number of mitochondria in $cnt1^{FD}$ were calculated and compared with those of control flies w^{1118} and $cnt1^{FD}$;*cnt1::GFP*. We show that $cnt1^{FD}$ mutants have an average of two defective spermatids per cyst compared with the controls (Supplementary Figure S7D). These features may account for the failed coiling process and the presence of tangled sperm tails in the TE region, where they could not move toward SV. This could be due to abnormal mitochondrial activity and other physiological changes that could affect the energy balance of the spermatids.

RNAseq analysis and data evaluation

To investigate the gene expression profile associated with the phenotype of the *cnt1* mutant, we performed RNAseq of reproductive oragans cDNA libraries of $cnt1^{FD}$ mutants and the control w^{1118} group (three biological replicates for each $cnt1^{FD}$ and w^{1118} strain). RNAseq analysis identified

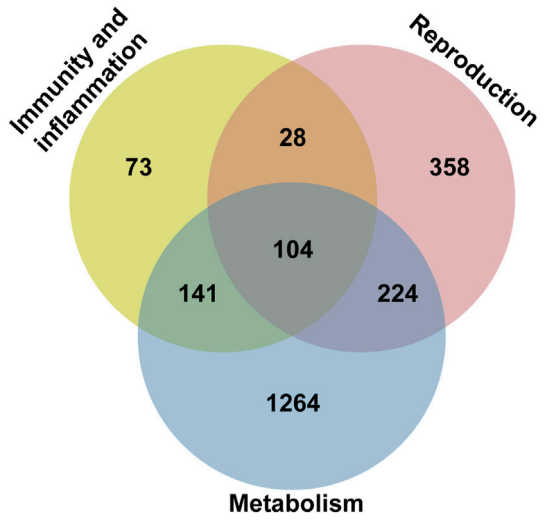

FIGURE 8
Functional classification of differentially regulated genes from the RNAseq data of $cnt1^{FD}$ and w^{1118} in a Venn diagram. The pie chart shows the distribution of genes in different categories with special emphasis on the reproduction domain. The Venn diagram shows genes with adj. p-value ≥ 0.05.

4,755 differentially expressed genes in the testes of the $cnt1^{FD}$ mutants, among which 2,472 were upregulated and 2,283 were downregulated (Supplementary Table S3). RNAseq data were validated through RT-qPCR (Supplementary Figure S8 and Supplementary Table S1). Ten representative genes were selected, and RT-qPCR showed concordant results with the RNA-sequencing data.

Pathview analysis of the differentially expressed genes (adj. p-value<0.05) revealed only one significant KEGG pathway, namely, the ribosomal pathway (dme03010). Two protein-coding ribosomal genes were upregulated, while 78 protein-coding ribosomal genes were downregulated (Supplementary Figure S9, Supplementary Table S3). By contrast, the expressions of genes encoding ribosomal RNAs of both subunits were stable (Supplementary Figure S9). The dysregulated genes were associated with both large and small ribosomal subunits involved in cytoplasmic translation (Supplementary Figures S9, S10). Subsequently, RNA sequencing data were further filtered for abs (log2FC) > 1 and annotated with GO terms from *Drosophila melanogaster*. The genes were sorted in a Venn diagram according to three main categories: reproduction (714 genes), immunity and Inflammation (346 genes), and metabolism (1733 genes) (Figure 8 and Supplementary Table S3). Among the genes in the common category, *death regulator Nedd2-like caspase* (*dronc*), and *death-associated inhibitor of apoptosis 1* (*diap1*) were dysregulated. These genes have previously been linked to impaired apoptotic machinery during spermatid individualization (Huh et al., 2004). Data analysis also revealed altered expressions of a number of genes known from previous studies to be involved in male fertility, including *sperm-specific dynein intermediate chain 4* (*sdic4*), a dynein gene essential for sperm tail motorization (Yeh et al., 2012).

Discussion

We have demonstrated that the *cnt1* gene, which is almost entirely expressed in the testis, is required for male fertility in *Drosophila*. We created a mutation in *cnt1* through targeted mutagenesis. The mutant showed alterations in reproductive behavior and defects in sperm maturation. Consequently, our characterization of the transcriptional responses to the *cnt1* mutation revealed changes in the expression of key genes that were previously reported to play a role in the above-mentioned aspects of male fertility.

Mating behavior

Our data indicate that male fertility caused by the *cnt1* mutation is partly due to a behavioral defect involving a short copulation duration. Previous reports have shown that the duration of copulation in *Drosophila* is primarily controlled by males (MacBean and Parsons, 1967; Lee and Hall, 2001; Acebes et al., 2004), with a considerable period to ensure successful sperm transfer beginning 5 minutes after copulation (Gilchrist and Partridge, 2000; Crickmore and Vosshall, 2013). Abnormal copulation duration has been found in a number of mutants, including null mutants of the clock genes *period* and *timeless* (Beaver and Giebultowicz, 2004), and *fru* mutants (Lee et al., 2001). For example, *fru* mutation affect copulation by altering fru neurons. These neurons localized in the abdominal ganglion exhibit innervation at the SV, accessory gland, and end base of the testis. Interestingly, knocking down a subset of these neurons, called sAbg-1 using the *UAS*-tetanus toxin (TNT) resulted in shortened copulation duration (Jois et al., 2018).

We have previously shown that mutations in the *equilibrative nucleoside transporter 2* (*ent2*) or the *adenosine receptor* (*AdoR*) of *Drosophila* impair synaptic transmission and memory (Knight et al., 2010). Therefore, we hypothesize that the $cnt1^{FD}$ induced loss of adenosine nucleoside transport in the testis may also impair adenosine signaling, thus affecting behavior (Leung et al., 2001). Accordingly, a recent study has shown that phosphodiesterase pde1, an enzyme that degrades cyclic AMP (a downstream signal of the adenosine receptor), causes male sterility and behavioral abnormalities that affect copulation in *Drosophila* (Morton et al., 2010). The adenosine pathway is known to cause neuromodulation in mammals and has been suggested to influence sex-dependent neuropsychiatric behavior

and erection in humans (Phatarpekar et al., 2010; Osborne et al., 2018).

Sperm maturation

Our results further showed that the effects of the $cnt1^{FD}$ mutation are pleiotropic and include morphological changes during spermiogenesis, where spermatid maturation is defective. The most striking phenotype of the *cnt1* mutation is a higher number of spermatid groups and mature sperms (Figure 5). We also showed that the tail coiling of mature sperm groups was disorganized and tangled, which probably prevented them from moving to the SV, where the sperm count was low. The higher number of spermatid groups contrasts with the low number of mature sperms in the SV, suggesting that spermatids accumulate in the TE region.

Thus, *cnt1* appears to play an important role in regulating mechanical movements in maturing sperms, which reportedly depend on intact mitochondria and dynein proteins (Ranz et al., 2003; Yeh et al., 2012), the latter of which require high ATP concentrations for proper function (Xie et al., 2006). A previous study has shown that knockdown of ATP synthase results in male infertility and abnormal spermatogenesis in *Drosophila* testes (Yu et al., 2019). In addition, ATP synthase has been reported to affect the elongated shape of mitochondria when knocked out (Sawyer et al., 2017). This finding is consistent with our RNAseq data that shows the dysregulation of genes belonging to the mitochondrial respiratory chain (*ATP synthase-coupling factor 6* (*ATPsyn-Cf6*), *NADH dehydrogenase 75* (*ND-75*), *cytochrome-c1* (*cyt-c1*), and *cytochrome c distal* (*cyt-c-d*)), of which *cyt-c1* was confirmed by RT-qPCR to be downregulated in $cnt1^{FD}$ mutants (Supplementary Figure S8). In addition, previous studies have shown that mutations in dynein, such as *dic61B*, play a crucial role in sperm motility (Fatima, 2011). The dynein mutation in *dic61B* has been associated with impaired spermatid individualization and motility, which eventually led to male sterility. Furthermore, the *dic61B* mutation has also been reported to contribute to a defect in the formation of major and minor mitochondria derivatives (Fatima, 2011), supporting the idea that alterations in both dynein and mitochondria may also affect sperm axoneme movement in $cnt1^{FD}$ mutants. Among the dysregulated dynein genes in our RNAseq data, we found and confirmed that the gene-encoding sperm-specific dynein (*sdic4*) is upregulated in $cnt1^{FD}$ mutants. Taken together, mitochondria and dynein functions may be altered in $cnt1^{FD}$ mutants.

In addition, our data showed an increased number of waste bags, consistent with the observed high number of spermatid groups and low count of mature sperms in the TE region. Furthermore, these bags left a trail as they moved to the end of the spermatid tail, suggesting that the bags could not process their degradation properly. A similar phenotype to the $cnt1^{FD}$ mutant was previously observed in the *driceless* mutant and associated with unusual active caspase signaling (Huh et al., 2004). Further phenotypic analysis using electron microscopy confirmed that, similar to *driceless* mutants (Huh et al., 2004), the spermatid cysts in $cnt1^{FD}$ underwent partial individualization, with the spermatid cysts containing sheathed spermatids in a common cytoplasmic membrane, while the other spermatids have their own cytoplasmic membrane. These mutants also showed a defect in the cystic bulges with trailing edge (Huh et al., 2004). Consistently, our RNAseq data show a dysregulation of a key gene involved in the apoptotic machinery during spermatid individualization: *dcp1* (Huh et al., 2004). It was reported in connection with the failure of the individualization process, like the $cnt1^{FD}$ mutant, in which multiple cysts contained many single spermatid units with excess cytoplasm.

Drosophila cnt1 and *cnt2* are similar genes which most probably have the same biochemical function (nucleoside transport) but they differ by tissue specificity of expression. Their phenotypes seem to be quite independent. In our experiments, the removal of one copy of *cnt2* did not enhance the *cnt1* fertility phenotype the heteroallelic flies $cnt1^{FD}/Df(2R)$ *BSC271* (this deletion lacks both *cnt1* and *cnt2*) (Supplementary Figure S3).

Similar to *Drosophila*, the expressions of Cnt isoforms were detected in both human and rat testes, mainly in the Sertoli cells, which are essential for sperm nutrition (Klein et al., 2013; Hau et al., 2020). The pharmacological blockade of nucleoside transporters in Sertoli cells seems to interfere with the spermatid maturation process, suggesting that nucleoside transport may be important for providing the nucleosides essential for sperm maturation (Leung et al., 2001; Kato et al., 2005). Previous research in mice has shown the relationship between sperm motility and mitochondrial dysfunction (Cardullo and Baltz, 1991; Ruiz-Pesini et al., 1998). These findings argue for similarities in the regulation of spermatogenesis in *Drosophila* and mammals.

In summary, we show that *cnt1* has a pleiotropic effect on mating behavior, spermatid maturation, and spermatid mitochondrial morphology in *Drosophila*. It affects the transcription of several key genes known from previous reports to be involved in these phenotypes, including dynein, ATP synthases, and apoptotic genes. Further work is needed to understand the relationship of these *cnt1* phenotypes to adenosine signaling and related metabolic pathways.

Data availability statement

The datasets presented in this study can be found in online repositories. The names of the repository/repositories and accession number(s) can be found below: SRA data: PRJNA838856, https://www.ncbi.nlm.nih.gov/sra/PRJNA838856.

Author contributions

HOM conceived the project, performed the experiments, made the illustrations, and prepared the manuscript. LP performed the fertility assay and immunohistochemical staining. Y-HL generated the *cnt1::GFP* tagged flies. BC-HW and LR analyzed the RNAseq data. LK performed the phylogeny tree. LV and MR generated the mutants. HS performed the electron microscopy. MH performed the RNAseq. MZ supervised the project and manuscript preparation.

Funding

This work was supported by the European fund for regional development "Interreg Austria/Czech Republic" (REGGEN-ATCZ207) and the junior grant project GACR (19-13784Y to LK).

Acknowledgments

We thank Dr. Mihail Sarov (MPI-CBG) for providing us with the plasmids (tagging cassettes) used to generate the GFP tag (Sarov et al., 2016). We also acknowledge the core facility of the Laboratory of Electron Microscopy, Biology Centre CAS supported by MEYS CR (LM2015129 Czech-BioImaging) and ERDF (No. CZ.02.1.01/0.0/0.0/13_013/0001445). We thank Jitka Pflegerova for her technical assistance and for preparing the TEM samples.

Conflict of interest

The authors declare that the research was conducted in the absence of any commercial or financial relationships that could be construed as a potential conflict of interest.

Publisher's note

All claims expressed in this article are solely those of the authors and do not necessarily represent those of their affiliated organizations, or those of the publisher, the editors and the reviewers. Any product that may be evaluated in this article, or claim that may be made by its manufacturer, is not guaranteed or endorsed by the publisher.

Supplementary material

The Supplementary Material for this article can be found online at: https://www.frontiersin.org/articles/10.3389/fcell.2022.945572/full#supplementary-material

References

Acebes, A., Grosjean, Y., Everaerts, C., and Ferveur, J. F. (2004). Cholinergic control of synchronized seminal emissions in *Drosophila*. *Curr. Biol.* 14, 704–710. doi:10.1016/j.cub.2004.04.003

Alzyoud, E., Vedelek, V., Réthi-Nagy, Z., Lipinszki, Z., and Sinka, R. (2021). Microtubule organizing centers contain testis-specific γ-turc proteins in spermatids of *Drosophila*. *Front. Cell Dev. Biol.* 9, 727264. doi:10.3389/fcell.2021.727264

Augière, C., Lapart, J.-A., Duteyrat, J.-L., Cortier, E., Maire, C., Thomas, J., et al. (2019). salto/CG13164 is required for sperm head morphogenesis in *Drosophila*. *Mol. Biol. Cell* 30, 636–645. doi:10.1091/mbc.E18-07-0429

Bader, M., Arama, E., and Steller, H. (2010). A novel F-box protein is required for caspase activation during cellular remodeling in *Drosophila*. *Development* 137, 1679–1688. doi:10.1242/dev.050088

Baker, B. S., Taylor, B. J., and Hall, J. C. (2001). Are complex behaviors specified by dedicated regulatory genes? Reasoning from *Drosophila*. *Cell* 105, 13–24. doi:10.1016/S0092-8674(01)00293-8

Baptissart, M., Vega, A., Martinot, E., and Volle, D. H. (2013). Male fertility: Is spermiogenesis the critical step for answering biomedical issues? *Spermatogenesis* 3, e24114. doi:10.4161/spmg.24114

Batut, B., Hiltemann, S., Bagnacani, A., Baker, D., Bhardwaj, V., Blank, C., et al. (2018). Community-driven data analysis training for biology. *Cell Syst.* 6, 752–758.e1. doi:10.1016/j.cels.2018.05.012

Beaver, L. M., and Giebultowicz, J. M. (2004). Regulation of copulation duration by period and timeless in *Drosophila melanogaster*. *Curr. Biol.* 14, 1492–1497. doi:10.1016/j.cub.2004.08.022

Cardullo, R. A., and Baltz, J. M. (1991). Metabolic regulation in mammalian sperm: Mitochondrial volume determines sperm length and flagellar beat frequency. *Cell Motil. Cytoskelet.* 19, 180–188. doi:10.1002/cm.970190306

Chen, X., Hiller, M., Sancak, Y., and Fuller, M. T. (2005). Tissue-specific TAFs counteract polycomb to turn on terminal differentiation. *Science* 310, 869–872. doi:10.1126/science.1118101

Chintapalli, V. R., Wang, J., and Dow, J. A. T. (2007). Using FlyAtlas to identify better *Drosophila melanogaster* models of human disease. *Nat. Genet.* 39, 715–720. doi:10.1038/ng2049

Clark, K., Karsch-Mizrachi, I., Lipman, D. J., Ostell, J., and Sayers, E. W. (2016). GenBank. *Nucleic Acids Res.* 44, D67–D72. doi:10.1093/nar/gkv1276

Crickmore, M. A., and Vosshall, L. B. (2013). Opposing dopaminergic and GABAergic neurons control the duration and persistence of copulation in *Drosophila*. *Cell* 155, 881–893. doi:10.1016/j.cell.2013.09.055

Demarco, R. S., Eikenes, Å. H., Haglund, K., and Jones, D. L. (2014). Investigating spermatogenesis in *Drosophila melanogaster*. *Methods* 68, 218–227. doi:10.1016/j.ymeth.2014.04.020

Dos Santos-Rodrigues, A., Pereira, M. R., Brito, R., de Oliveira, N. A., and Paes-de-Carvalho, R. (2015). Adenosine transporters and receptors: Key elements for retinal function and neuroprotection. *Vitam. Horm.* 98, 487–523. doi:10.1016/bs.vh.2014.12.014

Edgar, R. C. (2004). MUSCLE: Multiple sequence alignment with high accuracy and high throughput. *Nucleic Acids Res.* 32, 1792–1797. doi:10.1093/nar/gkh340

Ejsmont, R. K., Ahlfeld, P., Pozniakovsky, A., Stewart, A. F., Tomancak, P., and Sarov, M. (2011). Recombination-mediated genetic engineering of large genomic DNA transgenes. *Methods Mol. Biol.* 772, 445–458. doi:10.1007/978-1-61779-228-1_26

Ejsmont, R. K., Sarov, M., Winkler, S., Lipinski, K. A., and Tomancak, P. (2009). A toolkit for high-throughput, cross-species gene engineering in *Drosophila*. *Nat. Methods* 6, 435–437. doi:10.1038/nmeth.1334

Fabian, L., and Brill, J. A. (2012). *Drosophila* spermiogenesis: Big things come from little packages. *Spermatogenesis* 2, 197–212. doi:10.4161/spmg.21798

Fatima, R. (2011). *Drosophila* Dynein intermediate chain gene, Dic61B, is required for spermatogenesis. *PLoS One* 6, e27822. doi:10.1371/journal.pone.0027822

Fleischmannova, J., Kucerova, L., Sandova, K., Steinbauerova, V., Broz, V., Simek, P., et al. (2012). Differential response of *Drosophila* cell lines to extracellular adenosine. *Insect biochem. Mol. Biol.* 42, 321–331. doi:10.1016/j.ibmb.2012.01.002

Gilchrist, A. S., and Partridge, L. (2000). Why it is difficult to model sperm displacement in *Drosophila melanogaster*: The relation between sperm transfer and copulation duration. *Evolution* 54, 534–542. doi:10.1111/j.0014-3820.2000.tb00056.x

Gray, J. H., Owen, R. P., and Giacomini, K. M. (2004). The concentrative nucleoside transporter family, SLC28. *Pflugers Arch.* 447, 728–734. doi:10.1007/s00424-003-1107-y

Groth, A. C., Fish, M., Nusse, R., and Calos, M. P. (2004). Construction of transgenic *Drosophila* by using the site-specific integrase from phage phiC31. *Genetics* 166, 1775–1782. doi:10.1534/genetics.166.4.1775

Guindon, S., Dufayard, J.-F., Lefort, V., Anisimova, M., Hordijk, W., and Gascuel, O. (2010). New algorithms and methods to estimate maximum-likelihood phylogenies: Assessing the performance of PhyML 3.0. *Syst. Biol.* 59, 307–321. doi:10.1093/sysbio/syq010

Hau, R. K., Miller, S. R., Wright, S. H., and Cherrington, N. J. (2020). Generation of a hTERT-immortalized human Sertoli cell model to study transporter dynamics at the blood-testis barrier. *Pharmaceutics* 12, E1005. doi:10.3390/pharmaceutics12111005

Huh, J. R., Vernooy, S. Y., Yu, H., Yan, N., Shi, Y., Guo, M., et al. (2004). Multiple apoptotic caspase cascades are required in nonapoptotic roles for *Drosophila* spermatid individualization. *PLoS Biol.* 2, E15. doi:10.1371/journal.pbio.0020015

Jayaramaiah Raja, S., and Renkawitz-Pohl, R. (2005). Replacement by *Drosophila melanogaster* protamines and Mst77F of histones during chromatin condensation in late spermatids and role of sesame in the removal of these proteins from the male pronucleus. *Mol. Cell. Biol.* 25, 6165–6177. doi:10.1128/MCB.25.14.6165-6177.2005

Jois, S., Chan, Y. B., Fernandez, M. P., and Leung, A. K.-W. (2018). Characterization of the sexually dimorphic fruitless neurons that regulate copulation duration. *Front. Physiol.* 9, 780. doi:10.3389/fphys.2018.00780

Kato, R., Maeda, T., Akaike, T., and Tamai, I. (2005). Nucleoside transport at the blood-testis barrier studied with primary-cultured Sertoli cells. *J. Pharmacol. Exp. Ther.* 312, 601–608. doi:10.1124/jpet.104.073387

Klein, D. M., Evans, K. K., Hardwick, R. N., Dantzler, W. H., Wright, S. H., and Cherrington, N. J. (2013). Basolateral uptake of nucleosides by Sertoli cells is mediated primarily by equilibrative nucleoside transporter 1. *J. Pharmacol. Exp. Ther.* 346, 121–129. doi:10.1124/jpet.113.203265

Klein, D. M., Harding, M. C., Crowther, M. K., and Cherrington, N. J. (2017). Localization of nucleoside transporters in rat epididymis. *J. Biochem. Mol. Toxicol.* 31, e21911. doi:10.1002/jbt.21911

Knight, D., Harvey, P. J., Iliadi, K. G., Klose, M. K., Iliadi, N., Dolezelova, E., et al. (2010). Equilibrative nucleoside transporter 2 regulates associative learning and synaptic function in *Drosophila*. *J. Neurosci.* 30, 5047–5057. doi:10.1523/JNEUROSCI.6241-09.2010

Kondo, S., and Ueda, R. (2013). Highly improved gene targeting by germline-specific Cas9 expression in *Drosophila*. *Genetics* 195, 715–721. doi:10.1534/genetics.113.156737

Kumar, S., Stecher, G., Li, M., Knyaz, C., and Tamura, K. (2018). MEGA X: Molecular evolutionary genetics analysis across computing platforms. *Mol. Biol. Evol.* 35, 1547–1549. doi:10.1093/molbev/msy096

Larkin, A., Marygold, S. J., Antonazzo, G., Attrill, H., dos Santos, G., Garapati, P. V., et al. (2021). FlyBase: Updates to the *Drosophila melanogaster* knowledge base. *Nucleic Acids Res.* 49, D899–D907. doi:10.1093/nar/gkaa1026

Leatherman, J. L., and Dinardo, S. (2008). Zfh-1 controls somatic stem cell self-renewal in the *Drosophila* testis and nonautonomously influences germline stem cell self-renewal. *Cell Stem Cell* 3, 44–54. doi:10.1016/j.stem.2008.05.001

Lee, G., and Hall, J. C. (2001). Abnormalities of male-specific FRU protein and serotonin expression in the CNS of fruitless mutants in *Drosophila*. *J. Neurosci.* 21, 513–526. doi:10.1523/JNEUROSCI.21-02-00513.2001

Lee, G., Villella, A., Taylor, B. J., and Hall, J. C. (2001). New reproductive anomalies in fruitless-mutant *Drosophila* males: Extreme lengthening of mating durations and infertility correlated with defective serotonergic innervation of reproductive organs. *J. Neurobiol.* 47, 121–149. doi:10.1002/neu.1021

Lefort, V., Longueville, J.-E., and Gascuel, O. (2017). SMS: Smart model selection in PhyML. *Mol. Biol. Evol.* 34, 2422–2424. doi:10.1093/molbev/msx149

Leung, G. P., Ward, J. L., Wong, P. Y., and Tse, C. M. (2001). Characterization of nucleoside transport systems in cultured rat epididymal epithelium. *Am. J. Physiol. Cell Physiol.* 280, C1076–C1082. doi:10.1152/ajpcell.2001.280.5.C1076

Lin, Y.-H., Maaroufi, H. O., Ibrahim, E., Kucerova, L., and Zurovec, M. (2019). Expression of human mutant huntingtin protein in *Drosophila* hemocytes impairs immune responses. *Front. Immunol.* 10, 2405. doi:10.3389/fimmu.2019.02405

Lin, Y.-H., Maaroufi, H. O., Kucerova, L., Rouhova, L., Filip, T., and Zurovec, M. (2021). Adenosine receptor and its downstream targets, mod(mdg4) and Hsp70, work as a signaling pathway modulating cytotoxic damage in *Drosophila*. *Front. Cell Dev. Biol.* 9, 651367. doi:10.3389/fcell.2021.651367

Lindsley, D. I., and Tokuyasu, K. T. (1980). "Spermatogenesis," in *Genetics and Biology of Drosophila* (New York: Academic Press), 225–294.

Lotti, F., and Maggi, M. (2018). Sexual dysfunction and male infertility. *Nat. Rev. Urol.* 15, 287–307. doi:10.1038/nrurol.2018.20

MacBean, I. T., and Parsons, P. A. (1967). Directional selection for duration of copulation in *Drosophila melanogaster*. *Genetics* 56, 233–239. doi:10.1093/genetics/56.2.233

Machado, J., Abdulla, P., Hanna, W. J. B., Hilliker, A. J., and Coe, I. R. (2007). Genomic analysis of nucleoside transporters in Diptera and functional characterization of DmENT2, a *Drosophila* equilibrative nucleoside transporter. *Physiol. Genomics* 28, 337–347. doi:10.1152/physiolgenomics.00087.2006

Masino, S., and Boison, D. (2013). *Adenosine: A key link between metabolism and brain activity*. New York, NY: Springer. doi:10.1007/978-1-4614-3903-5

Molina-Arcas, M., and Pastor-Anglada, M. (2013). Nucleoside transporters (SLC28 and SLC29) family. *Pharmacogenomics of Human Drug Transporters.* 11, 243–270. doi:10.1002/9781118353240.ch11

Morton, D. B., Clemens-Grisham, R., Hazelett, D. J., and Vermehren-Schmaedick, A. (2010). Infertility and male mating behavior deficits associated with Pde1c in *Drosophila melanogaster*. *Genetics* 186, 159–165. doi:10.1534/genetics.110.118018

Nagarkar-Jaiswal, S., Lee, P.-T., Campbell, M. E., Chen, K., Anguiano-Zarate, S., Cantu Gutierrez, M., et al. (2015). A library of MiMICs allows tagging of genes and reversible, spatial and temporal knockdown of proteins in *Drosophila*. *Elife* 4, e05338. doi:10.7554/eLife.05338

Ng, C. L., Qian, Y., and Schulz, C. (2019). Notch and Delta are required for survival of the germline stem cell lineage in testes of *Drosophila melanogaster*. *PLoS One* 14, e0222471. doi:10.1371/journal.pone.0222471

Noguchi, T., Koizumi, M., and Hayashi, S. (2011). Sustained elongation of sperm tail promoted by local remodeling of giant mitochondria in *Drosophila*. *Curr. Biol.* 21, 805–814. doi:10.1016/j.cub.2011.04.016

Noguchi, T., and Miller, K. G. (2003). A role of actin dynamics in individualization during spermatogenesis in *Drosophila melanogaster*. *Development* 130, 1805–1816. doi:10.1242/dev.00406

Osborne, D. M., Sandau, U. S., Jones, A. T., Vander Velden, J. W., Weingarten, A. M., Etesami, N., et al. (2018). Developmental role of adenosine kinase for the expression of sex-dependent neuropsychiatric behavior. *Neuropharmacology* 141, 89–97. doi:10.1016/j.neuropharm.2018.08.025

Pavlou, H. J., and Goodwin, S. F. (2013). Courtship behavior in *Drosophila melanogaster*: Towards a 'courtship connectome. *Curr. Opin. Neurobiol.* 23, 76–83. doi:10.1016/j.conb.2012.09.002

Pérez-Torras, S., Mata-Ventosa, A., Drögemöller, B., Tarailo-Graovac, M., Meijer, J., Meinsma, R., et al. (2019). Deficiency of perforin and hCNT1, a novel inborn error of pyrimidine metabolism, associated with a rapidly developing lethal phenotype due to multi-organ failure. *Biochim. Biophys. Acta. Mol. Basis Dis.* 1865, 1182–1191. doi:10.1016/j.bbadis.2019.01.013

Phatarpekar, P. V., Wen, J., and Xia, Y. (2010). Role of adenosine signaling in penile erection and erectile disorders. *J. Sex. Med.* 7, 3553–3564. doi:10.1111/j.1743-6109.2009.01555.x

Porter, M. E. (1996). Axonemal dyneins: Assembly, organization, and regulation. *Curr. Opin. Cell Biol.* 8, 10–17. doi:10.1016/S0955-0674(96)80042-1

Ranz, J. M., Ponce, A. R., Hartl, D. L., and Nurminsky, D. (2003). Origin and evolution of a new gene expressed in the *Drosophila* sperm axoneme. *Genetica* 118, 233–244. doi:10.1023/A:1024186516554

Resende, L. P. F., Boyle, M., Tran, D., Fellner, T., and Jones, D. L. (2013). Headcase promotes cell survival and niche maintenance in the *Drosophila* testis. *PLoS One* 8, e68026. doi:10.1371/journal.pone.0068026

Rideout, E. J., Billeter, J.-C., and Goodwin, S. F. (2007). The sex-determination genes fruitless and doublesex specify a neural substrate required for courtship song. *Curr. Biol.* 17, 1473–1478. doi:10.1016/j.cub.2007.07.047

Ruiz-Pesini, E., Diez, C., Lapeña, A. C., Pérez-Martos, A., Montoya, J., Alvarez, E., et al. (1998). Correlation of sperm motility with mitochondrial enzymatic activities. *Clin. Chem.* 44, 1616–1620. doi:10.1093/clinchem/44.8.1616

Santel, A., Blümer, N., Kämpfer, M., and Renkawitz-Pohl, R. (1998). Flagellar mitochondrial association of the male-specific Don Juan protein in *Drosophila* spermatozoa. *J. Cell Sci.* 111 (2), 3299–3309. doi:10.1242/jcs.111.22.3299

Santel, A., Winhauer, T., Blümer, N., and Renkawitz-Pohl, R. (1997). The *Drosophila* don juan (dj) gene encodes a novel sperm specific protein component characterized by an unusual domain of a repetitive amino acid motif. *Mech. Dev.* 64, 19–30. doi:10.1016/s0925-4773(97)00031-2

Sarov, M., Barz, C., Jambor, H., Hein, M. Y., Schmied, C., Suchold, D., et al. (2016). A genome-wide resource for the analysis of protein localisation in *Drosophila*. *Elife* 5, e12068. doi:10.7554/eLife.12068

Sawyer, E. M., Brunner, E. C., Hwang, Y., Ivey, L. E., Brown, O., Bannon, M., et al. (2017). Testis-specific ATP synthase peripheral stalk subunits required for tissue-specific mitochondrial morphogenesis in *Drosophila*. *BMC Cell Biol.* 18, 16. doi:10.1186/s12860-017-0132-1

Schneider, C. A., Rasband, W. S., and Eliceiri, K. W. (2012). NIH image to ImageJ: 25 years of image analysis. *Nat. Methods* 9, 671–675. doi:10.1038/nmeth.2089

Siegel, R. W., and Hall, J. C. (1979). Conditioned responses in courtship behavior of normal and mutant *Drosophila*. *Proc. Natl. Acad. Sci. U. S. A.* 76, 3430–3434. doi:10.1073/pnas.76.7.3430

Soulavie, F., Piepenbrock, D., Thomas, J., Vieillard, J., Duteyrat, J.-L., Cortier, E., et al. (2014). Hemingway is required for sperm flagella assembly and ciliary motility in *Drosophila*. *Mol. Biol. Cell* 25, 1276–1286. doi:10.1091/mbc.e13-10-0616

Steinhauer, J. (2015). Separating from the pack: Molecular mechanisms of *Drosophila* spermatid individualization. *Spermatogenesis* 5, e1041345. doi:10.1080/21565562.2015.1041345

Tokuyasu, K. T. (1975). Dynamics of spermiogenesis in *Drosophila melanogaster*. VI. Significance of "onion" nebenkern formation. *J. Ultrastruct. Res.* 53, 93–112. doi:10.1016/S0022-5320(75)80089-X

Vedelek, V., Bodai, L., Grézal, G., Kovács, B., Boros, I. M., Laurinyecz, B., et al. (2018). Analysis of *Drosophila melanogaster* testis transcriptome. *BMC Genomics* 19, 697. doi:10.1186/s12864-018-5085-z

Wakimoto, B. T., Lindsley, D. L., and Herrera, C. (2004). Toward a comprehensive genetic analysis of male fertility in *Drosophila melanogaster*. *Genetics* 167, 207–216. doi:10.1534/genetics.167.1.207

White-Cooper, H. (2004). Spermatogenesis: Analysis of meiosis and morphogenesis. *Methods Mol. Biol.* 247, 45–75. doi:10.1385/1-59259-665-7:45

Witt, E., Benjamin, S., Svetec, N., and Zhao, L. (2019). Testis single-cell RNA-seq reveals the dynamics of de novo gene transcription and germline mutational bias in *Drosophila*. *Elife* 8, e47138. doi:10.7554/eLife.47138

Xie, P., Dou, S.-X., and Wang, P.-Y. (2006). Model for unidirectional movement of axonemal and cytoplasmic dynein molecules. *Acta Biochim. Biophys. Sin.* 38, 711–724. doi:10.1111/j.1745-7270.2006.00223.x

Yeh, S.-D., Do, T., Abbassi, M., and Ranz, J. M. (2012). Functional relevance of the newly evolved sperm dynein intermediate chain multigene family in *Drosophila melanogaster* males. *Commun. Integr. Biol.* 5, 462–465. doi:10.4161/cib.21136

Young, J. D. (2016). The SLC28 (CNT) and SLC29 (ENT) nucleoside transporter families: A 30-year collaborative odyssey. *Biochem. Soc. Trans.* 44, 869–876. doi:10.1042/BST20160038

Young, J. D., Yao, S. Y. M., Baldwin, J. M., Cass, C. E., and Baldwin, S. A. (2013). The human concentrative and equilibrative nucleoside transporter families, SLC28 and SLC29. *Mol. Asp. Med.* 34, 529–547. doi:10.1016/j.mam.2012.05.007

Yu, J., Chen, B., Zheng, B., Qiao, C., Chen, X., Yan, Y., et al. (2019). ATP synthase is required for male fertility and germ cell maturation in *Drosophila* testes. *Mol. Med. Rep.* 19, 1561–1570. doi:10.3892/mmr.2019.9834

Yuan, X., Zheng, H., Su, Y., Guo, P., Zhang, X., Zhao, Q., et al. (2019). *Drosophila* Pif1A is essential for spermatogenesis and is the homolog of human CCDC157, a gene associated with idiopathic NOA. *Cell Death Dis.* 10, 125. doi:10.1038/s41419-019-1398-3

Zhang, S. D., and Odenwald, W. F. (1995). Misexpression of the white (w) gene triggers male-male courtship in *Drosophila*. *Proc. Natl. Acad. Sci. U. S. A.* 92, 5525–5529. doi:10.1073/pnas.92.12.5525

Zhao, J., Klyne, G., Benson, E., Gudmannsdottir, E., White-Cooper, H., and Shotton, D. (2010). FlyTED: The *Drosophila* testis gene expression database. *Nucleic Acids Res.* 38, D710–D715. doi:10.1093/nar/gkp1006

Ziegler, A. B., Berthelot-Grosjean, M., and Grosjean, Y. (2013). The smell of love in *Drosophila*. *Front. Physiol.* 4, 72. doi:10.3389/fphys.2013.00072

Supplementary Material

Species name	Accession number	gene	Protein sequence
1. D.melanogaster	_A1Z7N3	CNT1	----------MAEPIEGEQEEKPP----------PSRAKRITYLVLHVLLHIIFISYFTAATIIF
2. D.erecta	_B3N816	CNT1	----------MADPQGGELEEKPP----------PSRTERITYLVLHVLLHVIFISYFTAATIIF
3. D.yakuba	_B4P3W2	CNT1	----------MADPQVDELEENPP----------PSRAKRITYLVLHVLLHVIFISYFTAATIIF
4. D.sechellia	_B4HSE4	CNT1	----------MADPAEGELDEKPP----------PSRAQRITYVILHVLLHVVFISYFTAATIIF
5. D.simulans	_B4QGR1	CNT1	----------MADPAEGELDEKPP----------PSRAQRIIYVILHVLLHVVFISYFTAATIIF
6. D.ananassae	_B3MI82	CNT1	----------MAEPAPAEESEEKP----------KPRWRRILERVILIFIHLLFIAYFIAATVIY
7. D.willistoni	_B4MUJ0	CNT1	----------MDESANIEEKPEK----------PSRKKKFLILLLHVIFHLILISYFIATSVVY
8. D.guanche	_A0A3B0JGG2	CNT1	----------MEPLDPEEE----------PSKKRALPKLLLHIFFHILLISYFIAATVVY
9. D.persimilis	_B4GHY4	CNT1	----------MEPLEDEEV----------PSKKRKILLLLLHILFHILWISYFIAATVVY
10. D.ficusphila	_A0A1W4UJK1	CNT1	----------MDNLAPEQQNPEEKPP----------RSKARRIVYLILHVLFHFLFILYFVAATVSY
11. D.melanogaster	_Q7K4A1	CNT2	---MSAESSKGAINNGYELDHKELDIRDSEEFTEHPLDDTSEV------ANKKGYFEKNPKVARLVRISIYVLLHLCVVGYFSYAT--Y
12. D.erecta	_B3N817	CNT2	---MSAESSKGSINNGYELDHKELDIRDSEEFKEIPLENISEV------PNKRGYFEKNPKVARLVRISIYVFLHLFVVGYFSYAT--Y
13. D.yakuba	_B4P3W1	CNT2	---MSAESSKGALNNGYELDHKELDIRDSEEYKEFPLEDLSED------PNKKGYFEKNPKVARLVKISIYVLLHLCVVGYFSYAT--Y
14. D.sechellia	_B4HSE3	CNT2	---MSAESSKGAINNGYELDHKELDIRDSEEFKELPLDDTSDA------PNKKGYFEKNPKVARLVRISLYVLLHLCVVGYFSYAT--Y
15. D.simulans	_B4QGR0	CNT2	---MSAESSKGAINNGYELDHKELDIRDSEEFKELPLDDTSDA------PNKKGYFEKNPKVARLVRISIYVLLHLCVVGYFSYAT--Y
16. D.ananassae	_B3MI83	CNT2	---MTDTSSIGAINNGYETDHKELSIPETEQFKELPPIGSTEK------APKPSYWDNNPKVKRIVKISLYVFLHLVVVGYFSYAT--Y
17. D.willistoni	_B4N641	CNT2	-------MEKGAINNGFELDQKDLTNKNDDLYETDVPVEILTT------QNGDLAQDNKAKITKWIKTFLKYFIHIVVIGYFSYAA--Y
18. D.guanche	_A0A3B0JP57	CNT2	---MTTDTSKGAINNGYELDHSELDIASVEPFKEIPQDGL-ELNLPRKMEDEKGFFNQNPKIARIVRISLYILLHLVVVGYFSYAT--Y
19. D.persimilis	_B4GHY3	CNT2	---MTTDTAKDVINNGYELDHRELEIPNSEPFKEIPREDRNLPQQG---EDGKGFFYNNPKMGRIVKISVYILLHVVVVGYFSYAT--Y
20. D.ficusphila	_A0A1W4UZY5	CNT2	---MSEDSSKGAINNGYELDHKQLEIHDSEEFKELPLENIKEV------SKKGGYFDDNPKVARLVRISLYILLHLVVVGYFSYAT--Y
21. D.busckii	_A0A0M4ED23	CNT2	---MDSKTDAGAINNSYELDHTDLERAKKTDYENDNAQDQVDSAAVMEQE--------QSKLPRFVKIILYVILHGLVVAYFSYAT--Y
22. D.virilis	_B4LP54	CNT2	---MDSKTSTGAINNAYELDHTDVGRSNPESHKTDYQVDYIHDQGPMQNDGGMETQN-YKKLIRWIKIGFQIVLQIGIVGYFSYAT--Y
23. D.navojoa	_A0A484BVE4	CNT2	MDSMGDKDSMGVTNNAYELDHT--DLRRSNPEFNNKTDYQVDYSHDHDLSVDRRETQENSEINKWIKRGLHLILQIAIVGYFVYAT--Y
24. D.grimshawi	_B4J5F4	CNT2	------MDNKGTINNAFELDHTDYEDYTNDDGAIERDRREQE----------NQKWHRWLKIGLLLILHIAIVVYFSYAT--Y
25. D.mojavensis	_B4KLQ3	CNT2	---MGDKESMGVNNNAYELDHTDLGRSNPEFNKT---DYQVDYSHDHDLSVDRRETQENNEINKWIKRGLHLILQIAIVGYFAYAT--Y
26. S.lebanonensis	_XP_030385480.1	CNT	---MATQTSKGVSNNSYELDQDMDALEPPNPANNKTDFQLANMTEVWSDGKLDAIDQPESKYKRLVRRLLIFLIHVAVVGYFSYAT--Y
27. S.lebanonensis	_XP_030379959.1	CNT	----------MAEPVTETETEPEE----------ESPRKKLIKRILLIIFHILFISYFIWCTVVF
28. S.lebanonensis	_XP_030387255.1	CNT	----------MAKRDNEAQPVLEDETEPEE----------ENKAKRICKLVCLIVFHIVFIAYFIWCTVVY
29. M.domestica	_XP_005188662.1	CNT	----------MEDTKSGEINKAFSGDEILENGAETHKTDFQIEDITSNVKEHSKIKRIVMSSLVWLIHIVVGSYFGYAT-HY
30. M.domestica	_XP_011294508.1	CNT	------MIRYKKPKLLWNNELKLLGDNEKKTHV----------ENEAKPL----------
31. C.capitata	_XM_004526264.3:148-1959	CNT	----------METNGQKNTAFEVDDAVENYTAVDTEVQEIDAMESKAEHNRSNT-KRRIKKVARNTLKVGVHFVVGGYFAYAT--Y
32. L.cuprina	_XP_023292620.1	CNT	----------MEESKEGEINKAYNIDESLENGVENYKTEFQIAEFEDKEKKIKP-KTTLEIWTKRSLLFILHAAVGAYFGYAT--Y

Supplementary Figure 1. Alignment of Cnt1 and Cnt2 protein of *Drosophila* and *Sophophora* subgenus and subgroup. The alignment of the Cnt paralogs shows a marked difference in the first 20 amino acids.

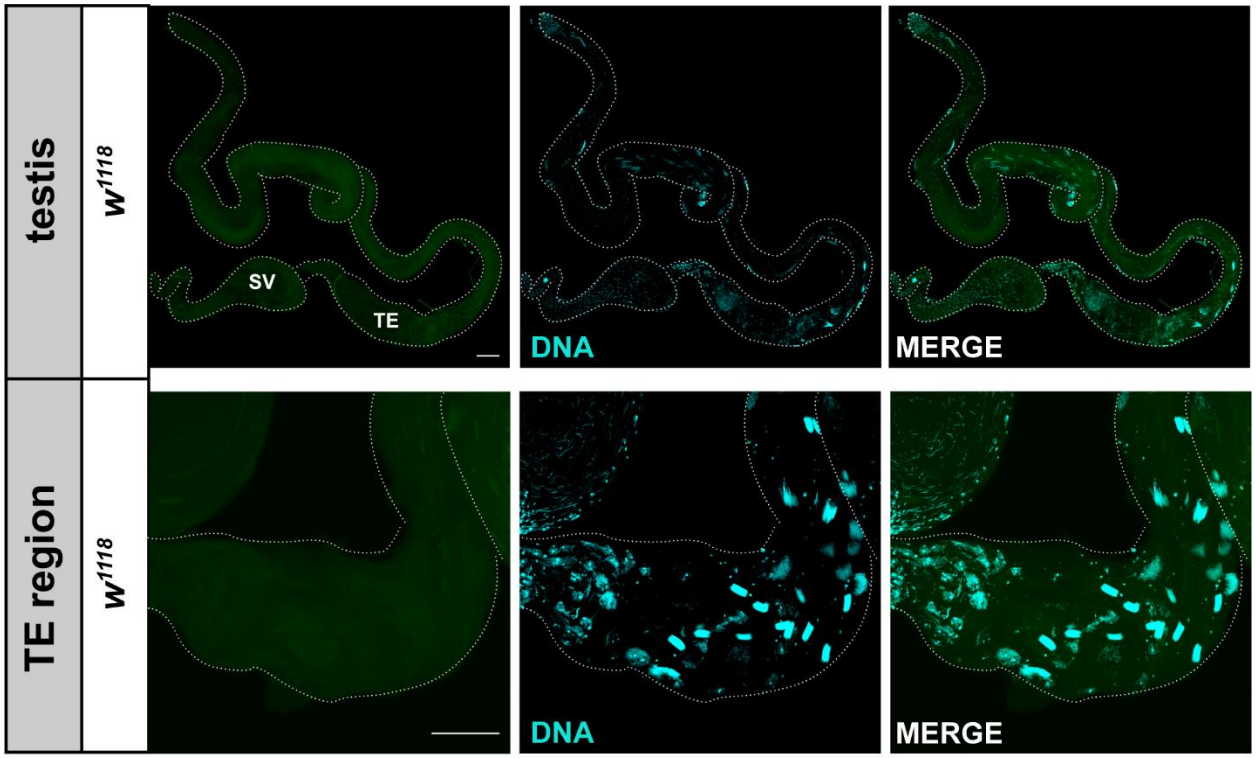

Supplementary Figure 2. Absence of GFP signaling in the w^{1118} fly strain. The figure shows the absence of GFP signal in the testis and its TE region. Scale bar: 40 µm; seminal vesicle (SV), terminal epithelium (TE).

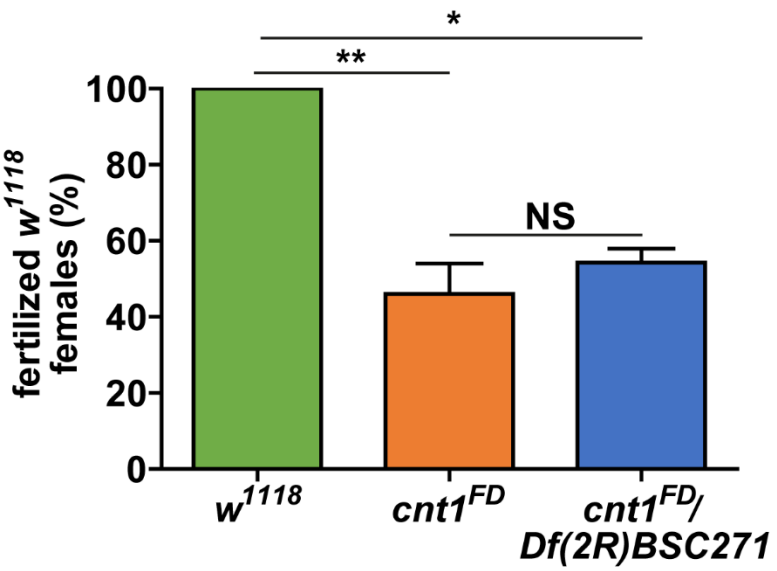

Supplementary Figure 3. The *cnt1* mutation causes partial sterility in *Drosophila* males. Naive mutant males ($cnt1^{FD}$) and control females (w^{1118}) were collected. After five to seven days, one male was placed in a vial with 10 females for 24 hours. Subsequently, each female was placed separately in a single vial, and the presence or absence of larvae was recorded. The chart shows the percentage of fertilized females after 24 hours of mating with $cnt1^{FD}$ males; n ≥6. Significance was analyzed by Kruskal–Wallis and labeled as follows: *P < 0.05, **P < 0.01, NS > 0.05. Error bars are presented as mean ± SEM.

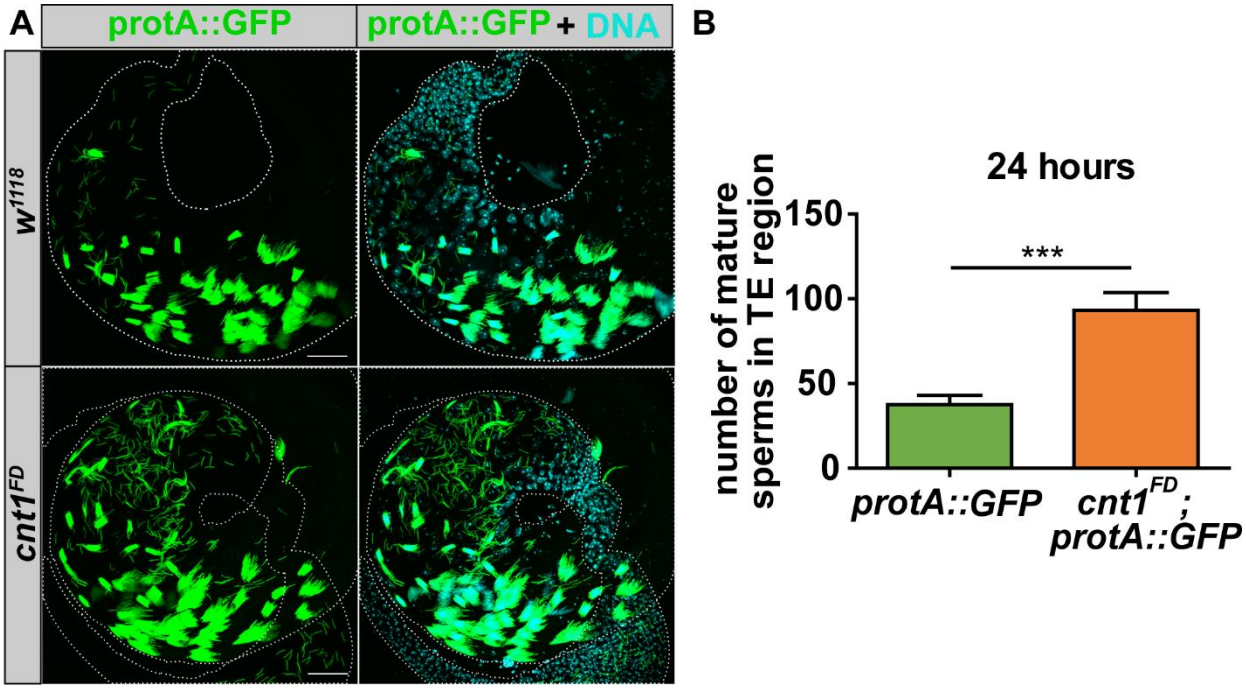

Supplementary Figure 4. The *cnt1* mutation increases the number of spermatid groups at an early age (24 hours old). **(A)** Microscopic observation of spermatids expressing protamine A signal in the TE region of the testis. w^{1118} is used as a control. In w^{1118}, the spermatid groups are localized at the beginning of the TE region whereas the $cnt1^{FD}$ mutants show that the spermatid groups are scattered along the TE region. Protamine A (green), DNA (cyan). Scale bar: 40 µm. **(B)** Number of mature sperms in the terminal epithelium region. Significance was analyzed with a one-tailed Student's t-test and labeled as follows: ***P < 0.001; n = 9. Error bars are shown as mean ± SEM.

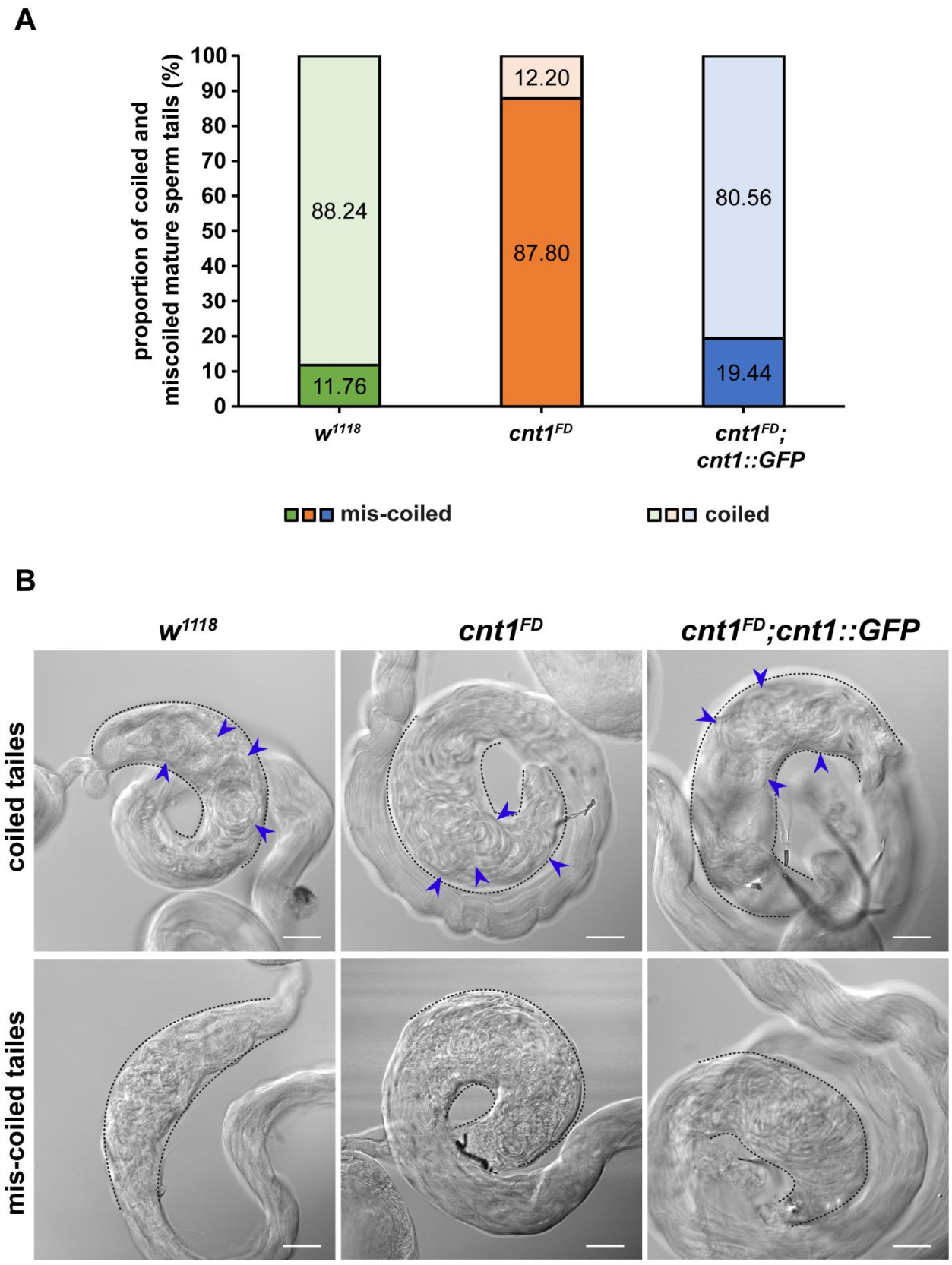
A
proportion of coiled and miscoiled mature sperm tails (%)
100
90
80
70
60
50
40
30
20
10
0
88.24
11.76
12.20
87.80
80.56
19.44
w1118
cnt1FD
cnt1FD; cnt1::GFP
mis-coiled
coiled
B
w1118
cnt1FD
cnt1FD;cnt1::GFP
coiled tailes
mis-coiled tailes

Supplementary Figure 5. The *cnt1* mutation causes a miscoiling of mature sperm groups. **(A)** Proportion of coiled and miscoiled mature sperm tails; n ≥34. **(B)** Microscopic observation of coiled and miscoiled mature sperm tails. The top panel shows an example of coiled tails in the TE region and the down panel shows the miscoiled tails in the TE region of in w^{1118}, $cnt1^{FD}$ and $cnt1^{FD}$;*cnt1::GFP* testis. The blue arrow points to the circular coiled tails. Scale bar: 40 µm.

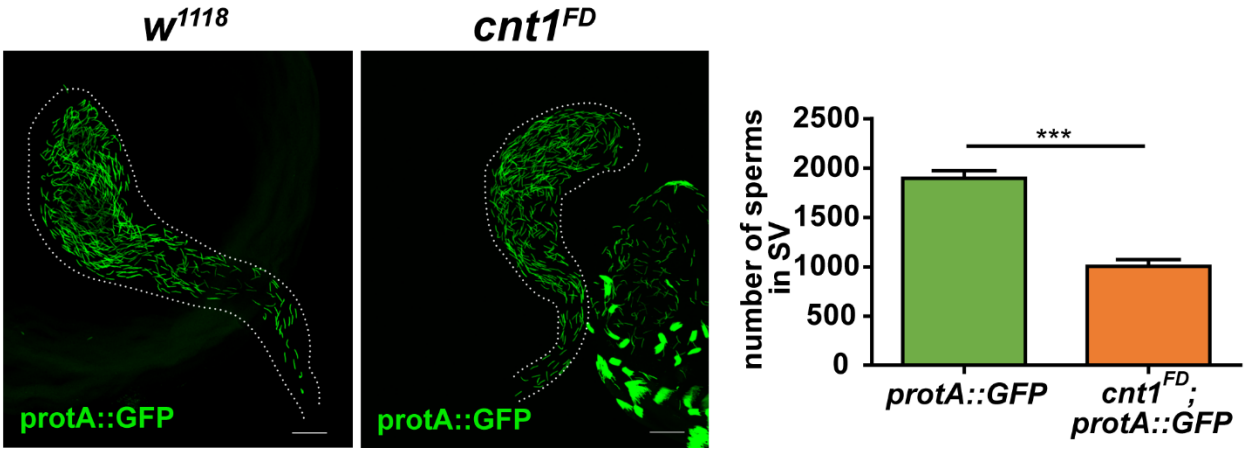

Supplementary Figure 6. *cnt1* mutation causes a defect in the movement of mature sperms toward the SV. **(A)** Microscopic observation of sperms in the SV expressing protamine A signal. Protamine A (green). Scale bar: 40 µm. **(B)** Number of sperms in the SV. Significance was analyzed using one-tailed Student's t-test and labeled as follows: ***P < 0.001; n ≥10. Error bars are shown as mean ± SEM.

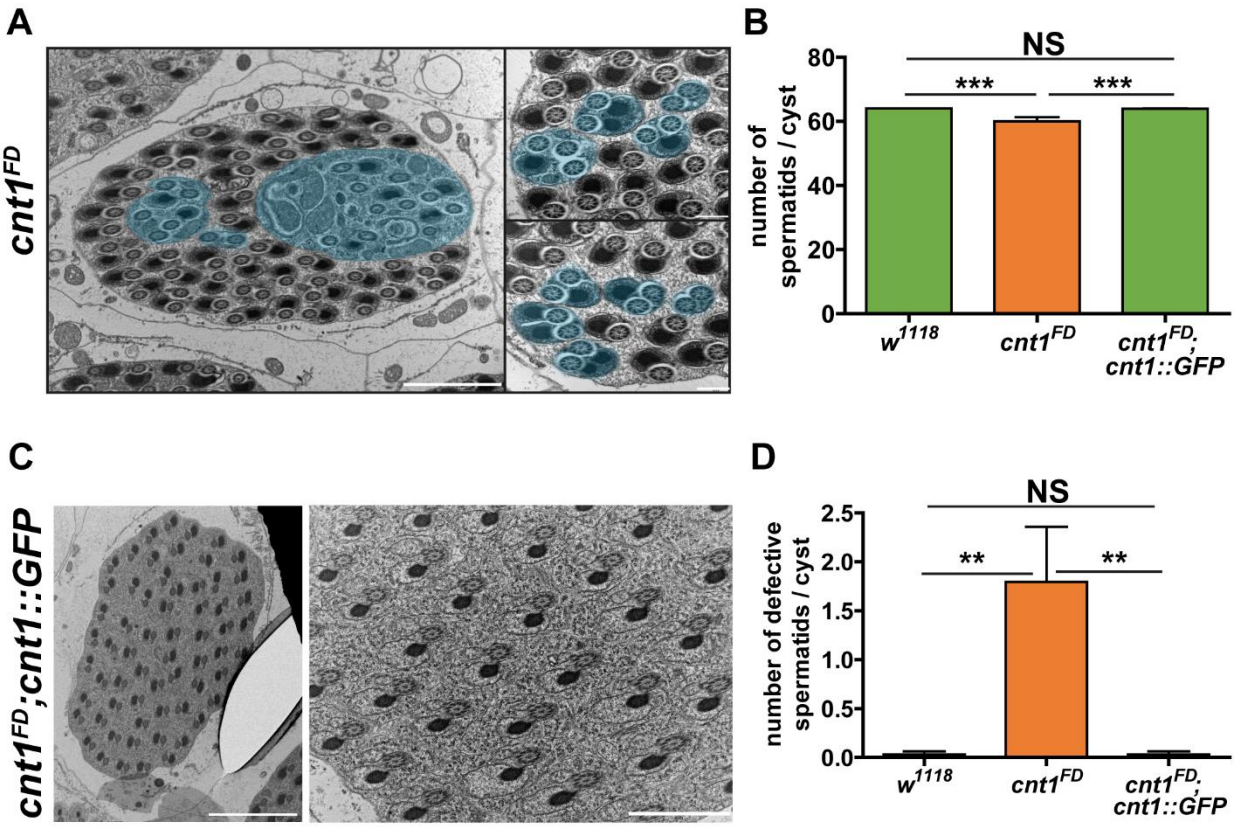

Supplementary Figure 7. *cnt1*^{FD} mutants exhibiting mitochondrial defects in spermatids. **(A)** Spermatid cysts of *cnt1*^{FD} mutants show either a lack of major mitochondria or a mitochondrial fusion of spermatids. Left panel, scale bar: 2 µm. Right panel, scale bar: 500 nm. **(B)** Number of spermatids per cyst. **(C)** Transversal section of *cnt1*^{FD}*;cnt1::GFP* mutant testes showing a cyst of elongating spermatids. Left panel, scale bar: 5 µm. Right panel, scale bar: 2 µm **(D)** Number of defective spermatids per cyst. **(B,D)**; n ≥ 32. Significance was analyzed by Kruskal–Wallis and labeled as follows: **P < 0.01, ***P < 0.001, NS > 0.05. Error bars are presented as mean ± SEM.

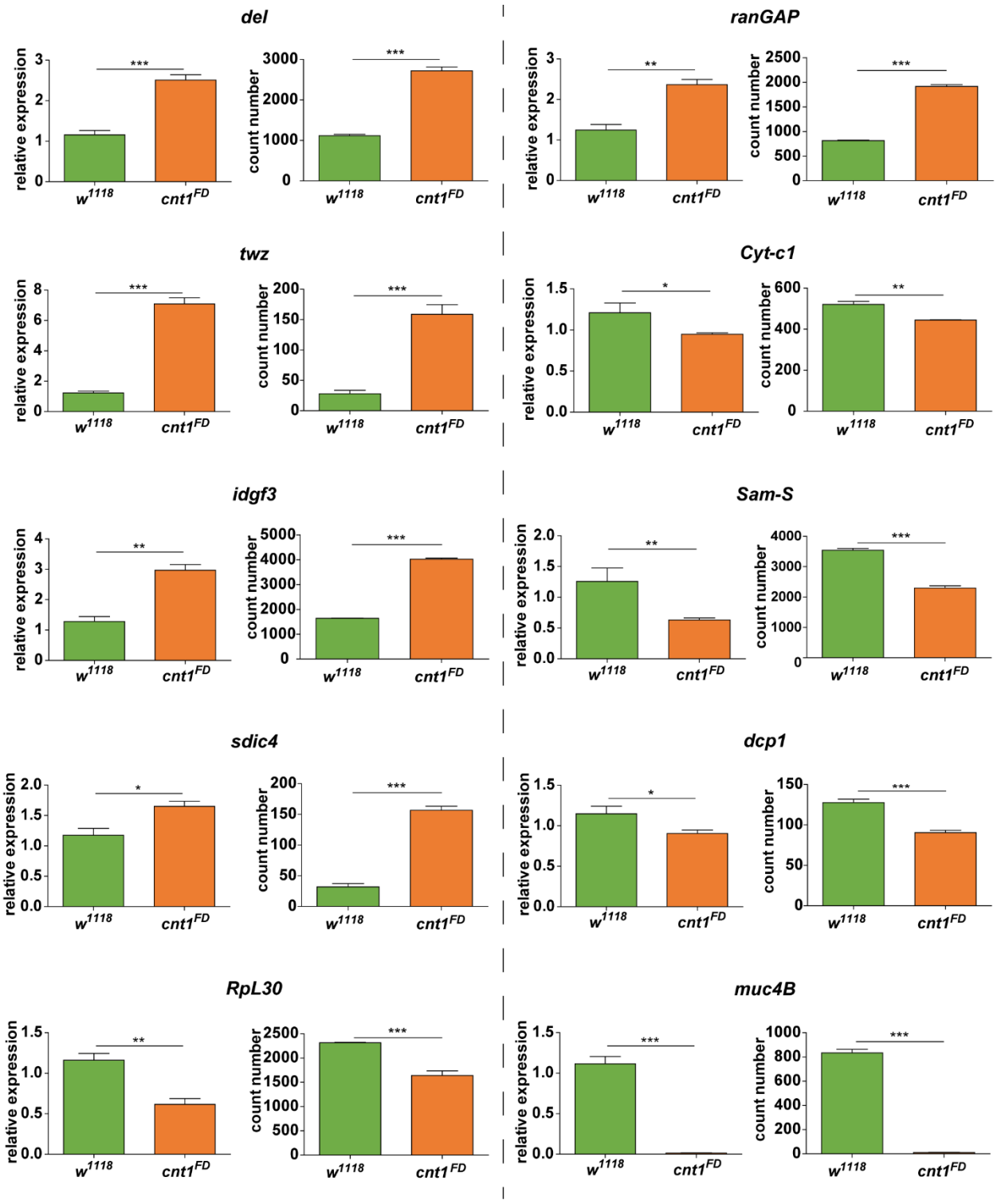

Supplementary Figure 8. Comparison of RNA sequencing and qPCR results for the transcription of 10 representative genes. The figure shows the plot of qPCR data (relative expression)on the left and the plot of RNAseq data (count number) on the right for the following genes: *del* (*deadlock*), *ranGAP* (*Ran GTPase activating protein*), *twz* (*tiwaz*), *Cyt-c1* (*Cytochrome c1*), idgf3 (*imaginal disc growth factor 3*), *Sam-S* (*S-*

adenosylmethionine synthetase), *sdic4* (*sperm-specific dynein intermediate chain 4*), *dcp1* (*death caspase 1*), *RpL30* (*ribosomal protein L30*) and *muc4B* (*mucin 4B*). Expressions were normalized to *αTub84B and act5C* transcripts (ΔΔCT). Significance was analyzed with a one-tailed Student's t-test and labeled as follows: *P < 0.05, **P < 0.01, ***P < 0.001; n = 3. Error bars are shown as mean ± SEM.

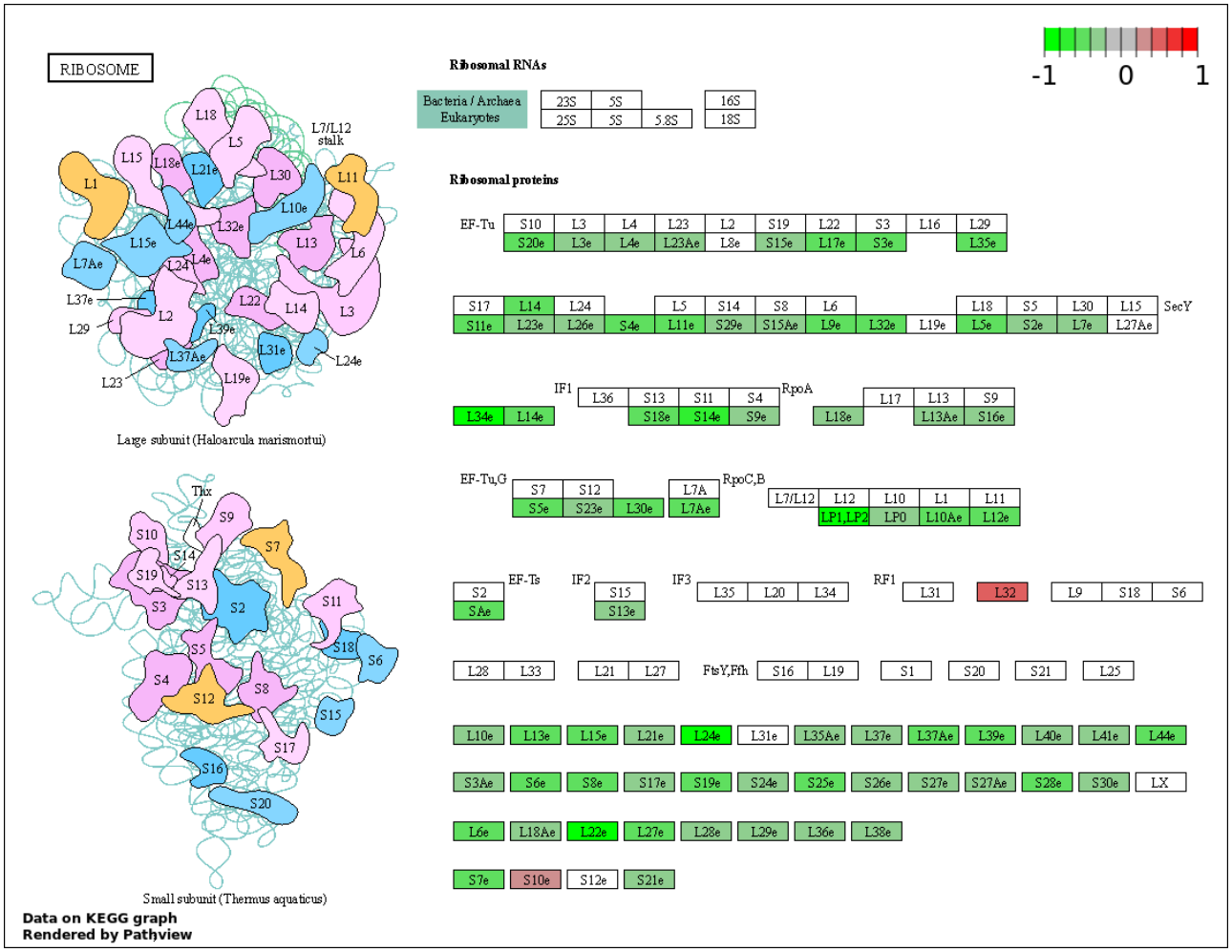

Supplementary Figure 9. KEGG ribosomal pathway: dme03010. Differential expression of ribosomal pathway genes. The figure shows up-regulated genes (red) and down-regulated genes (green).

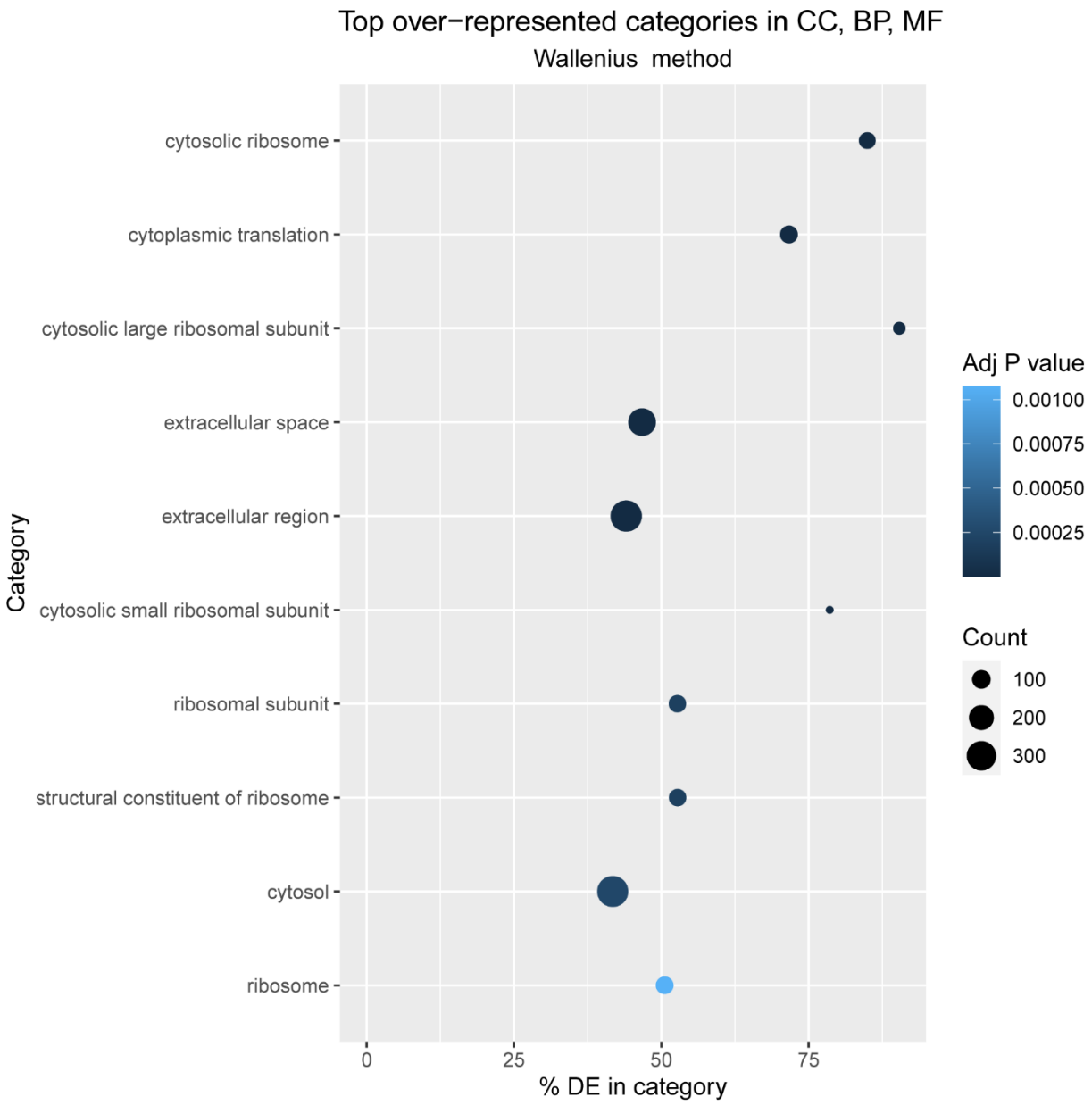

Supplementary Figure 10. A scatter plot of KEGG pathway enrichment statistics. The graph shows the top 10 over-represented GO terms. The x-axis shows the percentage of genes in the category identified as differentially expressed. Molecular Function - molecular activities of gene products (MF), Cellular Component - where gene products are active (CC), Biological Process - pathways and larger processes consisting of the activities of multiple gene products (BP).

Supplementary Table 1. List of used primers.

Supplementary Table 2. Results of the post-hoc tests in tabular form for all pairwise comparative analyses of three groups. Significance was established using parametric test: one-way ANOVA (combined with Tukey post-hoc test), or non-parametric test: Kruskal–Wallis (combined with comparisons of mean ranks of all pairs of groups post-hoc test).

Supplementary Table 3. List of the differentially expressed genes detected in *cnt1*^{FD} mutants compared with *w*^{1118}. The genes on the list are the differentially expressed genes based on the adj. P-value < 0.05. The highlighted genes in the Excel file belong to the discovered ribosomal pathway (the red ones are up-regulated, and the green ones are down-regulated). The table lists the genes in the following categories: immune system and inflammation, metabolism, and reproduction.

Table 1

	Primer sequence	
gene name	Forward	Reverse
Act5C	GTGCCCATCTACGAGGGTTA	TTGATGTCACGGACGATTTC
αTub84B	TCGAGCCCTACAACTCCATC	AATCAGACGGTTCAGGTTGG
cnt1	ACTTTACGGCAGCCACAATC	TTGGCTTAACCTCTGGCACT
sdic4	GGGTCAACGAGGTTTACGAA	TCCGGAGACGACAGAGAACT
Cyt-c1	CATGGCTTGAGATTGCTGAA	CTGCTCCAGGGCGTAGATAA
Sam-S	AATCAGCGACGCTATCTTGG	CAATGTGCTGCACTGTCTCA
del	GTGCACCAACTGATGATTCG	CTTGCGTCTGACCAACAGAA
ranGAP	GATTGGTGAGGGTCTGAAGC	TTCGGTCCTAAGGCATTGTC
twz	GTTCCGCCACATTCTGAACT	GCCACCAAATAGTTGCCATT
idgf3	GATCTGCTGCTCAGTCTCACC	TCGACGGGGCATCATAGTA
dcp1	CAAGGAGATCGTGGATTCGT	GGTGTTCAGTCGGTTGTTGA
muc4B	TGGAACCAGCTTGAACAATG	GCTGGCACTGTTGTTGATGT
RpL30	AGGCCAAACTGGTGCTCAT	TGCACACGCGGAAGTATTTA

Table 2

gene expression in male organs and female Tukey — Fig.2A

	reproductive organs	rest of the body	female
reproductive organs		0.013986	0.000190
rest of the body	0.013986		0.000192
female	0.000190	0.000192	

fertility assay (24h): Kruskal-Wallis — Fig.4B

	w1118	cnt1FD	cnt1FD;cnt1::GFP
w1118		0.040104	0.894157
cnt1FD	0.040104		0.001030
cnt1FD;cnt1::GFP	0.894157	0.001030	

copulation number: Kruskal-Wallis — Fig.4D

	w1118	cnt1FD	cnt1FD;cnt1::GFP
w1118		0.246833	1.000000
cnt1FD	0.246833		0.290041
cnt1FD;cnt1::GFP	1.000000	0.290041	

fertility assay (24h): Supplementary Fig. 3
Kruskal-Wallis

	w1118	cnt1FD	cnt1FD;cnt1::GFP
w1118		0.001935	0.043825
cnt1FD	0.001935		1.000000
cnt1FD/Df(2R)BSC271	0.043825	1.000000	

number of defective spermatids Supplementary Fig. 7D
Kruskal-Wallis

	w1118	cnt1FD	cnt1FD;cnt1::GFP
w1118		0.002420	1.000000
cnt1FD	0.002420		0.002420
cnt1FD;cnt1::GFP	1.000000	0.002420	

cnt1 expression in mutants Fig.3D
Tukey

	w1118	cnt1FD	cnt1FD;cnt1::GFP
w1118		0.000183	0.925695
cnt1FD	0.000183		0.000183
cnt1FD;cnt1::GFP	0.925695	0.000183	

fertility assay (48h): Fig.4C
Tukey

	w1118	cnt1FD	cnt1FD;cnt1::GFP
w1118		0.546384	0.780640
cnt1FD	0.546384		0.216237
cnt1FD;cnt1::GFP	0.780640	0.216237	

copulation length: Fig.4E
Kruskal-Wallis

	w1118	cnt1FD	cnt1FD;cnt1::GFP
w1118		0.000000	0.001000
cnt1FD	0.000000		0.015000
cnt1FD;cnt1::GFP	0.001000	0.015000	

number of spermatids/cyst Supplementary Fig. 7B
Kruskal-Wallis

	w1118	cnt1FD	cnt1FD;cnt1::GFP
w1118		0.000100	1.000000
cnt1FD	0.000100		0.000219
cnt1FD;cnt1::GFP	1.000000	0.000219	

Publication II

Yu-Hsien Lin, **Houda Ouns Maaroufi**, Lucie Kucerova, Lenka Rouhova, Tomas Filip, Michal Zurovec (2021). Adenosine signaling and its downstream target mod(mdg4) modify the pathogenic effects of polyglutamine in a *Drosophila* model of Huntington's disease. *Front. Cell Dev. Biol.* DOI: doi.org/10.3389/fcell.2021.651367

In this publication, we demonstrate the effects of the HTT mutation (mHTT) as a stressor on the Ado pathway, using *Drosophila* as a model organism (Q93). mHTT caused larval lethality associated with a decrease in Ado titer in hemolymph once expressed throughout the organism. We therefore hypothesised that the decrease in Ado levels was due to alterations in Ado metabolism or transport genes. Our results show that the expression of *adgf-A*, *adgf-D*, *ent1*, *ent2*, and *ent3* was decreased in the brain of Q93 larvae. Therefore, we genetically increased the metabolism of intracellular and extracellular Ado in flies by overexpressing *adgf-A* and *adenoK* in Q93 flies, which extended their lifespan in compared with Q93 flies. We also enhanced Ado signalling in Q93 flies by overexpressing *adoR* and caused a reduction of the lifespan of mHTT-expressing flies, in contrast to flies in which *adoR* was silenced. Furthermore, silencing *ent2* in Q93 flies reduced the lifespan of *Drosophila*, in contrast to overexpression of *ent2*. These results suggest that *adoR* and *ent2* are key regulators of mHTT effects and that the reduction of Ado in Q93 flies is a natural response to cytotoxic stress. We also identified new downstream targets of AdoR pathway, the modifier of mgd4 (Mod(mdg4)) and heat-shock protein 70 (Hsp70). Knock-down of *mod(mdg4)* and *adoR* suppressed the increased production of Hsp70 in Q93 flies involved in the response to various stress conditions. Overall, our data suggest that *ent2*, *adoR*, *mod(mdg4)*, and Hsp70 represent an important Ado pathway acting against cytotoxic stress.

frontiers in Cell and Developmental Biology

ORIGINAL RESEARCH
published: 12 March 2021
doi: 10.3389/fcell.2021.651367

Adenosine Receptor and Its Downstream Targets, Mod(mdg4) and Hsp70, Work as a Signaling Pathway Modulating Cytotoxic Damage in *Drosophila*

Yu-Hsien Lin[1,2†], Houda Ouns Maaroufi[1,2], Lucie Kucerova[1], Lenka Rouhova[1,2], Tomas Filip[1,2] and Michal Zurovec[1,2*]*

[1] Biology Centre of the Czech Academy of Sciences, Institute of Entomology, Ceske Budejovice, Czechia, [2] Faculty of Science, University of South Bohemia, Ceske Budejovice, Czechia

Adenosine (Ado) is an important signaling molecule involved in stress responses. Studies in mammalian models have shown that Ado regulates signaling mechanisms involved in "danger-sensing" and tissue-protection. Yet, little is known about the role of Ado signaling in *Drosophila*. In the present study, we observed lower extracellular Ado concentration and suppressed expression of Ado transporters in flies expressing mutant huntingtin protein (mHTT). We altered Ado signaling using genetic tools and found that the overexpression of Ado metabolic enzymes, as well as the suppression of Ado receptor (AdoR) and transporters (ENTs), were able to minimize mHTT-induced mortality. We also identified the downstream targets of the AdoR pathway, the modifier of mdg4 (Mod(mdg4)) and heat-shock protein 70 (Hsp70), which modulated the formation of mHTT aggregates. Finally, we showed that a decrease in Ado signaling affects other *Drosophila* stress reactions, including paraquat and heat-shock treatments. Our study provides important insights into how Ado regulates stress responses in *Drosophila*.

Keywords: heat-shock protein 70, modifier of mdg4, mutant huntingtin, cytotoxicity, neurodegeneration, equilibrative nucleoside transporter

OPEN ACCESS

Edited by:
Sameer Mohammad, King Abdullah International Medical Research Center (KAIMRC), Saudi Arabia

Reviewed by:
Rodrigo A. Cunha, University of Coimbra, Portugal
Pavel Hyršl, Masaryk University, Czechia

***Correspondence:**
Yu-Hsien Lin
r99632012@gmail.com
Michal Zurovec
zurovec@entu.cas.cz

†Present address:
Yu-Hsien Lin, Department of Plant Physiology, Swammerdam Institute for Life Sciences, University of Amsterdam, Amsterdam, Netherlands

Specialty section:
This article was submitted to Signaling, a section of the journal Frontiers in Cell and Developmental Biology

Received: *09 January 2021*
Accepted: *22 February 2021*
Published: *12 March 2021*

Citation:
Lin Y-H, Maaroufi HO, Kucerova L, Rouhova L, Filip T and Zurovec M (2021) Adenosine Receptor and Its Downstream Targets, Mod(mdg4) and Hsp70, Work as a Signaling Pathway Modulating Cytotoxic Damage in Drosophila. Front. Cell Dev. Biol. 9:651367. doi: 10.3389/fcell.2021.651367

INTRODUCTION

Tissue injury, ischemia, and inflammation activate organismal responses involved in the maintenance of tissue homeostasis. Such responses require precise coordination among the involved signaling pathways. Adenosine (Ado) represents one of the key signals contributing to the orchestration of cytoprotection, immune reactions, and regeneration, as well as balancing energy metabolism (Borea et al., 2016). Under normal conditions, the Ado concentration in blood is in the nanomolar range; however, under pathological circumstances the extracellular Ado (e-Ado) level may dramatically change (Moser et al., 1989). Ado has previously been considered a retaliatory metabolite, having general tissue protective effects. Prolonged adenosine signaling, however, can exacerbate tissue dysfunction in chronic diseases (Antonioli et al., 2019). As suggested for the nervous system in mammals, Ado seems to act as a high pass filter for injuries by sustaining viability with low insults and bolsters the loss of viability with more intense insults (Cunha, 2016).

Adenosine signaling is well-conserved among phyla. The concentration of Ado in the *Drosophila melanogaster* hemolymph is maintained in the nanomolar range, as in mammals, and increases dramatically in adenosine deaminase mutants or during infections (Dolezelova et al., 2005; Novakova and Dolezal, 2011). Unlike mammals, *D. melanogaster* contains only a single Ado receptor (AdoR) isoform (stimulating cAMP) and several proteins that have Ado metabolic and transport activities involved in the fine regulation of adenosine levels. *D. melanogaster* adenosine deaminase-related growth factors (ADGFs), which are related to human ADA2, together with adenosine kinase (AdenoK) are the major metabolic enzymes converting extra- and intra-cellular adenosine to inosine and AMP, respectively (Zurovec et al., 2002; Maier et al., 2005; Stenesen et al., 2013). The transport of Ado across the plasma membrane is mediated by three equilibrative and two concentrative nucleoside transporters (ENTs and CNTs, respectively) similar to their mammalian counterparts. Ado signaling in *Drosophila* has been reported to affect various physiological processes, including the regulation of synaptic plasticity in the brain, proliferation of gut stem cells, hemocyte differentiation, and metabolic adjustments during the immune response (Knight et al., 2010; Mondal et al., 2011; Bajgar et al., 2015; Xu et al., 2020).

The present study examined the role of *Drosophila* Ado signaling on cytotoxic stress and aimed to clarify the underlying mechanism. Earlier reports have shown that expression of the expanded polyglutamine domain from human mutant huntingtin protein (mHTT) induces cell death in both *Drosophila* neurons and hemocytes (Marsh et al., 2000; Lin et al., 2019). In our study, we confirmed the low-viability phenotype of mHTT-expressing larvae and observed that such larvae display a lower level of e-Ado in the hemolymph. Furthermore, we used genetic tools and altered the expression of genes involved in Ado metabolism and transport to find out whether changes in Ado signaling can modify the phenotype of mHTT-expressing flies. Finally, we uncovered a downstream mechanism of the *Drosophila* Ado pathway, namely *mod(mdg4)* and heat-shock protein 70 (Hsp70), which modify both the formation of mHTT aggregates and the stress response to heat-shock and paraquat treatments.

RESULTS

Decreased Hemolymph Ado Titer in mHTT-Expressing Larvae

To characterize the involvement of Ado signaling in the stress response, we used mHTT-expressing flies as a well-characterized genetic model for neurodegeneration and cytotoxic stress (Rosas-Arellano et al., 2018). We initially examined flies overexpressing normal exon 1 from human huntingtin (Q20 HTT), or its mutant pathogenic form (Q93 mHTT), driven by the ubiquitous *daughterless-Gal4* (*da-Gal4*) and pan-neuron driver (*elav-Gal4*). We observed that 100% of Q93-expressing larvae driven by *da-Gal4* died during the wandering stage. In contrast, those driven by *elav-Gal4* displayed no impact on larval development (**Supplementary Figure 1A**) but with a reduced adult eclosion rate (**Supplementary Figure 1B**) and lifespan (**Supplementary Figure 1C**). These results are consistent with previous observations (Song et al., 2013).

Measurement of the extracellular Ado (e-Ado) concentration in the hemolymph of Q93-expressing larvae (3rd instar) showed that its level was significantly lower compared to larvae expressing Q20 or control *da-GAL4* only (**Figure 1A**). Since e-Ado concentration may be associated with the level of extracellular ATP (e-ATP), we also examined its titer in larval hemolymph. However, as shown in **Figure 1B**, there was no significant difference in e-ATP levels between Q20, Q93, and control *da-GAL4* larvae.

We thus postulated that the lower level of e-Ado in Q93 larvae might be caused by changes in genes involved in Ado metabolism or transport. Therefore, we compared the expression of *adgf* genes (*adgf-a*, *adgf-c*, and *adgf-d*), adenosine kinase (*adenoK*), adenosine transporters (*ent1*, *ent2*, *ent3*, and *cnt2*), and *adoR* in the brains of Q93- and Q20-expressing larvae driven by *elav-Gal4* (**Figure 1C**). The results showed that the expression levels of *adgf-a* and *adgf-d*, as well as transporters *ent1*, *ent2*, and *ent3*, in the brain of Q93 larvae were significantly lower than in Q20 larvae. There was no difference in the expression of *cnt2* and *adoR* between Q93 and Q20 larvae.

Enhanced e-Ado Signaling Increased Mortality of mHTT Flies

To study the effect of e-Ado signaling on mHTT-induced cytotoxicity, we compared the survival of transgenic lines that co-express RNAi constructs of Ado metabolic, transport and receptor genes together with Q93 and Q20 driven by *elav-GAL4*. The results showed that knocking down *adgf-D*, *ent1*, *ent2*, and *adoR* resulted in a significantly increased eclosion rate (**Figure 1D**), and silencing *adgf-A* and *adenoK*, *ent1*, *ent2*, and *adoR* significantly extended the adult lifespan of mHTT-expressing flies (**Figure 1E**). Notably, the RNAi silencing of *ent2* and *adoR* extended the lifespan of mHTT-expressing flies to 30 and 40 days, respectively, which is about 1.5∼2 times longer than that of control *gfp*-RNAi-expressing mHTT flies. To ensure that the mortality of the Q93 flies was mainly caused by mHTT expression and not by the RNAi constructs, we examined the survival of flies co-expressing normal htt Q20 together with RNAi transgenes until all corresponding experimental flies (expressing Q93 together with RNAi constructs) died. We did not observe a significant effect for any of the RNAi transgenes on adult survival (**Supplementary Figure 2**).

It is generally assumed that gain- and loss-of-function manipulations of functionally important genes should lead to the opposite phenotypes. We therefore tested whether the overexpression of *adgf-A*, *adenoK*, *ent2*, and *adoR* would rescue mHTT phenotypes. As shown in **Figure 1F**, increasing either the intra- or extracellular Ado metabolism by overexpressing *adenoK* and *adgf-A* in Q93 flies extended their lifespan in comparison to control Q93 flies overexpressing GFP protein. In contrast, the overexpression of *ent2* and *adoR* significantly decreased the lifespan of mHTT-expressing flies. Therefore, the overexpression

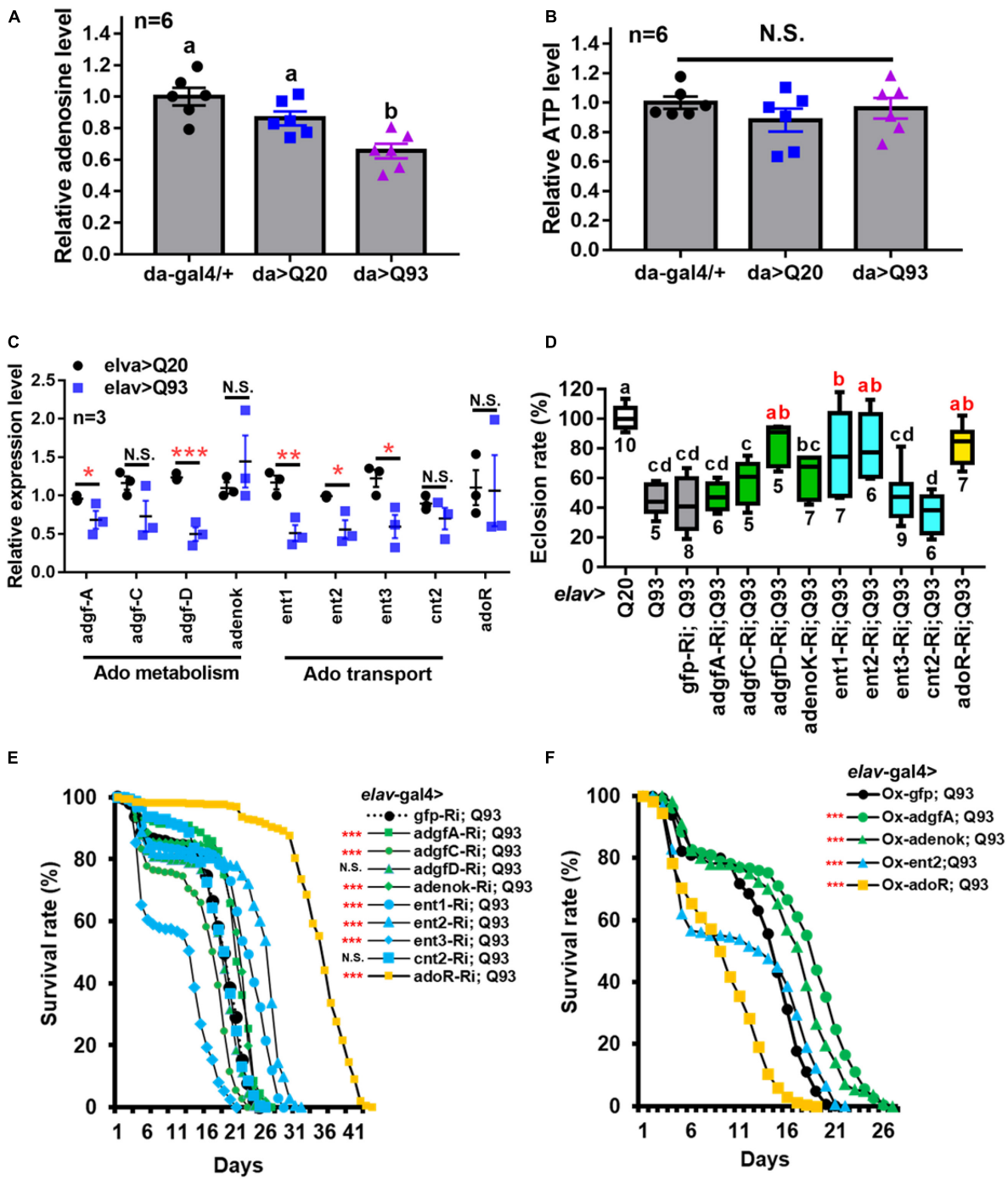

FIGURE 1 | Reduced extracellular Ado transport and receptor suppress mHTT induced lethality. **(A,B)** Relative level of extracellular Ado **(A)** and ATP **(B)** titers in Q93-expressing (da > Q93), Q20-expressing (da > Q20), and control *da*-GAL4 (da/+) larvae. Ado and ATP concentration are normalized to control larvae. Significance was analyzed by ANOVA; significant differences ($P < 0.05$) among treatment groups are marked with different letters; N.S., not significant; $n = 6$. Error bars are presented as mean ± SEM. **(C)** Transcription levels of genes involved in regulating Ado homeostasis in Q93-expressing (elav > Q93) and control Q20-expressing (elav > Q20) larval brains. Significance was analyzed by Student's *t*-test and labeled as follows: $^{*}P < 0.05$, $^{**}P < 0.01$, $^{***}P < 0.001$; N.S., not significant. $n = 3$. Error bars are presented as mean ± SEM. **(D)** Eclosion rate of mHTT-expressing adult females (elav > Q93) with RNAi silencing (Ri) Ado metabolic enzymes, transporters, *adoR*, and control *gfp*. Numbers below each column indicate the number of replicates (n). Significance was analyzed by ANOVA; significant differences ($P < 0.05$) among treatment groups are marked with different letters. **(E)** Survival of mHTT-expressing adult females (elav > Q93) with RNAi silencing (Ri) Ado metabolic enzymes, transporters, *adoR*, and control *gfp*. Significance was analyzed by weighted log-rank test; significant differences between each treatment group and control (*gfp*-Ri) are labeled as follows: $^{***}P < 0.001$; N.S., not significant. $n > 200$. **(F)** Survival of mHTT-expressing adult females (elav > Q93) overexpressing (Ox) Ado metabolic enzymes (*adgf-A* and *adenok*), transporters (*ent2*), *adoR*, and control *gfp*. Significance was analyzed by a weighted log-rank test; significant differences between each treatment group to control (*gfp*-Ri) are labeled as $^{***}P < 0.001$. $n > 200$.

of *adoR* and *ent2* genes resulted in a phenotype opposite to that observed in the knockdowns, thus supporting the importance of these genes as key regulators of mHTT phenotypes.

Knocking Down *ent2* and *adoR* Reduced Cell Death and mHTT Aggregate Formation

To determine whether the reduction of Ado signaling could affect other phenotypes of Q93 flies, we examined the effect of knocking down genes involved in Ado signaling and metabolism on *Drosophila* rhabdomere degeneration and mHTT aggregate formation. We expressed RNAi transgenes in the eyes of Q93 flies using the *gmr-GAL4* driver (Mugat et al., 2008; Kuo et al., 2013) and compared the levels of retinal pigment cell degeneration (**Figure 2A**). The results revealed that silencing Ado metabolic enzymes did not significantly influence the level of retinal pigment cell degeneration; however, retinal pigment cell degeneration was significantly reduced in *ent2* knockdown flies. Surprisingly we did not observe a significant rescue of cell death by silencing *adoR* (**Supplementary Figure 3**). We therefore assumed that it might be due to insufficient RNAi efficiency for suppressing AdoR signaling in the eye. To test this, we examined two combinations: mHTT-expressing flies with the adoR RNAi transgene under an adoR heterozygous mutant background ($AdoR^1/+$), and mHTT-expressing flies under an $AdoR^1$ homozygous mutant background. As shown in **Figure 2A**, both had significantly rescued retinal pigment cell degeneration, similar to that of *ent2* RNAi flies.

To examine the level of mHTT aggregate formation in the *Drosophila* brain, we drove the expression of transgenes using *elav-GAL4* and stained the brains with mHTT antibody (MW8), which exclusively stains mHTT inclusions (Ko et al., 2001). The results showed that mHTT inclusions were reduced to 50% in 10-day-old Q93 *adoR* RNAi flies (**Figures 2B,C**), with 20-day-old Q93 *adoR* RNAi flies exhibiting a similar level of suppression (**Supplementary Figure 4**). Our results demonstrate that decreased e-Ado signaling by either knocking down the transporter *ent2* or *adoR* has a strong influence on reducing mHTT-induced cell cytotoxicity and mHTT aggregate formation.

Epistatic Interaction of *adoR* and *ent2* on mHTT-Induced Mortality

The above results indicated that knockdown of *adoR*, *ent1*, or *ent2* expression significantly extended the adult longevity of mHTT files (**Figure 1E**). Therefore, we next tested whether there is a synergy between the effects of *adoR* and both transporters. First, we co-expressed *adoR* RNAi constructs with *ent1* RNAi in Q93-expressing flies. As shown in **Figure 3A**, the double knockdown of *ent1* and *adoR* shows a sum of individual effects on lifespan which is greater than the knockdown of *adoR* alone. There seems to be a synergy between *ent1* and *adoR*, suggesting that *ent1* may have its own effect which is partially independent from *adoR* signaling. In contrast, when we performed a double knockdown of *adoR* and *ent2* RNAi in Q93-expressing flies, the silencing of both had the same effect as silencing *adoR* only, indicating that they are involved in the same pathway.

Identification of Potential Downstream Targets of the AdoR Pathway

Our results indicate that *ent2* and *adoR* modify mHTT cytotoxicity and belong to the same pathway. To identify their potential downstream target genes, we compared the gene expression profiles of larvae carrying mutations in *adoR* or *ent2* as well as adult *adoR* mutants by using microarrays (Affymetrix). The data are presented as Venn diagrams, which show the intersection between differentially expressed genes for individual mutants in all three data sets, including six upregulated (**Figure 3B**) and seven downregulated mRNAs (**Figure 3C**). According to Flybase annotations[1], four of these genes were expressed in the nervous system (*ptp99A* was upregulated, while *CG6184*, *cindr*, and *mod(mdg4)* were downregulated) (**Supplementary Table 1**).

In order to examine the potential roles of these four genes in the interaction with mHTT, we co-expressed RNAi constructs of these candidate genes with mHTT and assessed the adult lifespan (**Figure 3D**). The results showed that only the knockdown of *mod(mdg4)* extended the lifespan of mHTT-expressing flies, and that the survival curve was not significantly different from that of *adoR* RNAi Q93 flies. Furthermore, *mod(mdg4)* RNAi was the only one of these constructs that significantly reduced retinal pigment cell degeneration (**Figure 3E**) and decreased the formation of mHTT inclusions (**Figures 3F,G**).

We next examined the possible epistatic relationship between *ent2*, *adoR*, and *mod(mdg4)* by combining the overexpression of *ent2* or *adoR* with *mod(mdg4)* RNAi in mHTT-expressing flies (**Figure 3H**). The results showed that the knockdown of *mod(mdg4)* RNAi was able to minimize the lethal effects caused by *ent2* and *adoR* overexpression in mHTT flies. This indicated that *mod(mdg4)* is a downstream target of the AdoR pathway. In addition, we found that increasing the e-Ado concentration by microinjecting Ado significantly increased *mod(mdg4)* expression in GAL4 control flies but not in the flies with *adoR* knockdown (**Figure 3I**). *mod(mdg4)* expression in the brain of mHTT Q93 larvae was lower than in control Q20 HTT larvae (**Figure 3J**). This result is consistent with a lower e-Ado level in Q93 mHTT larvae (**Figure 1A**).

Taken together, our results demonstrate that *mod(mdg4)* serves as a major downstream target of the AdoR pathway, modulating the process of mHTT inclusion formation and mHTT-induced cytotoxicity.

AdoR Pathway With Mod(mdg4) as Regulators of Hsp70 Protein Production

Earlier studies on *Drosophila* protein two-hybrid screening have indicated that Mod(mdg4) is able to interact with six proteins from the Hsp70 family (Giot et al., 2003; Oughtred et al., 2019). In addition, Hsp70 family proteins are known to contribute to suppressing mHTT aggregate formation (Warrick et al., 1999; Chan et al., 2000). In the present study, we compared the levels of Hsp70 protein in *adoR* and *mod(mdg4)* RNAi flies (**Figures 4A,B** and **Supplementary Figure 5**); the results showed that both

[1]http://flybase.org

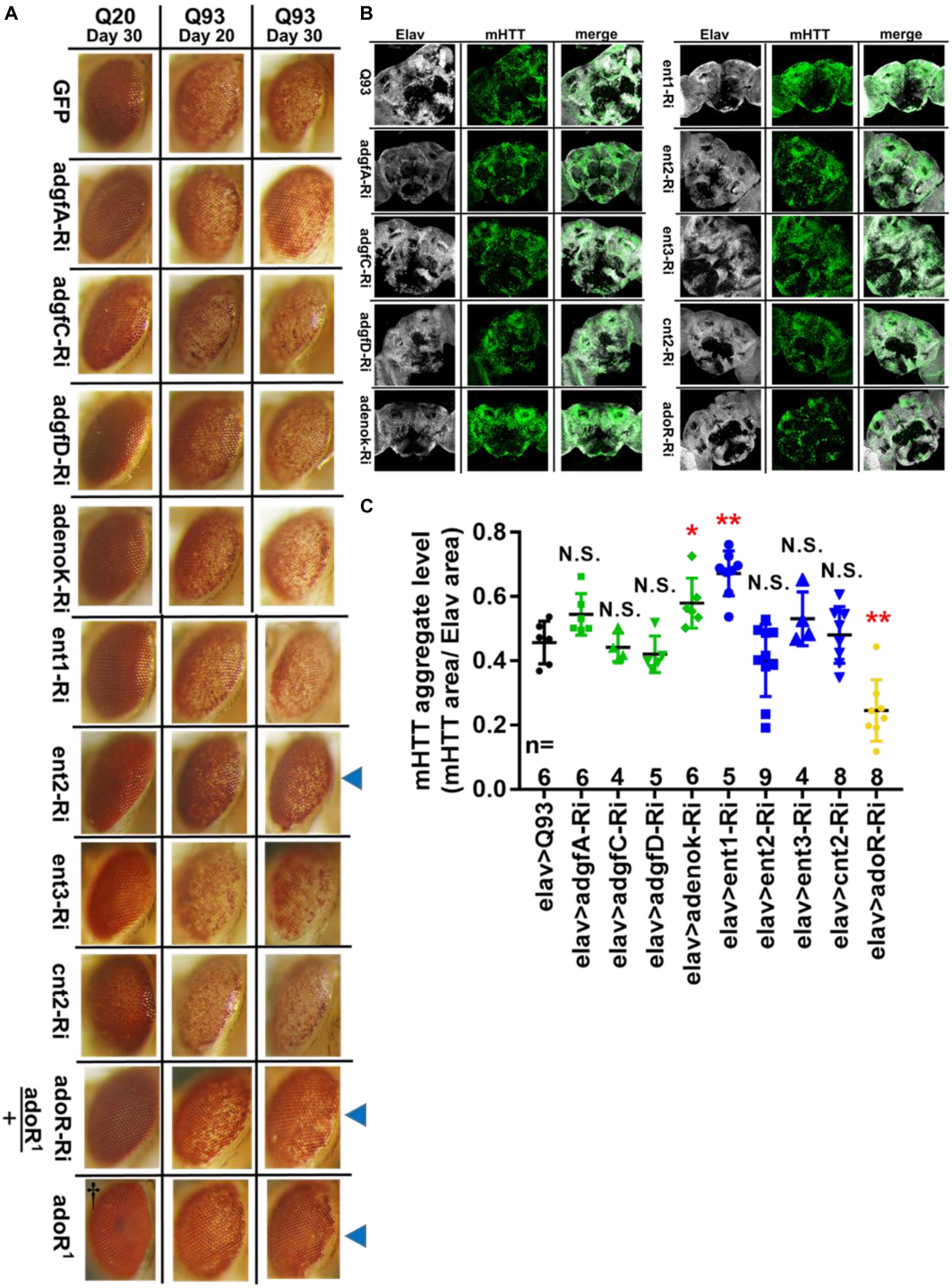

FIGURE 2 | Suppression of *ent2* and *adoR* decreased mHTT-induced cytotoxicity and mHTT aggregate formation. **(A)** Retinal pigment cell degeneration in mHTT-expressing adult females (gmr > Q93) with RNAi silencing Ado metabolic enzymes, transporters, *adoR* (*adoR* heterozygous mutant background), and mHTT-expressing flies under *adoR* homozygous mutant background. Blue arrows indicate treated groups showing a significantly reduced loss of pigment. †Eye image of control homozygous $adoR^1$ mutant without *htt* expression. Detailed methodologies for sample collection and eye imaging are described in section "Materials and Methods." **(B)** Representative confocal images of the brains of 10-day-old mHTT-expressing adult females (elav > Q93) with RNAi silencing Ado metabolic enzymes, transporters, and *adoR*. Neuronal cells were detected with anti-Elav; mHTT aggregates were detected with anti-HTT (MW8). **(C)** Level of mHTT aggregate formation was calculated by normalizing the area of mHTT signal to the area of Elav signal. Significance in mHTT aggregate levels was analyzed using a Mann–Whitney *U*-test; significant differences between control Q93 flies and each RNAi treatment group are labeled as follows: $*P < 0.05$; $**P < 0.01$; N.S., not significant. Error bars are presented as mean ± SEM. The number (n) of examined brain images are shown below each bar.

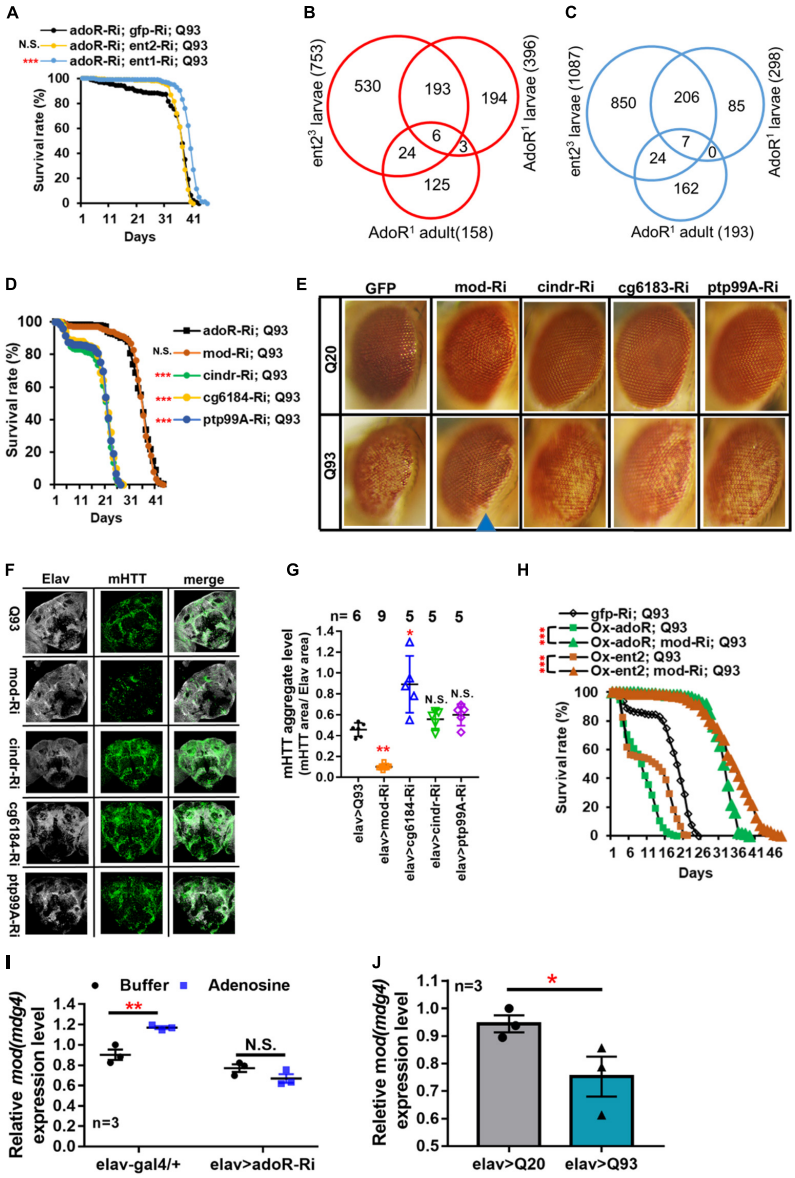

FIGURE 3 | Mod(mdg4) as a downstream target of ENT2/AdoR pathway modulated mHTT effects and aggregate formation. **(A)** Survival of mHTT-expressing adult females (elav > Q93) with RNAi co-silencing (Ri) transporters (*ent1* or *ent2*), and *adoR*. Significance was analyzed by a weighted log-rank test; significant differences between each treatment group and control (*gfp*-Ri) are labeled as follows: ***$P < 0.001$; N.S., not significant. $n > 200$. **(B,C)** Microarray analysis of the transcriptomes of *ent2* and *adoR* mutants. Venn diagram shows the number of common genes (in intersect region) which were upregulated **(B)** or downregulated **(C)** among the *adoR* mutant larvae vs. control (w^{1118}), *adoR* mutant adults vs. control (w^{1118}), and ent2 mutant larvae vs. control (w^{1118}). The cutoff values for expression differences were set at $Q < 0.05$ (false discovery rate, FDR). **(D)** Survival of mHTT-expressing adult females (elav > Q93) with RNAi co-silencing (Ri) of potential downstream genes of the ENT2/AdoR pathway. Significance was analyzed by a weighted log-rank test; significant differences between each treatment group to control (*adoR*-Ri) are labeled as follows: ***$P < 0.001$; N.S., not significant. $n > 200$. **(E)** Retinal pigment cell degeneration in mHTT-expressing adult females (gmr > Q93) with RNAi silencing potential downstream genes of the ENT2/AdoR pathway. Blue arrows indicate treated groups showing a significantly reduced loss of pigment. Detailed methodologies for sample collection and eye imaging are described in section "Materials and Methods." **(F)** Representative confocal images of the brains of 10-day-old mHTT-expressing adult females (elav > Q93) with RNAi silencing potential downstream genes of the ENT2/AdoR pathway. Neuronal cells were detected with anti-Elav and mHTT aggregates were detected with anti-HTT (MW8). **(G)** The level of mHTT aggregate formation was calculated by normalizing the area of mHTT signal to the area of Elav signal. Significance in mHTT aggregate levels was analyzed using a Mann–Whitney *U*-test; significant differences between control Q93 flies and each RNAi treatment group are labeled as follows: *$P < 0.05$; **$P < 0.01$; N.S., not significant. Error bars are presented as mean ± SEM. The number (n) of examined brain images are indicated above each bar. **(H)** Survival of mHTT-expressing adult females (elav > Q93) with co-RNAi silencing *mod(mdg4)* and co-overexpressing *adoR* or *ent2*. Significance was analyzed by a weighted log-rank test; significant differences are labeled as ***$P < 0.001$. $n > 200$. **(I)** Transcription level of *mod(mdg4)* 2 h after Ado injection into the whole body of 3- to 5-day old control adult females (elav-gal4/+) and *adoR* RNAi females (elav > adoR-Ri). Significance was analyzed by Student's *t*-test and labeled as follows: **$P < 0.01$; N.S., not significant. $n = 3$. Error bars are presented as mean ± SEM. **(J)** Transcription levels of *mod(mdg4)* in Q93-expressing (elav > Q93) and control Q20-expressing (elav > Q20) larval brains. Significance was analyzed by Student's *t*-test and labeled as *$P < 0.05$. $n = 3$. Error bars are presented as mean ± SEM.

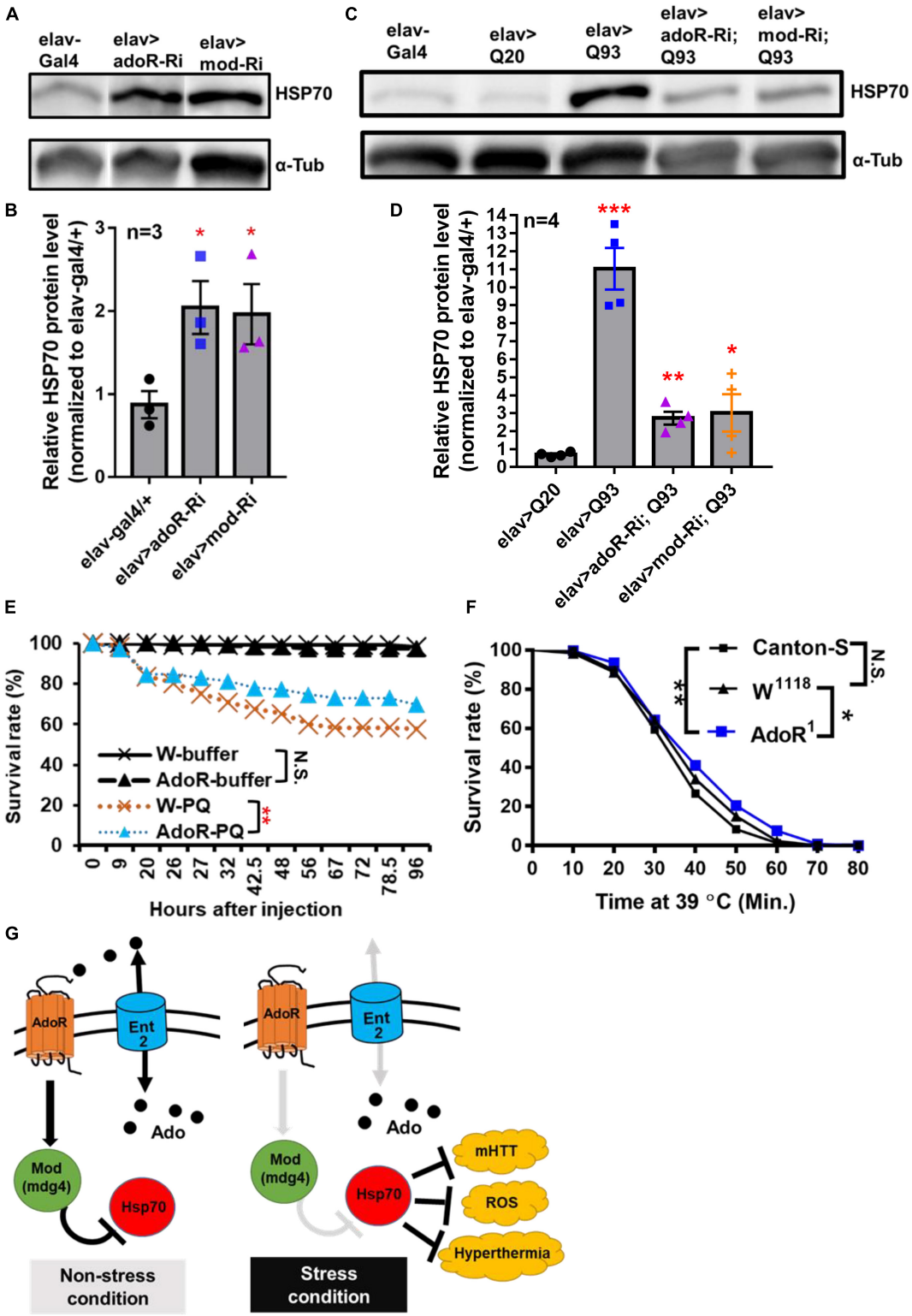

FIGURE 4 | AdoR regulated the Hsp70 protein level and influenced the stress response to paraquat and heat-shock treatments. **(A,B)** Representative images of western blot analysis. **(A)** Hsp70 protein level in the head of 10-day-old adult females with RNAi Silencing of (elav > adoR-Ri), *mod(mdg4)* (elav > mod-Ri), and control (elav-gal4/+). **(B)** The Hsp70 protein level was quantified by normalizing the intensity of the Hsp70 band to the α-tubulin band using ImageJ; values of RNAi treatment groups were further normalized to the elav-gal4 control. Significance was analyzed by Student's *t*-test; significant differences between the control

(Continued)

FIGURE 4 | Continued
and each RNAi treatment group are labeled as $^{*}P < 0.05$. $n = 3$. Error bars are presented as mean ± SEM. Original gel images are presented in the **Supplementary Figure 6**. **(C,D)** Representative images of western blot analysis. **(C)** Hsp70 protein level in the head of 10-day-old HTT (elav > Q20) or mHTT expressing (elav > Q93) adult females with RNAi silencing *adoR* and *mod(mdg4)*. **(D)** The Hsp70 protein level was quantified by normalizing the intensity of the Hsp70 band to the α-tubulin band by using ImageJ; values of each treatment group were further normalized to the elav-gal4 control. Significance was analyzed by Student's *t*-test; significant differences between HTT-expressing flies (elav > Q20) and each RNAi treatment of Q93-expressing flies are labeled as follows: $^{*}P < 0.05$, $^{**}P < 0.01$, $^{***}P < 0.001$. $n = 4$. Error bars are presented as mean ± SEM. Original gel images are presented in the **Supplementary Figure 7**. **(E)** Survival of w^{1118} and homozygous *adoR* mutant adult males after paraquat (PQ) injection. Control groups were injected with ringer buffer. Significance was analyzed by weighted log-rank test; significant differences are labeled as follows: $^{**}P < 0.01$, N.S., not significant. W-ringer, $n = 116$; $AdoR^{1}$-ringer, $n = 118$; W-PQ, $n = 118$; and $AdoR^{1}$-PQ, $n = 119$. **(F)** Survival of Cantons-S, w^{1118} and homozygous *adoR* mutant ($AdoR^{1}$) adult males during heat-shock treatment. Significance was analyzed by weighted log-rank test; significant differences are labeled as follows: $^{*}P < 0.05$, $^{**}P < 0.01$. Cantons-S and W^{1118}, $n = 300$; $AdoR^{1}$, $n = 370$. **(G)** Summary model of Ado signaling under stress response. Under a non-stress condition, the activated AdoR and Mod(mdg4) reduce Hsp70 production. In contrast, decreased Ado signaling under a stress condition resulted in Hsp70 production, which in turn enhanced stress tolerance.

knockdowns doubled the level of Hsp70 compared to *elav-Gal4* control flies under a non-stress condition (i.e., without mHTT expression). We next compared the level of Hsp70 in flies co-expressing mHTT with each RNAi construct (**Figures 4C,D** and **Supplementary Figure 6**). Interestingly, both *adoR* and *mod(mdg4)* RNAi flies co-expressing Q93 mHTT again showed levels around two-fold higher than the Q20 HTT-expressing control, although it was around ten times higher in Q93 mHTT-only flies. These results indicate that *adoR* and *mod(mdg4)* are able to suppress Hsp70 protein production under a non-stress condition. The knockdown of *adoR* and *mod(mdg4)* leads to an increase of Hsp70 production, thus preventing mHTT aggregate formation and decreasing mHTT cytotoxicity.

Decreased Susceptibility to Oxidative and Heat-Shock Stresses in *adoR* Mutant Flies

Since Hsp70 proteins are also involved in the response against oxidative stress (Azad et al., 2011; Shukla et al., 2014; Donovan and MarrII, 2016) and heat-shock stress (Gong and Golic, 2006; Bettencourt et al., 2008; Shilova et al., 2018) in *Drosophila*, we postulated that increased Hsp70 production by decreased e-Ado signaling may also enhance the resistance against both stresses. To test this, we treated flies with either paraquat (a potent oxidative stress inducer; **Figure 4E**) or a higher temperature (to induce heat-shock; **Figure 4F**). We then compared the survival rate between the mutant flies and w^{1118} or Canton-S control flies. The results showed that *adoR* mutant flies were more resistant to paraquat and heat-shock treatment. Our results therefore demonstrate that the *Drosophila* AdoR pathway with its downstream gene *mod(mdg4)* suppresses Hsp70 protein production under a non-stress condition. Thus, the knockdown of *ent2*, *AdoR*, and *mod*(*mdg4*) results in increased levels of Hsp70, which in turn helps flies to respond to various stresses, including mHTT cytotoxicity, oxidative, and heat-shock stresses (**Figure 4G**).

DISCUSSION

Adenosine signaling represents an evolutionarily conserved pathway affecting a diverse array of stress responses (Fredholm, 2007). As a ubiquitous metabolite, Ado has evolved to become a conservative signal among eukaryotes. In previous studies, *Drosophila adoR* mutants (Dolezelova et al., 2007; Wu et al., 2009) and mice with a knockout of all four *adoRs* (Xiao et al., 2019) both displayed minor physiological alteration under normal conditions. This is consistent with the idea that Ado signaling more likely regulates the response to environmental changes (stresses) rather than being involved in maintaining fundamental homeostasis in both insect and mammalian models (Cunha, 2019). Our study examined the impact of altering the expression of genes involved in Ado signaling and metabolism on the cytotoxicity and neurodegeneration phenotype of Q93 mHTT-expressing flies. We discovered a novel downstream target of this pathway, *mod(mdg4)*, and showed its effects on the downregulation of Hsp70 proteins, a well-known chaperone responsible for protecting cells against various stress conditions, including mHTT cytotoxicity, as well as thermal or oxidative stress (Soares et al., 2019).

The low level of Ado observed in our *da-Gal4* mHTT flies suggests that it might have a pathophysiological role; lowering of the Ado level might represent a natural response to cytotoxic stress. Consistently, our experimentally decreased Ado signal rescued the mHTT phenotype, while an increased Ado signal had deleterious effects. Interestingly, a high level of Ado in the hemolymph has previously been observed in *Drosophila* infected by a parasitoid wasp (Novakova and Dolezal, 2011; Bajgar et al., 2015). A raised e-Ado titer has not only been shown to stimulate hemocyte proliferation in the lymph glands (Mondal et al., 2011), but also to trigger metabolic reprogramming and to switch the energy supply toward hemocytes (Bajgar et al., 2015). In contrast, our experiments show that a lowered e-Ado titer results in increased Hsp70 production. Increased Hsp70 has previously been shown to protect the cells from protein aggregates and cytotoxicity caused by mHTT expression, as well as some other challenges including oxidative stress (paraquat treatment) or heat-shock (Garbuz, 2017). The fine regulation of extracellular Ado in *Drosophila* might mediate the differential Ado responses via a single receptor isoform. Our earlier experiments on *Drosophila* cells also suggested that different cell types have different responses to Ado signaling (Fleischmannova et al., 2012).

Our data also showed that altered adenosine signaling through the receptor is closely connected to Ado transport, especially to ent2 transporter function. We observed that *adoR* and *ent2*

knockdowns provide the most prominent rescue of mHTT phenotypes. In addition, the overexpression of *adoR* and *ent2* genes results in effects that are opposite to their knockdowns, thus supporting the importance of these genes as key regulators of mHTT phenotypes. Our previous report showed that responses to *adoR* and *ent2* mutations cause identical defects in associative learning and synaptic transmission (Knight et al., 2010). In the present study, we show that the phenotypic response of mHTT flies to *adoR* and *ent2* knockdowns are also identical. Our results suggest that the source of e-Ado for inducing AdoR signaling is mainly released by *ent2*. Consistently, the knockdown of *ent2* has previously been shown to block Ado release from *Drosophila* hemocytes upon an immune challenge (Bajgar et al., 2015), as well as from wounded cells stimulated by *scrib*-RNAi (Poernbacher and Vincent, 2018) or bleomycin feeding (Xu et al., 2020). These data support the idea that both *adoR* and *ent2* work in the same signaling pathway.

Our results revealed that lower AdoR signaling has a beneficial effect on mHTT-expressing flies, including increasing their tolerance to oxidative and heat-shock stresses. The effect of lower Ado signaling in mammals has been studied by pharmacologically blocking AdoRs, especially by the non-selective adenosine receptor antagonist caffeine. Interestingly, caffeine has beneficial effects on both neurodegenerative diseases and oxidative stress in humans (Rivera-Oliver and Diaz-Rios, 2014; Martini et al., 2016). In contrast, higher long-term Ado concentrations have cytotoxic effects by itself in both insect and mammalian cells (Schrier et al., 2001; Merighi et al., 2002). Chronic exposure to elevated Ado levels has a deleterious effect, causing tissue dysfunction, as has been observed in a mammalian system (Antonioli et al., 2019). Extensive disruption of nucleotide homeostasis has also been observed in mHTT-expressing R6/2 and Hdh150 mice (Toczek et al., 2016).

We identified a downstream target of the AdoR pathway, *mod(mdg4)*, which modulates mHTT cytotoxicity and aggregations. This gene has previously been implicated in the regulation of position effect variegation, chromatin structure, and neurodevelopment (Dorn and Krauss, 2003). The altered expression of *mod(mdg4)* has been observed in flies expressing untranslated RNA containing CAG and CUG repeats (Mutsuddi et al., 2004; Van Eyk et al., 2011). In addition, *mod(mdg4)* has complex splicing, including *trans*-splicing, producing at least 31 isoforms (Krauss and Dorn, 2004). All isoforms contain a common N-terminal BTB/POZ domain which mediates the formation of homomeric, heteromeric, and oligomeric protein complexes (Bardwell and Treisman, 1994; Albagli et al., 1995; Espinas et al., 1999). Among these isoforms, only two [including *mod(mdg4)*-56.3 (isoform H) and *mod(mdg4)*-67.2 (isoform T)] have been functionally characterized. *mod(mdg4)*-56.3 is required during meiosis for maintaining chromosome pairing and segregation in males (Thomas et al., 2005; Soltani-Bejnood et al., 2007). *mod(mdg4)*-67.2 interacts with suppressor of hairy wing [Su(Hw)] and Centrosomal protein 190 kD (CP190) forming a chromatin insulator complex which inhibits the action of adjacent enhancers on the promoter, and is important for early embryo development and oogenesis (Buchner et al., 2000; Soshnev et al., 2013; Melnikova et al., 2018). In the present study, we showed that *mod(mdg4)* is controlled by AdoR which consecutively works as a suppressor of Hsp70 chaperone. The downregulation of *adoR* or *mod(mdg4)* leads to the induction of Hsp70, which in turn suppresses mHTT aggregate formation and other stress phenotypes. Although our results showed that silencing all *mod(mdg4)* isoforms decreases cytotoxicity and mHTT inclusion formation, we could not clarify which of the specific isoforms is involved in such effects, since AdoR seems to regulate the transcriptions of multiple isoforms (**Supplementary Figure 7**). Further study will be needed to identify the specific *mod(mdg4)* isoform(s) connected to Hsp70 production.

In summary, our data suggest that the cascade (*ent2*)-*AdoR-mod(mdg4)-Hsp70* might represent an important general Ado signaling pathway involved in the response to various stress conditions, including reaction to mHTT cytotoxicity, oxidative damage, or thermal stress in *Drosophila* cells. The present study provides important insights into the molecular mechanisms of how Ado regulates mHTT aggregate formation and stress responses in *Drosophila*; this might be broadly applicable for understanding how the action of Ado affects disease pathogenesis.

MATERIALS AND METHODS

Fly Stocks

Flies were reared at 25°C on standard cornmeal medium. The following RNAi lines were acquired from the TRiP collection (Transgenic RNAi project) at Harvard Medical School: adgfA-Ri (BL67233), adgfC-Ri (BL42915), adgfD-Ri (BL56980), adenoK-Ri (BL64491), ent1-Ri (BL51055), adoR-Ri (BL27536), gfp-Ri (BL41552), mod(mdg4)-Ri (BL32995), cindr-Ri (BL38976), and ptp99A-Ri (BL57299). The following RNAi lines were acquired from the Vienna Drosophila RNAi Center (VDRC): ent2-Ri (ID100464), ent3-Ri (ID47536), cnt2-Ri (ID37161), and cg6184-Ri (ID107150).

Flies overexpressing human normal huntingtin (HTT) exon 1, Q20Httexon^{1111F1L}, mutant pathogenic fragments (mHTT), Q93Httexon^{14F132} and elav^{C155}-GAL4 were obtained from Prof. Lawrence Marsh (UC Irvine, United States) (Steffan et al., 2001). The UAS-overexpression lines, Ox-adenoK and Ox-adoR, were obtained from Dr. Ingrid Poernbacher (The Francis Crick Institute, United Kingdom) (Poernbacher and Vincent, 2018). gmr-GAL4 was obtained from Dr. Marek Jindra (Biology Centre CAS, Czechia). da-GAL4 was obtained from Dr. Ulrich Theopold (Stockholm University). The UAS overexpression strains Ox-adgfA, Ox-ent2, adoR^{1} and ent2^{3} mutant flies, were generated in our previous studies (Dolezal et al., 2003, 2005; Dolezelova et al., 2007; Knight et al., 2010).

Eclosion Rate and Adult Lifespan Assay

For assessing the eclosion rate, male flies containing the desired RNAi or overexpression transgene (RiOx) in the second chromosome with genotype w^{1118}/Y; RiOx/CyO; UAS-Q93/MKRS were crossed with females of *elav-GAL4*; +/+; +/+. The ratio of eclosed adults between *elav-GAL4*/+; RiOx/+; UAS-Q93/+ and *elav-GAL4*/+; RiOx/+; +/MKRS was then calculated.

If the desired RiOx transgene was in the third chromosome, female flies containing *elav-GAL4*; +/+; RiOx were crossed with male w^{1118}/Y; +/+; UAS-Q93/MKRS, and the ratio of eclosed adults between *elav-GAL4*; +/+; RiOx/UAS-Q93 and *elav-GAL4*; +/+; RiOx/MKRS was calculated. If the ratio showed higher than 100%, it indicated that the number of Q93 or Q20 flies containing RiOx was higher than the flies containing only RiOx construct without Q93 or Q20 expression.

For the adult survival assay, up to 30 newly emerged female adults were placed in each cornmeal-containing vial and maintained at 25°C. At least 200 flies of each genotype were tested and the number of dead flies was counted every day. Flies co-expressing RiOx and HTT Q20 were used for evaluating the effect of RNAi or overexpression of the desired transgenes.

Extracellular Adenosine and ATP Level Measurements

To collect the hemolymph, 6 third-instar larvae (96 h post-oviposition) were torn in 150 μl of 1× PBS containing thiourea (0.1 mg/ml) to prevent melanization. The samples were then centrifuged at 5000 × *g* for 5 min to separate the hemocytes and the supernatant was collected for measuring the extracellular adenosine or ATP level. For measuring the adenosine titer, 10 μl of hemolymph was mixed with the reagents of an adenosine assay kit (Biovision) following the manufacturer's instructions. The fluorescent intensity was then quantified (Ex/Em = 533/587 nm) using a microplate reader (BioTek Synergy 4). For measuring the ATP level, 10 μl of hemolymph was incubated with 50 μl of CellTiter-Glo reagent (Promega) for 10 min. Then, the luminescent intensity was quantified using an Orion II microplate luminometer (Berthold). To calibrate the standard curve of ATP concentration, 25 μM ATP standard solution (Epicenter) was used for preparing a concentration gradient (0, 2, 4, 6, 8, and 10 μM) of ATP solution and the luminescent intensity was measured for each concentration. The protein concentration of the hemolymph sample was determined by a Bradford assay. The adenosine and ATP concentrations were first normalized to protein concentration. Then, the values of Q20 and Q93 samples were normalized to values of the *GAL4* control sample. Six independent replicates for each genotype were performed for the analysis of adenosine and ATP levels.

RNA Extraction

The brains of 10 third-instar larvae (96 h post-oviposition) or 15 whole female flies were pooled for each replicate. The samples were first homogenized in RiboZol (VWR) and the RNA phase was separated by chloroform. For brain samples, the RNA was precipitated by isopropanol, washed in 75% ethanol, and dissolved in nuclease-free water. For whole fly samples, the RNA phase was purified using NucleoSpin RNA columns (Macherey-Nagel) following the manufacturer's instructions. All purified RNA samples were treated with DNase to prevent genomic DNA contamination. cDNA was synthesized from 2 μg of total RNA using a RevertAid H Minus First Strand cDNA Synthesis Kit (Thermo Fisher Scientific).

Adenosine Injection

Three- to five-day-old female adults were injected with 50 nl of 10 mM adenosine solution using a NANOJECT II (Drummond Scientific); control flies were injected with 50 nl of 1× PBS. Two hours post-injection, 15 injected flies for each replicate were collected for RNA extraction.

Microarray Analysis

The Affymetrix GeneChip® *Drosophila* genome 2.0 array system was used for microarray analysis following the standard protocol: 100 ng of RNA was amplified with a GeneChip 3′ express kit (Affymetrix), and 10 μg of labeled cRNA was hybridized to the chip according to the manufacturer's instructions. The statistical analysis of array data was as described in our previous studies (Arefin et al., 2014; Kucerova et al., 2016). Storey's *q* value [false discovery rate (FDR)] was used to select significantly differentially transcribed genes ($q < 0.05$). Transcription raw data are shown in **Supplementary Table 2** and have been deposited in the ArrayExpress database[2] (accession No. E-MTAB-8699 and E-MTAB-8704).

qPCR and Primers

5× HOT FIREPol® EvaGreen® qPCR Mix Plus with ROX (Solis Biodyne) and an Eco Real-Time PCR System (Illumina) were used for qPCR. Each reaction contained 4 μl of EvaGreen qPCR mix, 0.5 μl each of forward and reverse primers (10 μM), 5 μl of diluted cDNA, and ddH2O to adjust the total volume to 20 μl. The list of primers is shown in **Supplementary Table 3**. The expression level was calculated using the $2^{-\Delta\Delta Ct}$ method with the ct values of target genes normalized to a reference gene, ribosomal protein 49 (*rp49*).

Imaging of Retinal Pigment Cell Degeneration

Twenty- and thirty-day-old female adults were collected and their eye depigmentation phenotypes were recorded. At least 30 individuals for each genotype were examined under a microscope, and at least five representative individuals were chosen for imaging. Pictures were taken with an EOS 550D camera (Canon) mounted on a SteREO Discovery V8 microscope (Zeiss).

Brain Immunostaining

Brains dissected from 10- or 20-day-old adult females were used for immunostaining. The brains were fixed in 4% PFA, permeabilized with PBST (0.1% Triton X-100), blocked in PAT (PBS, 0.1% Triton X-100, 1% BSA), and stained with antibodies in PBT (PBS, 0.3% Triton X-100, 0.1% BSA). Primary antibodies used in this study were mouse anti-HTT; MW8, which specifically binds to mHTT aggregates (1:40, DSHB); and rat anti-Elav (1:40, DSHB), which is a pan-neuronal antibody. Secondary antibodies were Alexa Fluor 488 anti-mouse and Alexa Fluor 647 anti-rat (1:200, Invitrogen). The samples were mounted in Fluoromount-G (Thermo Fisher Scientific) overnight, prior to image examination.

[2]www.ebi.ac.uk/arrayexpress

Quantification of mHTT Aggregates

Images of aggregates were taken using a FluoView 100 confocal microscope (Olympus). The intensity of mHTT aggregates detected by anti-HTT antibody (MW8) or anti-Elav was quantified using ImageJ software. The level of mHTT aggregates was determined by calculating the ratio between areas of mHTT to the Elav signal. At least six brain images from each genotype were analyzed.

Western Blot

Twenty heads, collected from 10-day-old adult females, were pooled for each replicate. The samples were homogenized in 100 μl of RIPA buffer with 1 μl of Halt^{TM} proteinase inhibitor cocktail (Thermo Fisher Scientific). From each sample, 80 μl of supernatant was collected after 10 min of centrifugation at 12000 × *g*, which was then mixed with 16 μl of 6× loading buffer. After boiling at 95°C for 3 min, 10 μl were then loaded for running an SDS-PAGE gel. Proteins were then transfered to an Immobilon-E PVDF membrane (Millipore), which was then washed with 1× PBS containing 0.05% Tween 20 (three washes, each 15 min) and blocked in 5% BSA for 1 h at room temperature before staining. The membrane was subsequently stained with primary antibodies overnight at 4°C and secondary antibody for 1 h at room temperature. After immunostaining, the membrane was treated with 2 ml of SuperSignal^{TM} West Pico PLUS Chemiluminescent Substrate (Thermo Fisher Scientific) for 10 min at room temperature, and images were recorded using a Fujifilm LAS-3000 Imager. The primary antibodies used for staining were rat anti-Hsp70 (7FB) (1:2000, Thermo Fisher Scientific) and mouse anti-Tub (1:500, DSHB). The secondary antibodies were donkey anti-rat IgG (H + L) HRP (1:5000, Thermo Fisher Scientific) and donkey anti-Mouse IgG (H + L) HRP (1:5000, Thermo Fisher Scientific).

Paraquat Injection

Three- to five-day-old males were collected for paraquat injection. Each fly was injected with 50 nl of 3 mM paraquat ringer solution using a NANOJECT II (Drummond Scientific). Control flies were injected with ringer buffer. 70–20 of injected flies were pooled into one vial for each replicate, and six replicates were performed for each treatment.

Heat-Shock Treatment

The heat-shock procedure followed a previous study (Gong and Golic, 2006) with few modifications. Newly emerged males (0 or 1 day old) were collected and maintained on a standard cornmeal diet. The following day, 10 flies were transferred into each empty vial and given a mild heat-shock at 35°C for 30 min, then transferred to a circulating water bath at 39°C. The number of surviving flies was checked every 10 min; flies which did not move any part of their body were considered dead.

Statistical Analysis

A Shapiro–Wilk test was applied to determine data normality. For data which were not normally distributed ($P < 0.05$), statistical significance was analyzed using the Mann–Whitney *U*-test. For normally distributed data ($P > 0.05$), statistical significance was established using Student's *t*-test or one-way ANOVA with Tukey's HSD *post hoc* test. For the statistical analysis of survival curves, we used OASIS 2 to perform a weighted log-rank test (Han et al., 2016).

DATA AVAILABILITY STATEMENT

The datasets presented in this study can be found in online repositories. The names of the repository/repositories and accession number(s) can be found in the article/ **Supplementary Material**.

AUTHOR CONTRIBUTIONS

Y-HL performed the experiments and prepared the manuscript. HM assisted in recording the adult lifespan and eye phenotypes, and also as performed the brain dissection, immunochemistry, and confocal microscopy imaging. LK performed the microarray sample preparation, analyzed the microarray data and paraquat injection. LR assisted in recording the adult lifespan and eye phenotypes, prepared the fly strains, and performed the heat-shock treatment. TF established the methodologies for recording the eclosion rate and survival, and prepared the fly strains. MZ conceived the project and supervised the manuscript preparation. All authors contributed to the article and approved the submitted version.

FUNDING

This work was supported by the grant agency of the University of South Bohemia (065/2017/P to Y-HL), junior grant project GACR (19-13784Y to LK), and European Community's Program Interreg Österreich-Tschechische Republik (REGGEN/ATCZ207 to MZ).

ACKNOWLEDGMENTS

We thank Dr. Ingrid Poernbacher (The Francis Crick Institute, United Kingdom), Prof. Lawrence Marsh (UC Irvine, United States), Dr. Marek Jindra (Biology Centre CAS, Czechia), Dr. Tomas Dolezal (University of South Bohemia, Czechia), Dr. Ulrich Theopold (Stockholm University), Bloomington *Drosophila* Stock Center, and Vienna *Drosophila* Resource Center for providing us with fly strains.

SUPPLEMENTARY MATERIAL

The Supplementary Material for this article can be found online at: https://www.frontiersin.org/articles/10.3389/fcell.2021.651367/full#supplementary-material

REFERENCES

Albagli, O., Dhordain, P., Deweindt, C., Lecocq, G., and Leprince, D. (1995). The BTB/POZ domain: a new protein-protein interaction motif common to DNA- and actin-binding proteins. *Cell Growth Differ.* 6, 1193–1198.

Antonioli, L., Fornai, M., Blandizzi, C., Pacher, P., and Hasko, G. (2019). Adenosine signaling and the immune system: when a lot could be too much. *Immunol. Lett.* 205, 9–15. doi: 10.1016/j.imlet.2018.04.006

Arefin, B., Kucerova, L., Dobes, P., Markus, R., Strnad, H., Wang, Z., et al. (2014). Genome-wide transcriptional analysis of *Drosophila* larvae infected by entomopathogenic nematodes shows involvement of complement, recognition and extracellular matrix proteins. *J. Innate Immun.* 6, 192–204. doi: 10.1159/000353734

Azad, P., Ryu, J., and Haddad, G. G. (2011). Distinct role of Hsp70 in *Drosophila* hemocytes during severe hypoxia. *Free Radic. Biol. Med.* 51, 530–538. doi: 10.1016/j.freeradbiomed.2011.05.005

Bajgar, A., Kucerova, K., Jonatova, L., Tomcala, A., Schneedorferova, I., Okrouhlik, J., et al. (2015). Extracellular adenosine mediates a systemic metabolic switch during immune response. *PLoS Biol.* 13:e1002135. doi: 10.1371/journal.pbio.1002135

Bardwell, V. J., and Treisman, R. (1994). The POZ domain: a conserved protein-protein interaction motif. *Genes Dev.* 8, 1664–1677. doi: 10.1101/gad.8.14.1664

Bettencourt, B. R., Hogan, C. C., Nimali, M., and Drohan, B. W. (2008). Inducible and constitutive heat shock gene expression responds to modification of Hsp70 copy number in *Drosophila melanogaster* but does not compensate for loss of thermotolerance in Hsp70 null flies. *BMC Biol.* 6:5. doi: 10.1186/1741-7007-6-5

Borea, P. A., Gessi, S., Merighi, S., and Varani, K. (2016). Adenosine as a multi-signalling guardian angel in human diseases: when, where and how does it exert its protective effects? *Trends Pharmacol. Sci.* 37, 419–434. doi: 10.1016/j.tips.2016.02.006

Buchner, K., Roth, P., Schotta, G., Krauss, V., Saumweber, H., Reuter, G., et al. (2000). Genetic and molecular complexity of the position effect variegation modifier mod(mdg4) in *Drosophila*. *Genetics* 155, 141–157.

Chan, H. Y., Warrick, J. M., Gray-Board, G. L., Paulson, H. L., and Bonini, N. M. (2000). Mechanisms of chaperone suppression of polyglutamine disease: selectivity, synergy and modulation of protein solubility in *Drosophila*. *Hum. Mol. Genet.* 9, 2811–2820. doi: 10.1093/hmg/9.19.2811

Cunha, R. A. (2016). How does adenosine control neuronal dysfunction and neurodegeneration? *J. Neurochem.* 139, 1019–1055. doi: 10.1111/jnc.13724

Cunha, R. A. (2019). Signaling by adenosine receptors-homeostatic or allostatic control? *PLoS Biol.* 17:e3000213. doi: 10.1371/journal.pbio.3000213

Dolezal, T., Dolezelova, E., Zurovec, M., and Bryant, P. J. (2005). A role for adenosine deaminase in *Drosophila* larval development. *PLoS Biol.* 3:e201. doi: 10.1371/journal.pbio.0030201

Dolezal, T., Gazi, M., Zurovec, M., and Bryant, P. J. (2003). Genetic analysis of the ADGF multigene family by homologous recombination and gene conversion in *Drosophila*. *Genetics* 165, 653–666.

Dolezelova, E., Nothacker, H. P., Civelli, O., Bryant, P. J., and Zurovec, M. (2007). A *Drosophila* adenosine receptor activates cAMP and calcium signaling. *Insect Biochem. Mol. Biol.* 37, 318–329.

Dolezelova, E., Zurovec, M., Dolezal, T., Simek, P., and Bryant, P. J. (2005). The emerging role of adenosine deaminases in insects. *Insect Biochem. Mol. Biol.* 35, 381–389. doi: 10.1016/j.ibmb.2004.12.009

Donovan, M. R., and Marr, M. T. II (2016). dFOXO activates large and small heat shock protein genes in response to oxidative stress to maintain proteostasis in *Drosophila*. *J. Biol. Chem.* 291, 19042–19050. doi: 10.1074/jbc.M116.723049

Dorn, R., and Krauss, V. (2003). The modifier of mdg4 locus in *Drosophila*: functional complexity is resolved by trans splicing. *Genetica* 117, 165–177. doi: 10.1023/A:1022983810016

Espinas, M. L., Jimenez-Garcia, E., Vaquero, A., Canudas, S., Bernues, J., and Azorin, F. (1999). The N-terminal POZ domain of GAGA mediates the formation of oligomers that bind DNA with high affinity and specificity. *J. Biol. Chem.* 274, 16461–16469. doi: 10.1074/jbc.274.23.16461

Fleischmannova, J., Kucerova, L., Sandova, K., Steinbauerova, V., Broz, V., Simek, P., et al. (2012). Differential response of *Drosophila* cell lines to extracellular adenosine. *Insect Biochem. Mol. Biol.* 42, 321–331. doi: 10.1016/j.ibmb.2012.01.002

Fredholm, B. B. (2007). Adenosine, an endogenous distress signal, modulates tissue damage and repair. *Cell Death Differ.* 14, 1315–1323. doi: 10.1038/sj.cdd.4402132

Garbuz, D. G. (2017). Regulation of heat shock gene expression in response to stress. *Mol. Biol.* 51, 352–367. doi: 10.1134/S0026893317020108

Giot, L., Bader, J. S., Brouwer, C., Chaudhuri, A., Kuang, B., Li, Y., et al. (2003). A protein interaction map of *Drosophila melanogaster*. *Science* 302, 1727–1736. doi: 10.1126/science.1090289

Gong, W. J., and Golic, K. G. (2006). Loss of Hsp70 in *Drosophila* is pleiotropic, with effects on thermotolerance, recovery from heat shock and neurodegeneration. *Genetics* 172, 275–286. doi: 10.1534/genetics.105.048793

Han, S. K., Lee, D., Lee, H., Kim, D., Son, H. G., Yang, J. S., et al. (2016). OASIS 2: online application for survival analysis 2 with features for the analysis of maximal lifespan and healthspan in aging research. *Oncotarget* 7, 56147–56152. doi: 10.18632/oncotarget.11269

Knight, D., Harvey, P. J., Iliadi, K. G., Klose, M. K., Iliadi, N., Dolezelova, E., et al. (2010). Equilibrative nucleoside transporter 2 regulates associative learning and synaptic function in *Drosophila*. *J. Neurosci.* 30, 5047–5057. doi: 10.1523/JNEUROSCI.6241-09.2010

Ko, J., Ou, S., and Patterson, P. H. (2001). New anti-huntingtin monoclonal antibodies: implications for huntingtin conformation and its binding proteins. *Brain Res. Bull.* 56, 319–329. doi: 10.1016/S0361-9230(01)00599-8

Krauss, V., and Dorn, R. (2004). Evolution of the trans-splicing *Drosophila* locus mod(mdg4) in several species of Diptera and Lepidoptera. *Gene* 331, 165–176. doi: 10.1016/j.gene.2004.02.019

Kucerova, L., Broz, V., Arefin, B., Maaroufi, H. O., Hurychova, J., Strnad, H., et al. (2016). The *Drosophila* chitinase-like protein IDGF3 is involved in protection against nematodes and in wound healing. *J. Innate Immun.* 8, 199–210. doi: 10.1159/000442351

Kuo, Y., Ren, S., Lao, U., Edgar, B. A., and Wang, T. (2013). Suppression of polyglutamine protein toxicity by co-expression of a heat-shock protein 40 and a heat-shock protein 110. *Cell Death Dis.* 4:e833. doi: 10.1038/cddis.2013.351

Lin, Y. H., Maaroufi, H. O., Ibrahim, E., Kucerova, L., and Zurovec, M. (2019). Expression of human mutant huntingtin protein in *Drosophila* hemocytes impairs immune responses. *Front. Immunol.* 10:2405. doi: 10.3389/fimmu.2019.02405

Maier, S. A., Galellis, J. R., and Mcdermid, H. E. (2005). Phylogenetic analysis reveals a novel protein family closely related to adenosine deaminase. *J. Mol. Evol.* 61, 776–794. doi: 10.1007/s00239-005-0046-y

Marsh, J. L., Walker, H., Theisen, H., Zhu, Y.-Z., Fielder, T., Purcell, J., et al. (2000). Expanded polyglutamine peptides alone are intrinsically cytotoxic and cause neurodegeneration in *Drosophila*. *Hum. Mol. Genet.* 9, 13–25. doi: 10.1093/hmg/9.1.13

Martini, D., Del Bo, C., Tassotti, M., Riso, P., Del Rio, D., Brighenti, F., et al. (2016). Coffee consumption and oxidative stress: a review of human intervention studies. *Molecules* 21:979. doi: 10.3390/molecules21080979

Melnikova, L., Kostyuchenko, M., Parshikov, A., Georgiev, P., and Golovnin, A. (2018). Role of Su(Hw) zinc finger 10 and interaction with CP190 and Mod(mdg4) proteins in recruiting the Su(Hw) complex to chromatin sites in *Drosophila*. *PLoS One* 13:e0193497. doi: 10.1371/journal.pone.0193497

Merighi, S., Mirandola, P., Milani, D., Varani, K., Gessi, S., Klotz, K. N., et al. (2002). Adenosine receptors as mediators of both cell proliferation and cell death of cultured human melanoma cells. *J. Invest. Dermatol.* 119, 923–933. doi: 10.1046/j.1523-1747.2002.00111.x

Mondal, B. C., Mukherjee, T., Mandal, L., Evans, C. J., Sinenko, S. A., Martinez-Agosto, J. A., et al. (2011). Interaction between differentiating cell- and niche-derived signals in hematopoietic progenitor maintenance. *Cell* 147, 1589–1600. doi: 10.1016/j.cell.2011.11.041

Moser, G. H., Schrader, J., and Deussen, A. (1989). Turnover of adenosine in plasma of human and dog blood. *Am. J. Physiol.* 256, C799–C806. doi: 10.1152/ajpcell.1989.256.4.C799

Mugat, B., Parmentier, M. L., Bonneaud, N., Chan, H. Y., and Maschat, F. (2008). Protective role of engrailed in a *Drosophila* model of Huntington's disease. *Hum. Mol. Genet.* 17, 3601–3616. doi: 10.1093/hmg/ddn255

Mutsuddi, M., Marshall, C. M., Benzow, K. A., Koob, M. D., and Rebay, I. (2004). The spinocerebellar ataxia 8 noncoding RNA causes neurodegeneration and associates with staufen in *Drosophila*. *Curr. Biol.* 14, 302–308. doi: 10.1016/j.cub.2004.01.034

Novakova, M., and Dolezal, T. (2011). Expression of *Drosophila* adenosine deaminase in immune cells during inflammatory response. *PLoS One* 6:e17741. doi: 10.1371/journal.pone.0017741

Oughtred, R., Stark, C., Breitkreutz, B. J., Rust, J., Boucher, L., Chang, C., et al. (2019). The BioGRID interaction database: 2019 update. *Nucleic Acids Res.* 47, D529–D541. doi: 10.1093/nar/gky1079

Poernbacher, I., and Vincent, J. P. (2018). Epithelial cells release adenosine to promote local TNF production in response to polarity disruption. *Nat. Commun.* 9:4675. doi: 10.1038/s41467-018-07114-z

Rivera-Oliver, M., and Diaz-Rios, M. (2014). Using caffeine and other adenosine receptor antagonists and agonists as therapeutic tools against neurodegenerative diseases: a review. *Life Sci.* 101, 1–9. doi: 10.1016/j.lfs.2014.01.083

Rosas-Arellano, A., Estrada-Mondragon, A., Pina, R., Mantellero, C. A., and Castro, M. A. (2018). The tiny *Drosophila Melanogaster* for the biggest answers in Huntington's disease. *Int. J. Mol. Sci.* 19:2398. doi: 10.3390/ijms19082398

Schrier, S. M., Van Tilburg, E. W., Van Der Meulen, H., Ijzerman, A. P., Mulder, G. J., and Nagelkerke, J. F. (2001). Extracellular adenosine-induced apoptosis in mouse neuroblastoma cells: studies on involvement of adenosine receptors and adenosine uptake. *Biochem. Pharmacol.* 61, 417–425. doi: 10.1016/S0006-2952(00)00573-6

Shilova, V. Y., Zatsepina, O. G., Garbuz, D. G., Funikov, S. Y., Zelentsova, E. S., Schostak, N. G., et al. (2018). Heat shock protein 70 from a thermotolerant Diptera species provides higher thermoresistance to *Drosophila* larvae than correspondent endogenous gene. *Insect Mol. Biol.* 27, 61–72. doi: 10.1111/imb.12339

Shukla, A. K., Pragya, P., Chaouhan, H. S., Tiwari, A. K., Patel, D. K., Abdin, M. Z., et al. (2014). Heat shock protein-70 (Hsp-70) suppresses paraquat-induced neurodegeneration by inhibiting JNK and caspase-3 activation in *Drosophila* model of Parkinson's disease. *PLoS One* 9:e98886. doi: 10.1371/journal.pone.0098886

Soares, T. R., Reis, S. D., Pinho, B. R., Duchen, M. R., and Oliveira, J. M. A. (2019). Targeting the proteostasis network in Huntington's disease. *Ageing Res. Rev.* 49, 92–103. doi: 10.1016/j.arr.2018.11.006

Soltani-Bejnood, M., Thomas, S. E., Villeneuve, L., Schwartz, K., Hong, C. S., and Mckee, B. D. (2007). Role of the mod(mdg4) common region in homolog segregation in *Drosophila* male meiosis. *Genetics* 176, 161–180. doi: 10.1534/genetics.106.063289

Song, W., Smith, M. R., Syed, A., Lukacsovich, T., Barbaro, B. A., Purcell, J., et al. (2013). Morphometric analysis of Huntington's disease neurodegeneration in *Drosophila*. *Methods Mol. Biol.* 1017, 41–57. doi: 10.1007/978-1-62703-438-8_3

Soshnev, A. A., Baxley, R. M., Manak, J. R., Tan, K., and Geyer, P. K. (2013). The insulator protein Suppressor of Hairy-wing is an essential transcriptional repressor in the *Drosophila* ovary. *Development* 140, 3613–3623. doi: 10.1242/dev.094953

Steffan, J. S., Bodai, L., Pallos, J., Poelman, M., Mccampbell, A., Apostol, B. L., et al. (2001). Histone deacetylase inhibitors arrest polyglutamine-dependent neurodegeneration in *Drosophila*. *Nature* 413, 739–743. doi: 10.1038/35099568

Stenesen, D., Suh, J. M., Seo, J., Yu, K., Lee, K. S., Kim, J. S., et al. (2013). Adenosine nucleotide biosynthesis and AMPK regulate adult life span and mediate the longevity benefit of caloric restriction in flies. *Cell Metab.* 17, 101–112. doi: 10.1016/j.cmet.2012.12.006

Thomas, S. E., Soltani-Bejnood, M., Roth, P., Dorn, R., Logsdon, J. M. Jr., and Mckee, B. D. (2005). Identification of two proteins required for conjunction and regular segregation of achiasmate homologs in *Drosophila* male meiosis. *Cell* 123, 555–568. doi: 10.1016/j.cell.2005.08.043

Toczek, M., Zielonka, D., Zukowska, P., Marcinkowski, J. T., Slominska, E., Isalan, M., et al. (2016). An impaired metabolism of nucleotides underpins a novel mechanism of cardiac remodeling leading to Huntington's disease related cardiomyopathy. *Biochim. Biophys. Acta* 1862, 2147–2157. doi: 10.1016/j.bbadis.2016.08.019

Van Eyk, C. L., O'keefe, L. V., Lawlor, K. T., Samaraweera, S. E., Mcleod, C. J., Price, G. R., et al. (2011). Perturbation of the Akt/Gsk3-beta signalling pathway is common to *Drosophila* expressing expanded untranslated CAG, CUG and AUUCU repeat RNAs. *Hum. Mol. Genet.* 20, 2783–2794. doi: 10.1093/hmg/ddr177

Warrick, J. M., Chan, H. Y., Gray-Board, G. L., Chai, Y., Paulson, H. L., and Bonini, N. M. (1999). Suppression of polyglutamine-mediated neurodegeneration in *Drosophila* by the molecular chaperone HSP70. *Nat. Genet.* 23, 425–428. doi: 10.1038/70532

Wu, M. N., Ho, K., Crocker, A., Yue, Z., Koh, K., and Sehgal, A. (2009). The effects of caffeine on sleep in *Drosophila* require PKA activity, but not the adenosine receptor. *J. Neurosci.* 29:11029–11037. doi: 10.1523/JNEUROSCI.1653-09.2009

Xiao, C., Liu, N., Jacobson, K. A., Gavrilova, O., and Reitman, M. L. (2019). Physiology and effects of nucleosides in mice lacking all four adenosine receptors. *PLoS Biol.* 17:e3000161. doi: 10.1371/journal.pbio.3000161

Xu, C., Franklin, B., Tang, H. W., Regimbald-Dumas, Y., Hu, Y., Ramos, J., et al. (2020). An in vivo RNAi screen uncovers the role of AdoR signaling and adenosine deaminase in controlling intestinal stem cell activity. *Proc. Natl. Acad. Sci. U.S.A.* 117, 464–471. doi: 10.1073/pnas.1900103117

Zurovec, M., Dolezal, T., Gazi, M., Pavlova, E., and Bryant, P. J. (2002). Adenosine deaminase-related growth factors stimulate cell proliferation in *Drosophila* by depleting extracellular adenosine. *Proc. Natl. Acad. Sci. U.S.A.* 99, 4403–4408. doi: 10.1073/pnas.062059699

Conflict of Interest: The authors declare that the research was conducted in the absence of any commercial or financial relationships that could be construed as a potential conflict of interest.

Supplementary Material

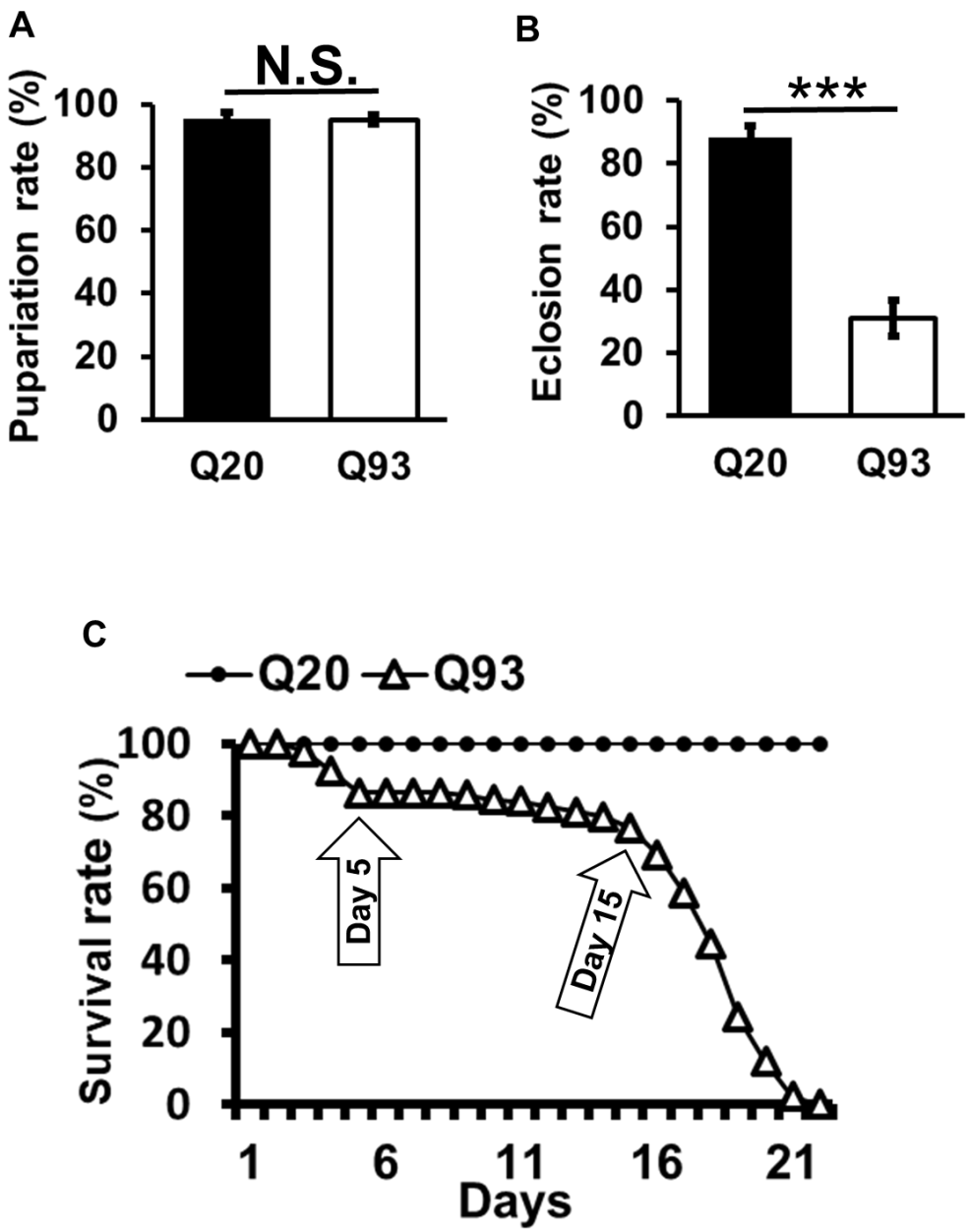

Figure S1. mHTT expression decreased viability in *Drosophila*. Flies expressing normal HTT (Q20) and mHTT (Q93) were driven by the pan-neuron driver (elav-GAL4), and the larval pupariation rate (A), adult eclosion rate (B), and adult survival (C) were recorded. At least five independent replicates were measured. Significance was examined using Student's t-test: ***$P < 0.001$; N.S., not significant. Error bars are presented as mean ± SEM

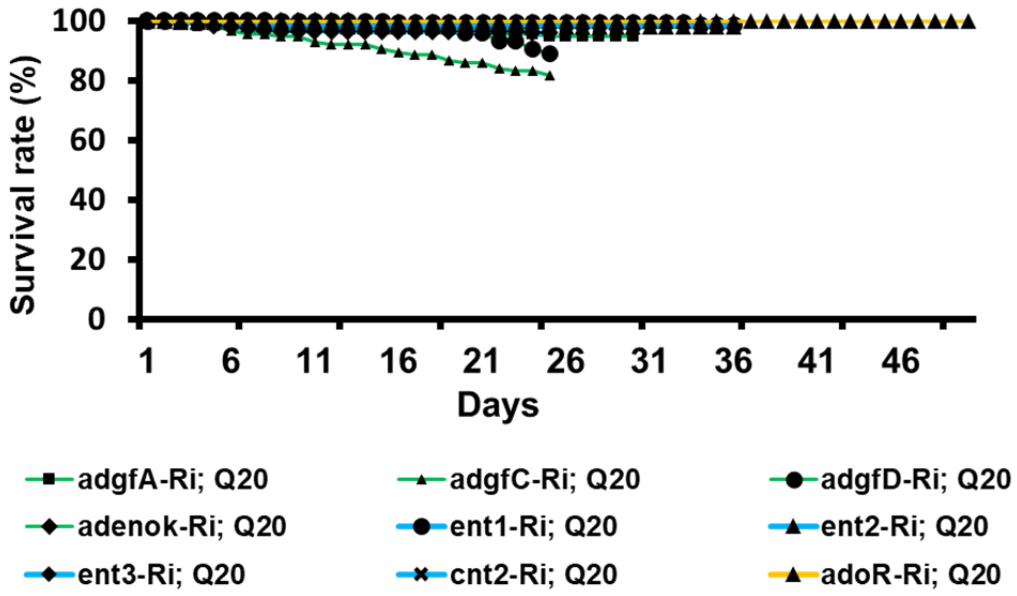

Figure S2. RNAi of Ado metabolic, transport and receptor genes did not influence viability of flies. Co-expression of normal Q20 HTT with RNAi of *adgf-A*, *adgf-C*, *adgf-D*, *adenoK*, *ent1*, *ent2*, *ent3*, *cnt2*, and *adoR* driven by the pan-neuronal driver (elav-GAL4). The number of dead flies was recorded until all corresponding experimental flies (expressing Q93 together with RNAi constructs) had died

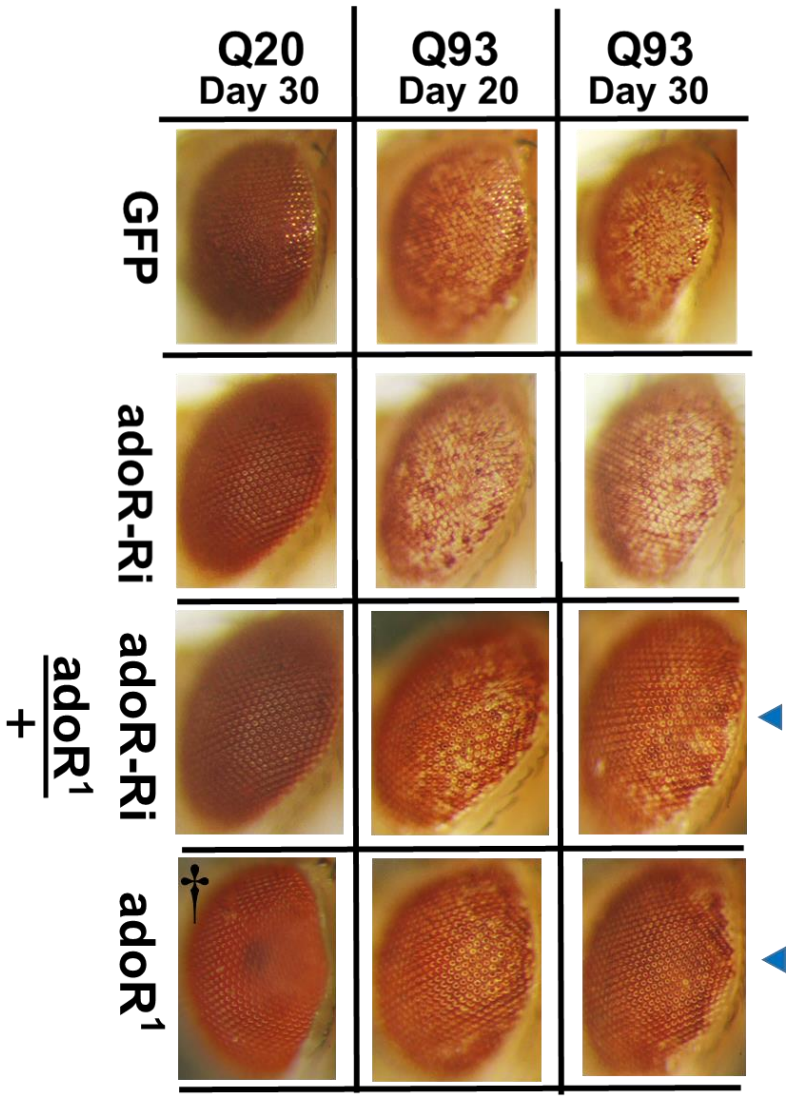

Figure S3. Co-expression of Q93 with heterozygous adoR RNAi construct could not significantly rescue retinal pigment cell degeneration. Retinal pigment cell degeneration in mHTT-expressing adult females (gmr>Q93) with RNAi silencing *adoR* or with *adoR* heterozygous and homozygous mutation

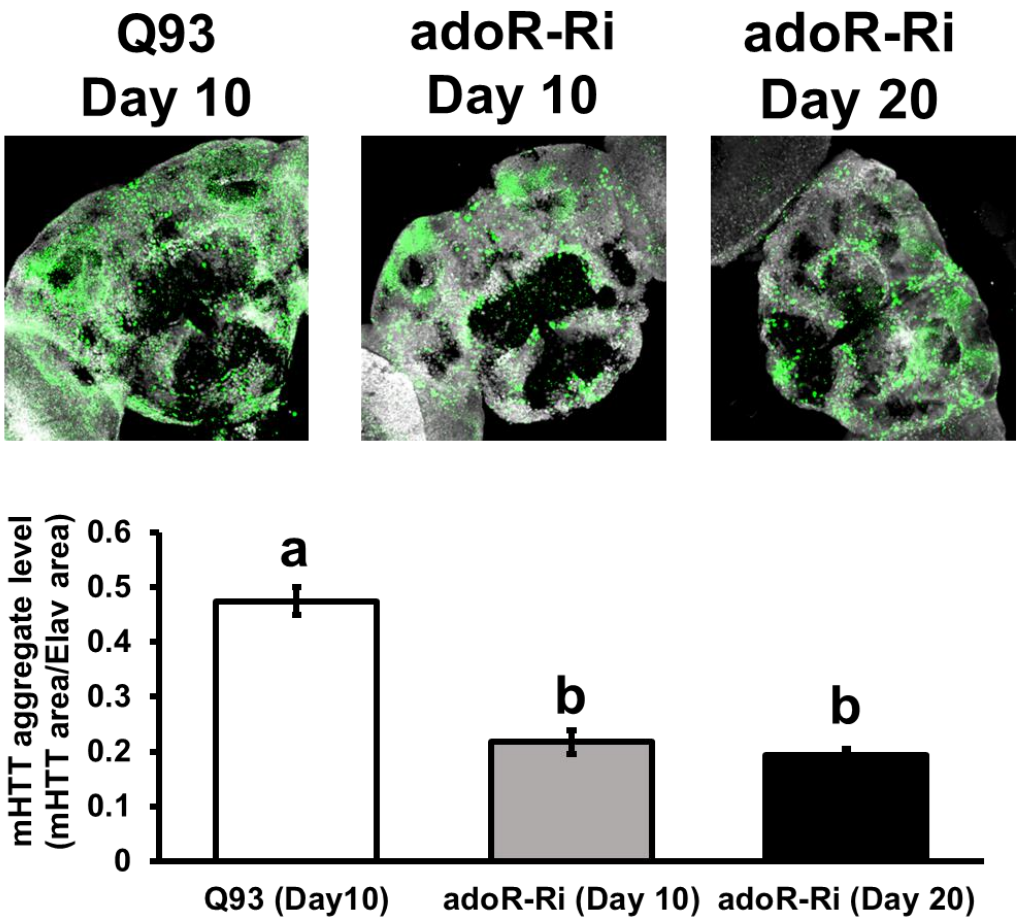

Figure S4. AdoR RNAi suppressed mHTT aggregate formation in the brains of 10- and 20-day-old mHTT flies. Representative confocal images of the brains of mHTT-expressing adult females (elav>Q93) with RNAi silencing *adoR*. Neuronal cells were detected with anti-Elav; mHTT aggregates were detected with anti-HTT (MW8). The level of mHTT aggregate formation was calculated by normalizing the area of mHTT signal to the area of Elav signal. Significance values of mHTT aggregates levels were analyzed by ANOVA; significant differences ($P < 0.05$) among treatment groups are marked with different letters. Error bars are presented as mean ± SEM. n = 6

probe ID	Gene name	Symbol	CG	Ent2^{3}-L	AdoR^{1}-L	AdoR^{1}-A	Localization
1641190_at	Jonah 65Aii	Jon65Aii	CG6580	2.79	2.5	3.18	MG
1627771_at	---		CG13075	2.58	2.91	1.93	HG, MT
1630590_at	---		CG18417	2.02	3.48	4.35	MG, HG
1624393_at	white	w	CG2759	1.77	4.97	4.5	MT
1632003_a_at	Protein tyrosine phosphatase 99A	Ptp99A	CG11516	1.53	1.41	2.32	ID, NS, T
1632404_at	tetracycline resistance	rtet	CG5760	1.02	0.85	2.09	MG, HG, I
1633369_s_at	---		CG6184	-0.23	-0.21	-0.68	NS, tes
1637389_at	Ionotropic receptor 100a	Ir100a	CG11575	-0.67	-0.68	-2.61	non-spec
1635901_at	Protein S-acyltransferase		CG17197	-0.85	-0.63	-1.09	ID, tes
1624020_at	modifier of mdg4	mod(mdg4)	CG32491	-1	-1.4	-0.57	NS, ID
1640850_at	CIN85 and CD2AP orthologue	cindr	CG31012	-1.11	-1.1	-1.02	NS, SS, ID, tes
1627953_at	modifier of mdg4	mod(mdg4)	CG32491	-1.28	-1.08	-1.19	NS, ID
1633748_at	NADH dehydrogenase (ubiquinone) 20 kDa subunit-like	ND-20L	CG2014	-1.94	-2.05	-0.82	ID, tes

Table S1. Intersection genes between the three datasets of microarray analysis. Genes highlighted in red and blue were significantly up- and downregulated (q<0.05), respectively, in the larvae of *ent2* (Ent2^{3}-L) mutant and *adoR* mutants (AdoR^{1}-L) as well as adult of *adoR* mutant (AdoR^{1}-A). Tissue localization of each gene expression was obtained from Flybase (http://flybase.org/). Tissue abbreviations: midgut (MG), hindgut (HG), Malpighian tubule (MT), imaginal disc (ID), integument (I), sensory system (SS), nervous system (NS), trachea (T), testis (tes), non-specific expression (non-spec)

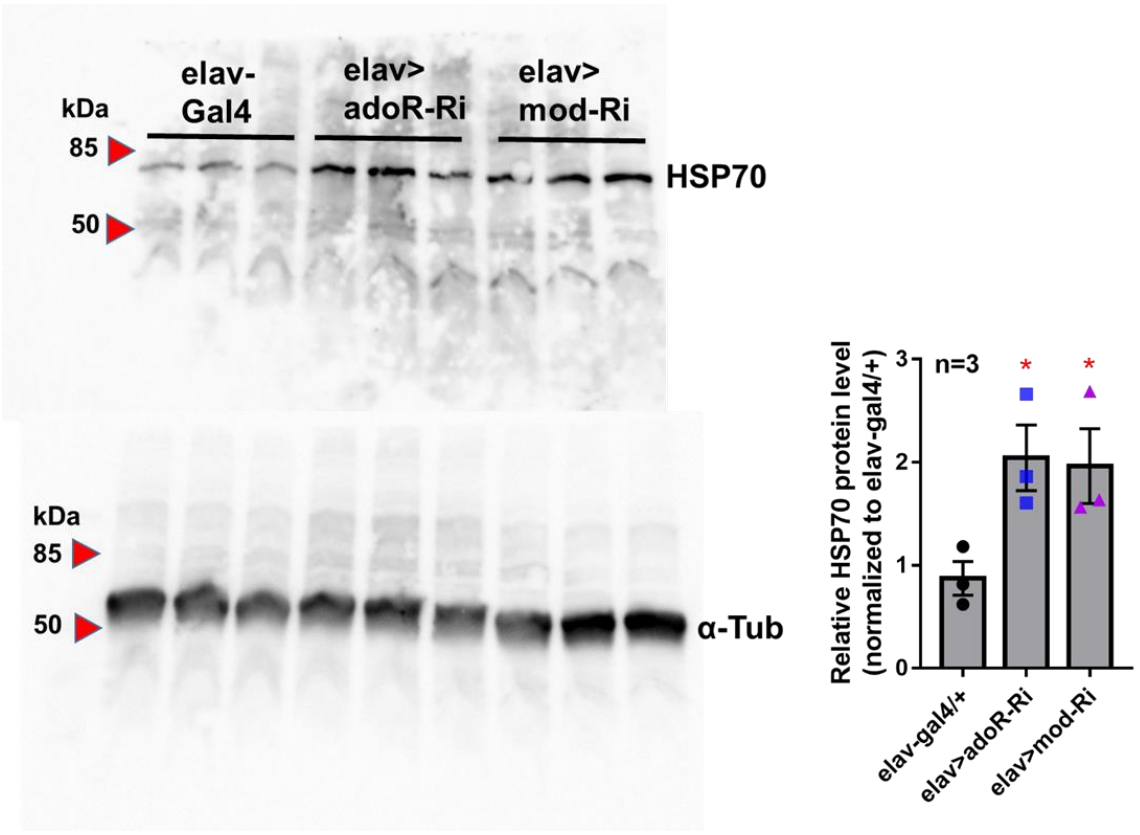

Figure S5. Full image of western blot results shown in Figure 4A. Hsp70 protein levels in the heads of 10-day-old adult females with RNAi silencing adoR (elav>adoR-Ri), mod(mdg4) (elav>mod-Ri) and control (elav-gal4/+). The Hsp70 protein level was quantified by normalizing the intensity of the Hsp70 band to the α-Tubulin band using ImageJ; values of RNAi treatment groups were further normalized to the elav-gal4 control. Significance was analyzed by Student's t-test; significant differences between the control and each RNAi treatment group are labeled as $*P < 0.05$. Error bars are presented as mean ± SEM. n = 3

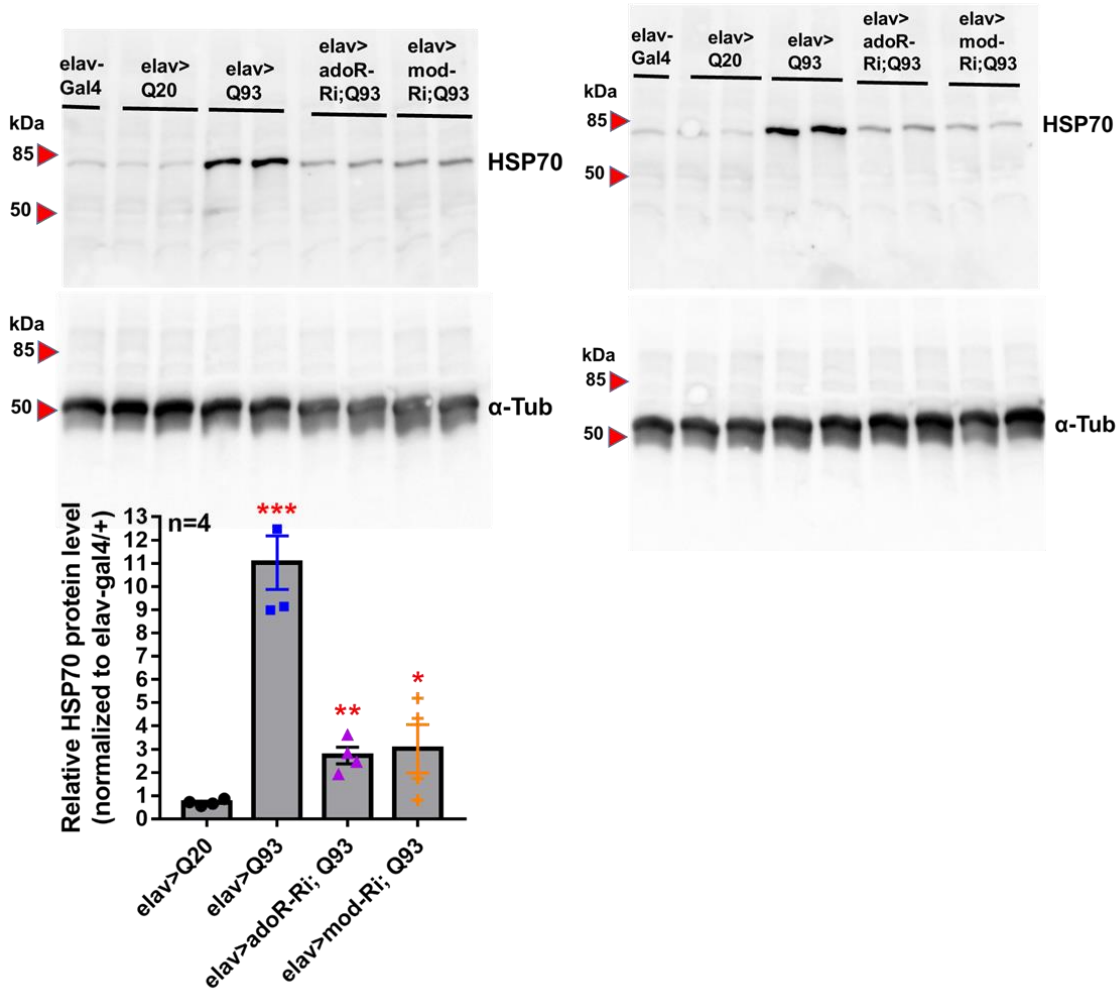

Figure S6. Full image of western blot results shown in Figure 4C. Hsp70 protein levels in the heads of 10-day-old HTT (elav>Q20) or mHTT-expressing (elav>Q93) adult females with RNAi silencing adoR and mod(mdg4). The Hsp70 protein level was quantified by normalizing the intensity of the Hsp70 band to the α-Tubulin band using ImageJ; values for each treatment group were further normalized to the elav-gal4 control. Significance was analyzed by Student's t-test; significant differences between HTT-expressing flies (elav>Q20) with each RNAi treatment of Q93 expressing flies are labeled as follows: $*P < 0.05$, $**P < 0.01$, $***P < 0.001$. Error bars are presented as mean ± SEM. n = 4

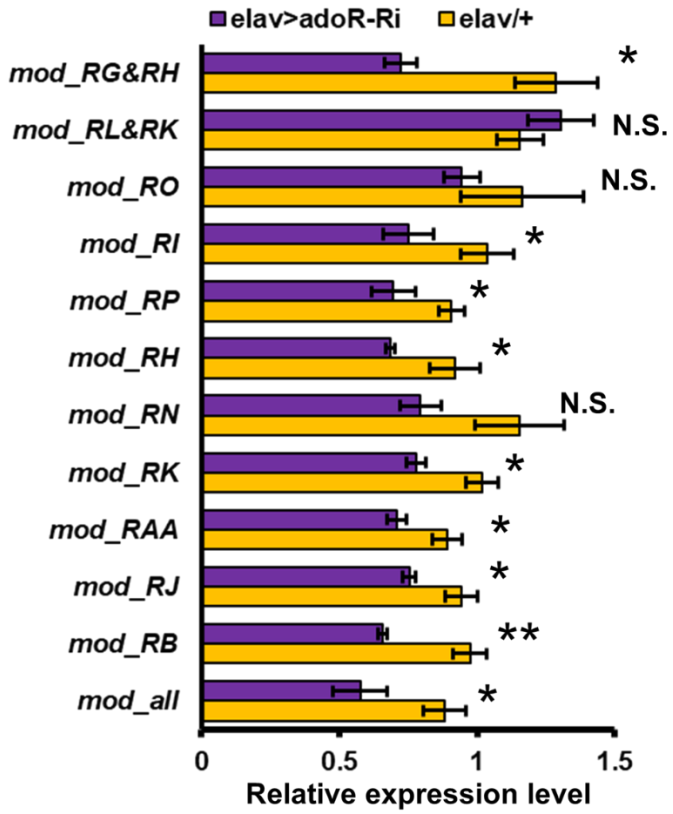

Figure S7. Multiple isoforms of *mod(mdg4)* were downregulated by adoR RNAi. *adoR* RNAi transgene (adoR-Ri) expression was driven by the pan-neuronal driver (elav>adoR-Ri); control flies contained only *elav*-GAL*4* (elav/+). Mod_all indicates that the primers targeted all *mod(mdg4)* isoforms. Isoforms L and G do not have their own unique exonal region, therefore it is possible for the qPCR primers to target two isoforms simultaneously (presented as RG&RG and RL&RK). qPCR result significance was examined using Student's t-test: *$P < 0.05$; **$P < 0.01$; N.S., not significant

genes	left 5'-3'	right 5'-3'
adgf-a	AGGCTCATCCAGATTTCATT	CGGGTACTTTTCCTTTATTTGTT
adgf-c	TGTACACAGAGATTCGGACCAG	TAGACGGCCATAATGACTTTGA
adgf-d	CTGACCACCACCAATAATCTGTA	AGCGCTCCCAAATCTTCTT
adenoK	GAGGATCGGTACGCCAATATCT	AGGAAGAAGCCCGAAATGTAGT
ent1	TCCCTGCGCACCAAGAT	ATAAACTCGGAGGGAAATAGACG
ent2	AAGGGATCAACGTCGGTGT	AATAGGACTTGGCCGTGATG
ent3	CATCGCTCTGGGCATCAC	CCACCGTCAGACCAACATTAT
cnt2	CTTTGCCAATCCCAGTTCC	TAGTTCGCCCGCTCGTC
AdoR	TTTTGCCACCATTATCACTCC	AGGCGGGGTTCATCGTA
mod(mdg4)	CAAGATGTTCACTCAGATGC	CCGAGTGGCTGACGTTGTTC
cindr	ATGACCACAACGAACTCAAGC	CTACTGCTCCCGGTCTTCT
ptp99A	GGGAAGTGCCCGTTAAGATCG	CTGAATCCAATGTCCCCGTC
CG6184	CCCAGATCAGTGTCCAGAAGC	ATCGCCATTCAGATCAGCCG
mod(mdg4)_RO	CCACAGTCGCAAGAGCAATA	GCGGCTGGTGGTTATGTAGT
mod(mdg4)_RI	CATAAAGGAGGAGGGTGACG	TCTCGATTCATTGCAGGTTG
mod(mdg4)_RT	TTCAGTGCTGCTACCGTGAG	GCGACAGCGAGGATATGACT
mod(mdg4)_RAA	CGCTGCTCCATGTACAAAAA	CGAGCACTCTGGGAACAAAT
mod(mdg4)_RN	GACAGAAGAGGCCAAGCATC	CCTTCCGTGGTTCGAGATAA
mod(mdg4)_RH	CACAAGTGATAAGACACTCCCAAG	CGTTTTGGAAGAGCAGCAC
mod(mdg4)_RG+RH	CCGCCTCTCGTACTTATTGG	TGATGATTCGCTCCTGTGAG
mod(mdg4)_RB	CGTAAAACCCGATCAACACC	GTAACGATGCTCCCCACAGT
mod(mdg4)_RJ	CAAGACCTCGGGATTGAAAA	TAGGGCGGATGGTTATGTTG
mod(mdg4)_RL+RK	CCATTGCTTGACCAGGAACT	CGGATTCGGCCTATGACTAC
mod(mdg4)_RP	CATGCTCAAGCAACACACCT	GCTGTTCAGGATGGTGAGTG
mod(mdg4)_RK	CAAGCGTTTGAACGAGAACA	GGATGATTGTGGGCATTCTT

Table S1. Table S1. List of qPCR primers used in the present study

Publication III

Yu-Hsien Lin, **Houda Ouns Maaroufi**, Emad Ibrahim, Lucie Kucerova, Michal Zurovec (2019). Expression of human mutant huntingtin protein in *Drosophila* hemocytes impairs immune responses. *Frontiers in immunology*. DOI: 10.3389/fimmu.2019.02405

As an extension of the previous publication, we examined one of the less studied effects of the mHTT mutation, namely immune system impairment. In this publication, we expressed mHTT in *Drosophila* hemocytes. We found that the number of circulating hemocytes was decreased in Q93 flies. Therefore, we investigated whether the immune response to infection was impaired in Q93 larvae. We infected larvae with the nematodes *Heterorhabditis bacteriophora* or *Steinernema carpocapsae* and found that Q93 larvae had higher mortality than the control group. We also observed a decrease in the clotting activity of the hemolymph of Q93 larvae, suggesting that the susceptibility to infection was due to the poor quality of the hemolymph clot. Similarly, infection of Q93 larvae with a parasitic wasp *Leptopilina boulardi* showed a high number of emerging wasps compared to the control, indicating that the wasps overwhelmed the larval immune system. This phenotype was associated with a defect in wasp eggs melanization. We further investigated whether mHTT expression alters hemocyte function by using S2 cell lines expressing mHTT. The S2 cells were infected with E. coli particles conjugated with a pH-sensitive dye (pHrodo), and we observed decreased phagocytic activity in mHTT-expressing cells. We also checked whether the phagocytic activity of S2 cells was affected by mitochondrial dysfunction and impaired energy metabolism. In mHTT-expressing cells, ATP levels were significantly decreased, which could limit the cellular immune responses against pathogenic infections. The phenotype was associated with increased expression of cytokines, with *upd3* strongly expressed in mHTT-expressing cells compared with controls. In addition, expression of *dome* receptor and several downstream targets of the JAK/STAT pathway were also increased. The phenotype was associated with a decrease in antimicrobial peptide production upon bacterial infection. This study provides a novel system to study tissue-specific effects of mHTT in *Drosophila* immune cells.

frontiers in Immunology

ORIGINAL RESEARCH
published: 16 October 2019
doi: 10.3389/fimmu.2019.02405

Expression of Human Mutant Huntingtin Protein in *Drosophila* Hemocytes Impairs Immune Responses

Yu-Hsien Lin[1,2]*, *Houda Ouns Maaroufi*[1,2], *Emad Ibrahim*[1,2], *Lucie Kucerova*[1] and *Michal Zurovec*[1,2]*

[1] Biology Centre of the Czech Academy of Sciences, Institute of Entomology, Ceske Budejovice, Czechia, [2] Faculty of Science, University of South Bohemia, Ceske Budejovice, Czechia

The pathogenic effect of mutant HTT (mHTT) which causes Huntington disease (HD) are not restricted to nervous system. Such phenotypes include aberrant immune responses observed in the HD models. However, it is still unclear how this immune dysregulation influences the innate immune response against pathogenic infection. In the present study, we used transgenic *Drosophila melanogaster* expressing mutant HTT protein (mHTT) with hemocyte-specific drivers and examined the immune responses and hemocyte function. We found that mHTT expression in the hemocytes did not affect fly viability, but the numbers of circulating hemocytes were significantly decreased. Consequently, we observed that the expression of mHTT in the hemocytes compromised the immune responses including clot formation and encapsulation which lead to the increased susceptibility to entomopathogenic nematode and parasitoid wasp infections. In addition, mHTT expression in *Drosophila* macrophage-like S2 cells *in vitro* reduced ATP levels, phagocytic activity and the induction of antimicrobial peptides. Further effects observed in mHTT-expressing cells included the altered production of cytokines and activation of JAK/STAT signaling. The present study shows that the expression of mHTT in *Drosophila* hemocytes causes deficient cellular and humoral immune responses against invading pathogens. Our findings provide the insight into the pathogenic effects of mHTT in the immune cells.

Keywords: Huntington's disease, immunity, infection, *Drosophila* melanogaster, phagocytosis, cytokines, antimicrobial peptide (AMPs)

OPEN ACCESS

Edited by:
Susanna Valanne,
University of Tampere, Finland

Reviewed by:
Jenny Sassone,
Vita-Salute San Raffaele University, Italy
Ioannis Eleftherianos,
George Washington University, United States

***Correspondence:**
Yu-Hsien Lin
r99632012@gmail.com
Michal Zurovec
zurovec@entu.cas.cz

Specialty section:
This article was submitted to Comparative Immunology, a section of the journal Frontiers in Immunology

Received: *20 June 2019*
Accepted: *25 September 2019*
Published: *16 October 2019*

Citation:
Lin Y-H, Maaroufi HO, Ibrahim E, Kucerova L and Zurovec M (2019) Expression of Human Mutant Huntingtin Protein in Drosophila Hemocytes Impairs Immune Responses. Front. Immunol. 10:2405. doi: 10.3389/fimmu.2019.02405

INTRODUCTION

Huntington's disease (HD) is an inherited neurodegenerative disorder caused by an abnormal expansion of CAG trinucleotide in the Huntingtin (*htt*) gene. Mutant HTT protein (mHTT) contains an extended polyglutamine tract encoded by 40 to over 150 CAG repeats, which causes cytotoxicity and leads to neurodegeneration; this results in involuntary movement, cognitive impairment, and psychiatric abnormalities (1). Although many clinical symptoms of HD are related to neuronal dysfunction, emerging evidence indicates that the expression of mHTT in non-neuronal cells of the brain or in the peripheral tissues also contributes to the pathogenesis of HD (2). Abnormal phenotypic effects caused by the dysfunction of non-neuronal cells have been described in cardiac cells, muscles, the endocrine system, adipose tissue, testes and immune cells of HD patients, and also in mouse HD models (2, 3).

Abnormalities related to the immune system were observed in a number of studies of HD patients (4). The expression of mHTT in both brain and peripheral immune cells (microglial and myeloid cells) induces the NF-κB signaling pathway which elevates levels of pro-inflammatory cytokines and chemokines, leading to systemic inflammation (5). In addition, macrophages isolated from HD model mice exhibited migration deficits, and microglia showed a delayed response to laser-induced injury in the brain (6). Although several studies proposed that the immune cell response is impaired in HD, this phenomenon is still poorly characterized in relation to host responses to pathogens. One recent study reported increased proliferation of a parasite, *Toxoplasma gondii*, in HD model mice, causing premature mortality and thus suggesting that expression of mHTT in immune cells may suppress immune responses (7).

Drosophila melanogaster has been long-term established as a HD model. *In vivo* experiments have revealed that the ectopic overexpression of mutant human *htt* (exon 1 with expanded CAG repeats) in the neural tissue of transgenic flies causes neurodegeneration (8, 9). The mechanisms of cellular pathology observed in the HD flies seem similar to those in human patients, including the suppression of mitochondrial function, transcriptional dysregulation, and neuronal apoptosis (10, 11). Genetic screening for disease modifiers in HD model flies led to the identification of the effects of sumoylation and HSP70 chaperone machinery on neurodegeneration. The subsequent confirmation that these pathways are involved in the pathology of human patients validates the *Drosophila* model for investigating HD (12, 13). Furthermore, since the tissue-specific expression of transgenes in *Drosophila* can be easily controlled using the UAS-Gal4 system, *Drosophila* have also been used to study the effects of HD on non-neuronal cells, including glial cells, photoreceptors, cardiac cells, and salivary glands (14–18).

The present study aimed to survey the physiological impact of mHTT expression in *Drosophila* hemocytes. We used the *Drosophila* UAS-Gal4 system to express mHTT with hemocyte-specific drivers and investigated the effect of mHTT on survival, hemocyte development, and susceptibility to pathogens. We also expressed mHTT in a *Drosophila* macrophage-like cell line, S2 cells, and assessed the effect of mHTT on phagocytic activity, ATP levels, antimicrobial peptides, and production of cytokines. Our results suggest that the expression of mHTT in hemocytes does not directly affect survival but causes immune dysregulation, which leads to an impaired immune response against pathogenic invasion.

RESULTS

Expression of mHTT in Hemocytes Did Not Affect Larval Viability but Decreased the Number of Circulating Hemocytes

In order to characterize the effects of mHTT in *Drosophila* hemocytes, we used a tissue-specific UAS-Gal4 system by expressing wild-type human HTT (Q20) or mutant HTT (Q93) under the control of a pan-neuronal driver, *elav-gal4*, or hemocyte drivers, *hml-gal4,* and *he-gal4.* The flies devoid of plasmatocytes (*phago*^{less}) generated by expressing pro-apoptosis genes, *rpr* and *hid* with *hml-gal4* were used as negative control (19, 20). The results showed that the ectopic expression of Q93 with the pan-neuronal driver (*elav-gal4*) decreased both the eclosion rate and the longevity of the adult flies, but not the rate of pupariation (**Figure 1**). The expression of Q20 and Q93 with both hemocyte drivers (*hml-gal4* and *he-gal4*) had no effect on pupariation and eclosion rates. Furthermore, the differences in longevity between Q20 and Q93 flies were not significant, and their survival rate was higher than *phago*^{less} flies (**Figure 1C**). These results indicated that the hemocyte-specific expression of mHTT did not influence fly viability, unlike its expression in the brain.

Although the expression of mHTT did not affect fly survival, we observed a significant decrease in the number of circulating hemocytes. In first-instar larvae, the number of hemocytes differed significantly only in the *phago*^{less} flies (**Figure 2A**). However, a reduced amount of circulating and sessile hemocytes was apparent in the Q93 mutants from second-instar larvae. As shown in **Figure 2B**, the circular hemocyte numbers in Q93 larvae were still higher than in *phago*^{less} flies, showing about 50% of the numbers observed in the Q20 control (**Figure 2B**). These results showed that the expression of mHTT with two different hemocyte-specific drivers reduced the number of hemocytes.

Expression of mHTT in Hemocytes Impaired the Immune Response to Parasites

To examine whether mHTT expression in *Drosophila* hemocytes affects the innate immune response and whether such larvae are still able to restrain parasite development, we tested the sensitivity of such flies to entomopathogenic nematode and parasitoid wasp infections, which are two *Drosophila* pathogenic models for examining the cellular immune response (21, 22). Early third-instar larvae expressing mHTT (Q93), wild-type HTT (Q20) or *phago*^{less} were infected with nematode species, *Heterorhabditis bacteriophora* or *Steinernema carpocapsae*, which contain the bacterial symbionts *Photorhabdus luminescens* and *Xenorhabdus nematophila*, respectively. Mortality was calculated at 24 and 48 h post-infection. As shown in **Figure 3**, both *phago*^{less} and Q93 larvae displayed significantly higher mortality than Q20 controls. Previous studies revealed that the formation of hemolymph clot is an important innate immune response against entomopathogenic nematode infection in *Drosophila* (23, 24). To determine whether the expression of mHTT in the hemocytes caused clotting defects, we used an established bead aggregation assay (24, 25). Compared to the larvae expressing normal HTT (Q20), the hemolymph collected from mHTT (Q93)-expressing larvae displayed poor bead aggregation similar to *phago*^{less} larvae (**Figure 3E**). This results indicated that the expression of mHTT suppresses the clotting activity and thus increases the susceptibility to nematode infection.

Similarly, we infected *Drosophila* larvae with a parasitoid wasp, *Leptopilina boulardi* and calculated the number of emerged

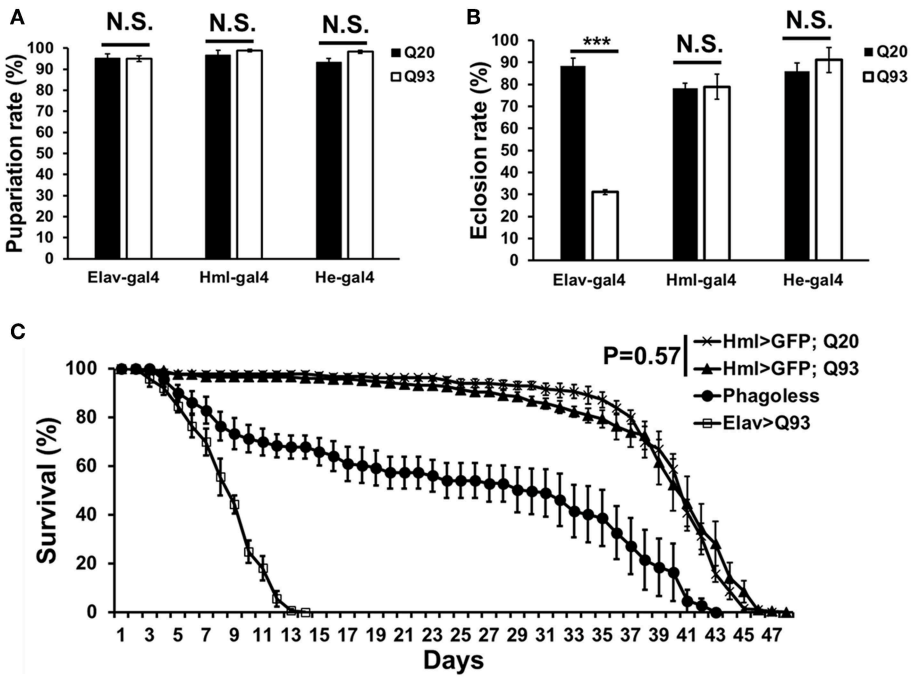

FIGURE 1 | The viability assays of mHTT-expressing flies under the control of the pan-neuronal driver (*elav-gal4*) and hemocyte drivers (*hml-gal4* and *he-gal4*). **(A)** The effect of mHTT expression on pupariation (survival to pupal stage). **(B)** Eclosion (survival to adulthood) and **(C)** adult longevities were measured in control Q20 and mHTT Q93. All the experiments performed in at least six independent replicates. Data are presented as averages ± SEM. *P*-values for pupariation and eclosion rate using Student's *t*-test, ***$P < 0.001$, N.S., not significant. Significance analysis for longevity curve using weighted log-rank test.

fly and wasp adults. The number of eclosed *Drosophila* adults was not significantly different between Q20 and Q93 driven by *hml-gal4* and *he-gal4*, while *phago*^{less} showed lower eclosion rates than both Q20 and Q93 (**Figures 4A,B**). However, the number of emerged wasps were significantly higher in both Q93 and *phago*^{less} flies, thus indicating that a greater number of wasps overwhelmed the immune reaction of Q93 hosts and successfully developed to adult stage. In addition, the higher number of wasp eggs successfully hatched in both Q93 and phagoless larvae (**Figure 4C**); these results indicated that Q93 and *phago*^{less} larvae have less efficient immune reaction against wasp infection. Since the encapsulation and melanization are major defense mechanisms against parasitoid wasp infection, we quantified the number of the melanized capsules to assess the immune activity after 72 h post-infection. We found that there were more intact melanized capsules in Q20 larvae (79%) than in those expressing Q93 (51.6%) or in *phago*^{less} (17.7%) (**Figures 4D,G** left). We also observed a higher amount of melanization pieces in Q93 or *phago*^{less} individuals than in Q20 larvae (**Figures 4E,G** middle). The formation of such defective capsules was described previously in immune-deficient mutant flies (26). Moreover, 37% of the infected *phago*^{less} larvae formed no melanization capsules compared to Q20 (0%) or Q93 (4.8%) infected larvae (**Figures 4F,G** right). These results could explain a lower proportion of *phago*^{less} adults successfully eclosed after wasp infection (**Figures 4A,B**). Taken together, our results suggest, that mHTT expression impairs the innate immune reactions to nematode and parasitoid wasp infections due to the deficient cellular immune responses such as clot formation and encapsulation.

Reduced Phagocytic Activity and ATP Levels in mHTT Cells

To find out whether mHTT expression could cause a detrimental effect on hemocyte functions, we expressed mHTT or wild-type HTT in *Drosophila* S2 cells. The S2 cell line consists of macrophage-like cells with phagocytic activity and the ability to produce antimicrobial peptides (AMPs) (27). We transfected the cells with four different recombinant constructs encoding green fluorescent protein (GFP) fused to HTT repeats under an inducible metallothionein promoter. We created stable cell lineages and confirmed that the S2 cells expressed HTT-fusion proteins by observing the GFP. As shown in **Supplemental Figure 1**, most of the cells in all cell lineages were positive for the fluorophore. Furthermore, the cells containing the mHTT Q46, Q72, and Q97 constructs (all except wild-type Q25) showed formation of mHTT aggregates.

We further treated the HTT-expressing cells with *E. coli* particles conjugated by pH-sensitive dye (pHrodo) to examine their phagocytic activity. This causes bright fluorescence to be visible after particle engulfment in the acidic environment of phagolysosome. The results showed that after inducing mHTT expression, the fluorescence signals were significantly lower in Q46, Q72, and Q97 mHTT-expressing cells but not in cells expressing wild-type Q25 HTT (**Figure 5A**). Quantification of the cells containing fluorescent signals showed a significant

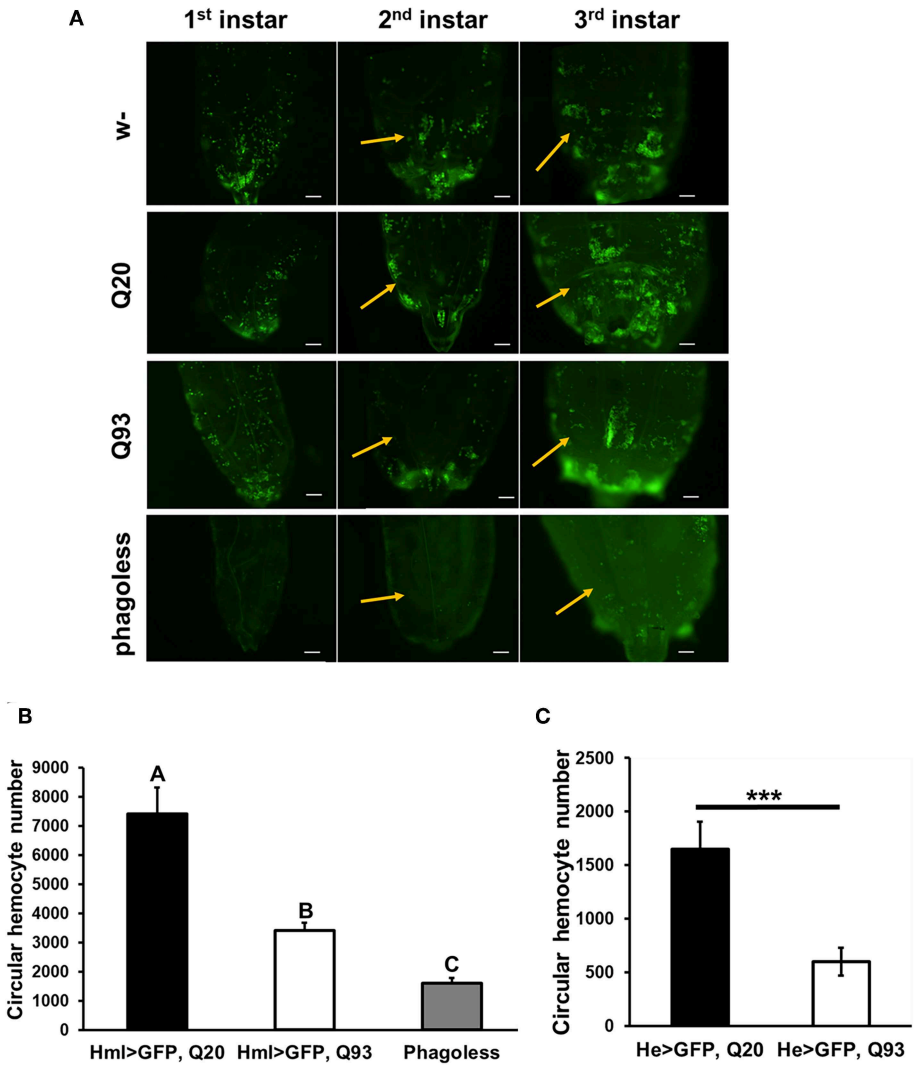

FIGURE 2 | Ectopic expression of mHTT decreased hemocyte numbers. **(A)** Microscope images indicated the decreased number of circulating and sessile hemocytes in mHTT-expressing second-instar larvae. Quantification of hemocytes by ectopic co-expression of HTT with GFP using *hml-gal4* **(B)** or *he-gal4* **(C)**. *Phago*^{less} flies with hemocyte ablation (*hml > UAS-rpr, hid*) were used as a negative control. The number of the circular hemocyte corresponded to the total number of GFP positive cells in 25 μL of collected sample. At least five independent replicates were analyzed. Data are presented as averages ± SEM. Significances were analyzed by ANOVA with Fisher LSD *post-hoc* test **(B)**, and the significant differences among treatment groups are marked with different letters ($P < 0.05$). Student's *t*-test was used for **(C)**, $^{***}P < 0.001$.

reduction (20–30%) of fluorescent-positive cells in mHTT-expressing cells compared to the control cells (Q25) (**Figure 5B**), thus supporting the hypothesis that expression of mHTT in immune cells impairs phagocytic activity.

The phagocytic capacity of immune cells has been associated with mitochondrial activity (28–30); mHTT has been shown to cause impairment of energy metabolism and mitochondrial dysfunction in human peripheral blood cells (31). To test whether mHTT can also impair the energy metabolism of *Drosophila* immune cells, we measured the ATP levels in S2 lineages after mHTT induction. The results showed that ATP levels significantly decreased in cells expressing Q72 and Q97 mHTT after 72 h of induction (**Figure 6A**). The ATP levels in cells expressing Q46, Q72, and Q97 mHTT were further reduced after 120 h of induction (**Figure 6B**). This indicated that the expression of mHTT reduces ATP levels, which may further limit the cellular immune responses against pathogenic infection.

The studies in human and mouse have demonstrated that the expression of Bcl-2 family proteins associated with mitochondrial dysfunction is activated by mHTT expression (32). To assess whether the level of *Drosophila* Bcl-2 proteins is also altered by mHTT expression, we compared the transcription levels of two of *Bcl-2* genes, *buffy* and *debcl*, in Q25- and Q97-expressing S2 cells (**Figure 6C**). We found that *buffy* expression is five times higher in Q97- than in Q25- expressing cells, but we did not detect any significant difference in *debcl* mRNA

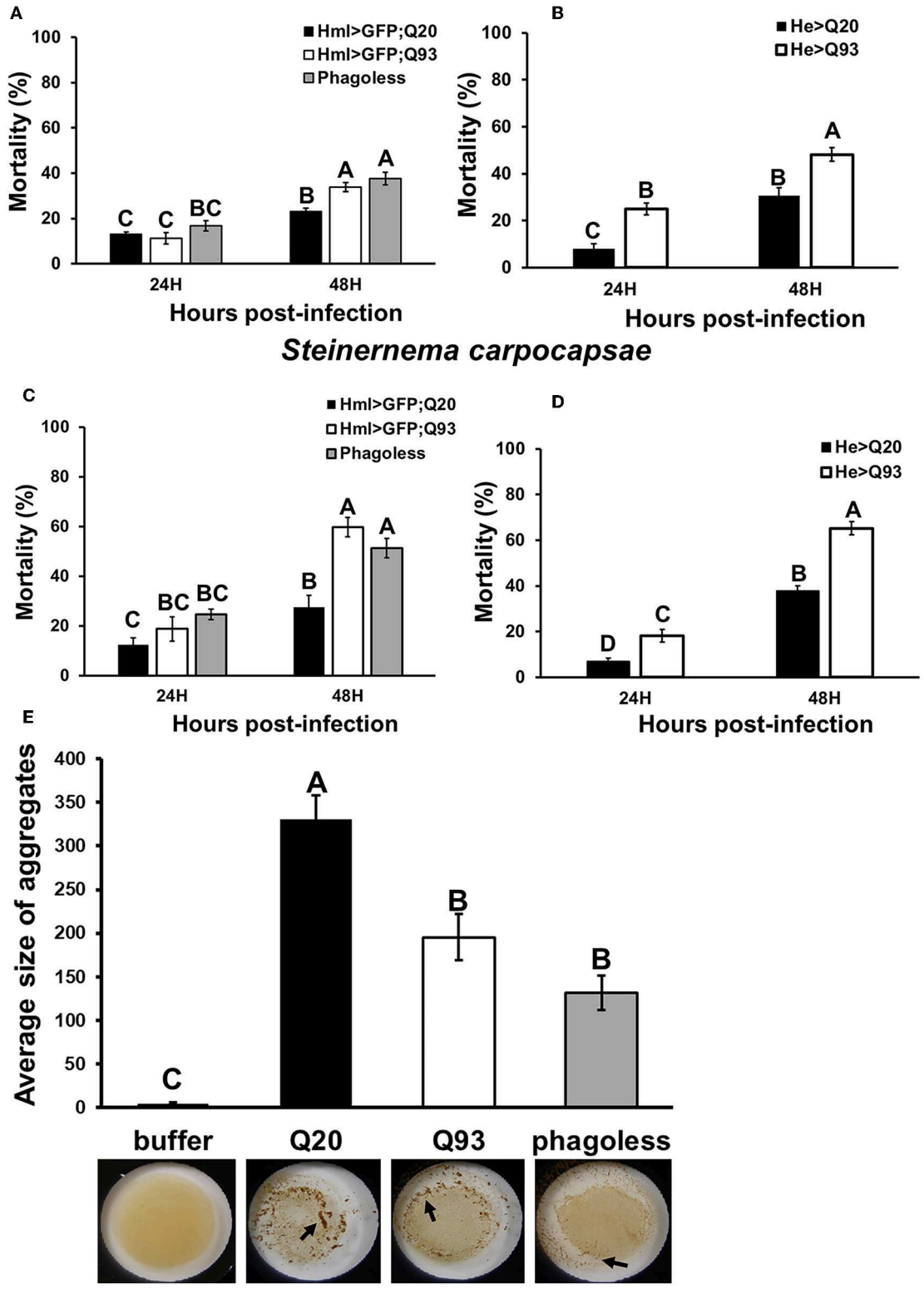

FIGURE 3 | Immune challenge with entomopathogenic nematode infection and clotting assay. Larvae expressing mHTT Q93 or HTT Q20 with *hml-gal4* or *he-gal4* hemocyte drivers were infected with *H. bacteriophora* **(A,B)**, or *S. carpocapsae* **(C,D)**. Mortality was calculated 24 and 48 h after infection. *Phago*^{less} flies with

(Continued)

FIGURE 3 | hemocyte ablation (*hml > UAS-rpr, hid*) were used as negative control. Bead aggregation assay was used for assessing the clotting activity **(E)**. Hemolymph was collected from Q93, Q20, and *Phago*^{less} (*hml-gal4*) larvae, mixed with a bead suspension, and the aggregates were quantified by ImageJ software. All the experiments were performed in five to six independent replicates. Data are presented as averages ± SEM. Significances were analyzed by ANOVA with Fisher LSD *post-hoc* test; significant differences among treatment groups are marked with different letters ($P < 0.05$).

level. Different from pro-apoptotic function of *debcl*, *buffy* was suggested to play an anti-apoptotic role under stress conditions which is similar to mammalian Bcl-2 proteins (33, 34). We conclude that the alternation of ATP synthesis and *buffy* expression indicate the abnormality of mitochondrial function in mHTT expressing cells, and the induction of *buffy* might be a protective mechanism for preventing the cell death caused by mitochondrial dysfunction.

Upregulation of Cytokines Expression and Downstream JAK/STAT Signaling in mHTT Expression Cells

It has been reported that the level of cytokines and chemokines are abnormally increased in the plasma of HD patients (35). Consistently, the production of cytokines from monocytes and macrophages of HD patients have shown hyper-activation after lipopolysaccharide stimulation (36). To test whether mHTT has a similar effect in *Drosophila*, we used Schneider 2 (S2) cells and measured the effect of mHTT expression on three *Drosophila* cytokines, *upd1*, *upd2*, and *upd3*, as well as *dome*, *jak* (*hop*) and downstream targets of JAK-STAT signaling (**Figure 7A**). The results showed that the expression of cytokine *upd3* is significantly increased in Q97 mHTT-expressing cells compared to Q25 controls (**Figure 7B**). In addition, the expression of *dome* receptor and four downstream targets, *tep1*, *totA*, *totB,* and *totC* were also significantly increased in Q97-expressing cells. These results indicated that the expression of mHTT induced the production of cytokines and activates JAK/STAT signaling.

Decreased Antimicrobial Peptide (AMP) Production in Response to Bacteria

Drosophila Toll and Imd pathways control the humoral immune response against invasive microorganisms by regulating the induction of downstream AMP genes in both hemocytes and the fat body (37). To examine whether AMP induction was affected by mHTT expression in *Drosophila* S2 cells, we treated mHTT-expressing cells with a mixture of heat-inactivated Gram-negative bacteria, *Escherichia coli*, and Gram-positive bacteria, *Micrococcus luteus*. The induction of AMPs was assessed using qPCR. As shown in **Figure 8**, there was no difference in the expression of AMPs between Q25 and Q97 in the absence of bacterial treatment. In contrast, all AMP genes were significantly induced in both Q25- and Q97-expressing cells at 8 h after bacterial treatment. However, AMP induction levels were significantly lower in cells expressing Q97 (**Figure 8A**). We further assessed the AMP expression levels under *in vivo* condition after infecting larvae with phytopathogenic bacteria, *Erwinia carotovora carotovora 15* (Ecc15). We examined the expression levels of *dpt*, *dptB*, *attA,* and *cecA* which were known as being highly induced after Ecc15 infection (38). Our results of larval infections showed that except for *attA*, the induction levels of *dpt*, *dptB,* and *cecA* in Q93 or *phago*^{less} larvae were significantly lower than in Q20 controls (**Figure 8B**). These results confirm that the induction of AMPs in response to bacteria was significantly suppressed in mHTT-expressing cells or larvae.

DISCUSSION

Peripheral immune dysregulation is considered as one of the clinical features of HD pathogenesis (39). Previous studies in mice and HD patients have suggested that mHTT expression in immune cells accelerates the neurodegenerative process. The activation of pro-inflammatory products in mHTT-expressing microglial cells elevate the reactive oxygen species (ROS) and cause neuroinflammation, which contributes to neurodegeneration (5, 40). Genetic ablation or pharmacologically-blocked cannabinoid receptor 2 (interleukin-6 regulator), as well as drug suppression of the cytokine-responsive kynurenine pathway, can both slow neurodegeneration and improve the phenotype of R6/2 HD mice (41, 42). Since the expression of mHTT in HD mice and human patients is ubiquitous, it is still unclear whether mHTT expression in blood cells directly contributes to the lethal effect of HD. The present study examined mHTT expressed specifically in *Drosophila* blood cells and assessed its impacts on development and longevity (**Figure 1**). We found that the expression of mHTT in hemocytes did not cause mortality or a shortening in life span, which is in contrast to expression in the brain. Our results, therefore, suggest that expression of mHTT in immune cells does not directly contribute to mortality.

A reduced proliferation of immune cells has been observed in *T. gondii*-infected HD mice, in which the expansion of $CD8^+$ T-cells in the spleen and brain was significantly suppressed during infection (7). Our results showed that the expression of mHTT in flies with hemocyte-specific drivers causes a significant reduction in the number of circulating hemocytes (**Figure 2**), and this decrease might be caused by dysfunction of mitochondria (**Figure 7**). The mitochondrial abnormalities resulting in metabolic dysregulation in peripheral blood cells of HD patients increase oxidative damage and suppress their anti-oxidant capacity (40). The activation of caspase-3 and caspase-9 in lymphoblasts of HD patients increases apoptosis under stress conditions (43).

The mHTT-expressing larvae revealed a higher susceptibility to wasp and nematode infections and this phenotype was caused by defects of clot formation and encapsulation (**Figures 3**, **4**). It has been shown that wasp egg recognition by circulating plasmatocytes and their differentiation to lamellocytes for further encapsulation are important processes of the immune response against wasp invasion in *Drosophila* (44). The production of clotting components from hemocytes also contributes to

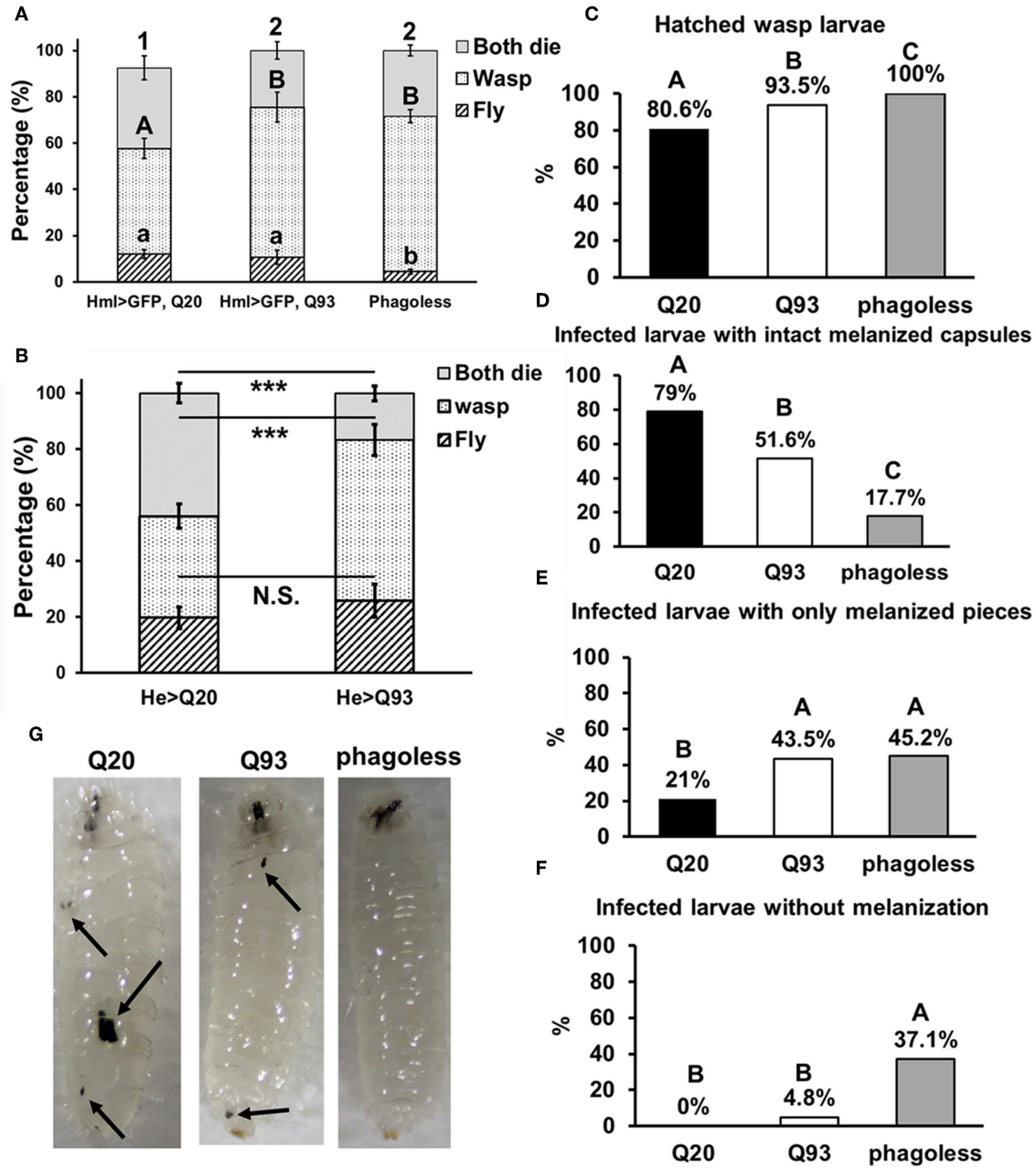

FIGURE 4 | Immune challenge with parasitoid wasp infection and encapsulation activity assay. Larvae expressing mHTT Q93 and HTT Q20 with *hml-gal4* **(A)** or *he-gal4* **(B)** hemocyte driver were infected with parasitoid wasp, *L. boulardi*. *Phago*^{less} flies (which underwent hemocyte ablation) were used as negative control. Thirty infected larvae were collected and the numbers of eclosed flies and wasps were calculated, indicating the number of flies overcoming the wasp infection and the number of wasps successfully escaping the fly's immune reaction, respectively. Data are presented as average ± SEM with more than 10 biological replicates. The significances of results for **(A)** were analyzed by ANOVA with a Fisher LSD *post-hoc* test; different letters on the treatment group indicate significant differences at $P < 0.05$. The significances of results for **(B)** were examined using Student's *t*-test, $^{***}P < 0.001$, N.S., not significant. For assessing the encapsulation activity, the numbers of fly larvae containing larvae of parasitic wasps **(C)**, intact melanized capsules **(D)**, melanized pieces **(E)** as well the numbers of the infected larvae without melanization **(F)** were recorded. The significances of the results were analyzed by Mann-Whitney *U*-test (paired); significant differences among treatment groups are marked with different letters ($P < 0.05$). The photos show examples of intact melanized capsule in Q20 larvae, melanized pieces in Q20 and Q93 larvae and infected *phago*^{less} without melanization reaction **(G)**.

wound healing and melanization, which are important against nematode or wasp infections (24, 45). mHTT-expressing macrophages and monocytes from HD mice and patients also showed migration defects toward an inflammatory stimulus (6). Hemocyte migration and adhesion are important factors for the development of embryonic macrophages, as well as successful

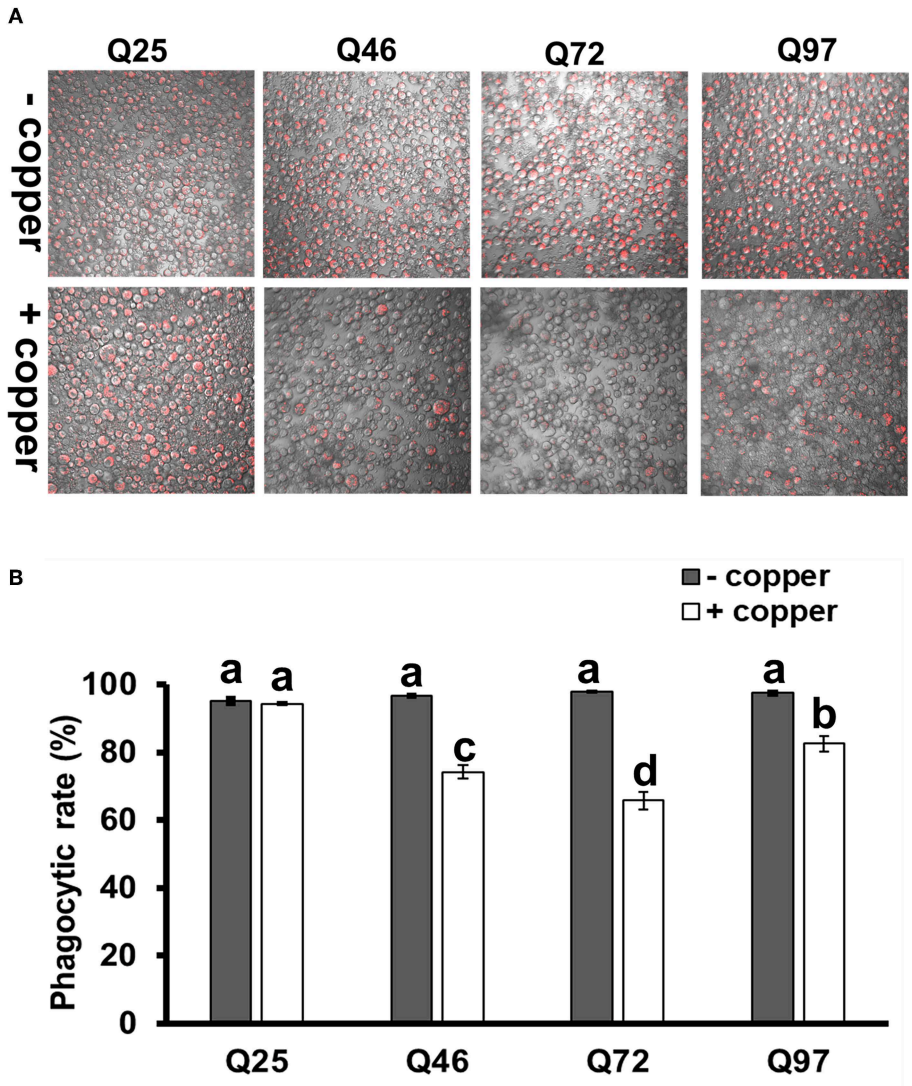

FIGURE 5 | Impairment of phagocytic activities in mHTT-expressing S2 cells. S2 cell lineages expressing wild-type HTT (Q25) and mHTT (Q46, Q72, and Q97) were treated with pHrodo Red *E. coli* for 8 h. **(A)** Fluorescence microscope images show the decreased intensity of red fluorescence signals in mHTT-expressing cells. **(B)** The phagocytic rate was calculated as the percentage of cells showing a red fluorescence signal to the total number of cells in each image. Each treatment was performed in three independent replicates with (+copper) or without (–copper) $CuSO_4$ induction. Data are presented as average ± SEM. Significances were analyzed by ANOVA with Tukey HSD *post-hoc* test; different letters on the treatment group indicate significant differences at $P < 0.05$.

wound healing and encapsulation during wasp infection (46). Furthermore, decreased phagocytic activity toward bacterial particles (**Figure 5**) and a suppressed induction of antimicrobial peptides (**Figure 8**) can also contribute to immune deficiency against the bacterial symbionts of nematodes (23, 47).

A previous study showed that macrophages isolated from HD patients and R6/2 mice displayed increased phagocytosis when incubated with fluorescent polystyrene beads (48). Our results seemingly differ because we observed reduced phagocytic activity of the *Drosophila* macrophage-like cells expressing different mHTT fragments (**Figure 5**). Unlike their approach, we tested phagocytic activity using *E. coli* particles with a pH-sensitive fluorescent dye that can accurately confirm phagosome formation and initiation of the phagolysosome acidification. However, similar to their results, we found that S2 cells expressing mHTT were able to initiate phagocytosis. We tested this by treating the S2 cells with heat-inactivated *E. coli* labeled with DNA-specific fluorescent dye (without pH-sensor); the results showed that mHTT-expressing cells were indeed able to engulf *E. coli* (**Supplemental Figure 2**). Thus, our results suggest that mHTT-expressing cells were unable to complete the process of phagocytosis to final phagolysosome acidification. In addition, a defective actin function has been reported in HD mouse immune cells leading to failure of membrane ruffling (6),

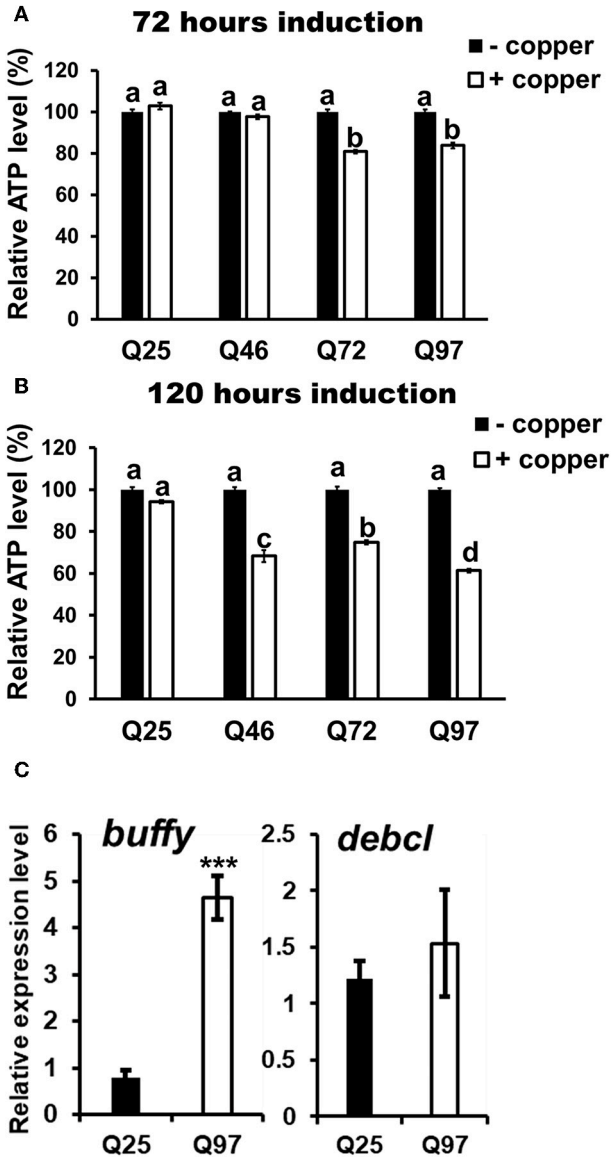

FIGURE 6 | Decrease of ATP level and alternation of Bcl-2 protein expression in mHTT-expressing S2 cells. ATP levels of HTT- and mHTT-expressing S2 cells (5×10^4 cells) were measured after 72 **(A)** and 120 h **(B)** of copper induction. Each treatment was performed in five independent replicates with (+copper) or without (–copper) copper induction. Data are presented as average ± SEM. Significances were analyzed by ANOVA with Tukey HSD *post-hoc* test; different letters on the treatment group indicate significant differences at $P < 0.05$. The mRNA levels of *Drosophila* Bcl-2 proteins, *buffy* and *debcl* were measured in Q25 HTT and Q97 mHTT-expressing S2 cells after 120 h of induction **(C)**. All the expressions were normalized to *rp49* transcript and Q25 control (ΔΔCT). Data are presented as average ± SEM from three independent replicates. *P*-values were determined using Student's *t*-test, $^{***}P < 0.001$.

which supports our results since actin assembly is required to trigger engulfment and phagolysosome maturation for successful phagocytosis (49).

Consistent with previous observations in HD mice and patients, we also found that *Drosophila* hemocyte cytokine *udp3* was upregulated in mHTT-expressing cells (**Figure 8**). *Udp3* binds to the JAK/STAT signaling receptor, Dome, and initiates phosphorylation cascades which translocate the transcription factor, Stat92E, into the nucleus and activates downstream target genes (**Figure 7A**) (50). Two selected downstream target genes, *tep1* and *totA*, were highly expressed in mHTT-expressing cells (**Figure 7B**). Notably, we found that the induction of antimicrobial peptides was significantly suppressed in mHTT-expressing cells after bacterial treatments, which has not yet been observed in other HD models. It is known that several human antimicrobial peptides are expressed in blood cells including neutrophils and macrophages (51). Since the transcriptomic analysis in HD blood cells has shown dysregulation of transcription in large genomic regions (52), further studies will be needed to understand whether the production of antimicrobial peptides is impaired in the blood cells of patients or HD mice during infection.

In summary, the present study demonstrates immune dysregulation in flies expressing mHTT in hemocytes (**Figure 9**). This expression does not directly cause a lethal effect, although it does reduce the number of circulating hemocytes and decrease ATP levels. Cytokine expression and downstream JAK/STAT signaling are activated upon mHTT expression, which has also been observed in HD patients and mice. In addition, the induction of antimicrobial peptides as well as the immune response against different pathogenic infections are impaired in mHTT-expressing *Drosophila* cells. The present study introduces a system for studying the tissue-specific effects of mHTT in *Drosophila* immune cells. Further studies can be applied to clarify the molecular interaction between mHTT and antimicrobial peptide pathways (Toll and IMD signaling) as well as the mechanisms of phagocytosis suppression.

MATERIALS AND METHODS

Fly Stocks

Flies were reared at 25°C on standard cornmeal medium. The fly strains used were UAS-Q20Httexon1^{111F1L} and UAS-Q93Httexon1^{4F132} obtained from Prof. Lawrence Marsh (UC Irvine, USA) (8), which contain 20 (wild-type) and 93 (mutant HTT) polyglutamine repeats, respectively. The pan-neuronal driver, *elav-gal4*[C155], and hemocyte drivers, *he-gal4* and *hml-gal4*, were obtained from Bloomington *Drosophila* Stock Center and Dr. Tomas Dolezal (University of South Bohemia), respectively (53–55). Hemocyte-ablated flies (*phago^{less}*) were used as negative controls and were generated by overexpressing pro-apoptotic proteins (*UAS-rpr*, *-hid*) with *hml-gal4* (19, 20, 56).

Developmental and Longevity Assay

Thirty first-instar larvae collected from a juice plate were transferred into vials to measure the number of pupae and adults for each replicate. For the longevity assay, about 20–30 newly emerged male adults were collected for each replicate and maintained at 29°C. Q93 expression driven by pan-neuronal driver, *elav-gal4* and *phgo^{less}* flies were used as positive controls for longevity assay. Since expression of Q93 driven by *elav-gal4* (X chromosome insertion) results in high mortality of male progeny (dosage compensation) (57), female progeny were used for recording the longevity. The number of dead flies was counted

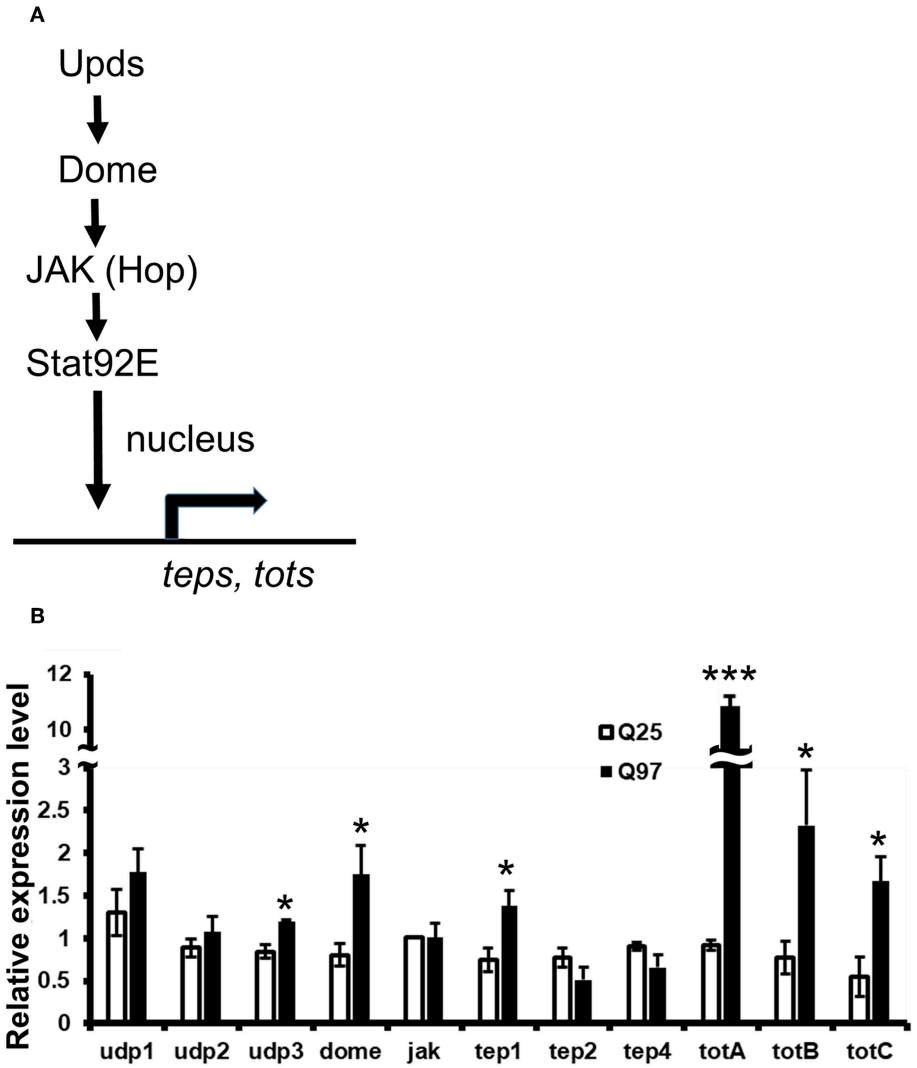

FIGURE 7 | Activation of cytokine expression and JAK/STAT signaling in the mHTT-expressing S2 cells. **(A)** Schematic representation of the interaction between Upds and JAK/STAT pathway. **(B)** The gene expression of cytokines (*udp1-3*), *dome*, *jak*(*hop*), and JAK/STAT downstream target genes (*teps* and *tots*) were measured in Q25 HTT and Q97 mHTT-expressing S2 cells after 120 h of copper induction. All the expressions were normalized to *rp49* expression and Q25 control (ΔΔCT). Data are presented as average ± SEM from three independent replicates. *P*-values using Student's *t*-test, $^{*}P < 0.05$, $^{***}P < 0.001$.

every day. All the experiments were performed in at least six independent replicates.

Circulating Hemocyte Counting

Circulating hemocytes were obtained from larvae by cuticle tearing in Ringer's buffer with thiourea to prevent melanization (25 μl of buffer per 6 larvae). The number of hemocytes expressing GFP (*hml-gal4* or *he-gal4 > UAS-gfp*) were counted using a hemocytometer. At least five independent replicates were analyzed for each genotype.

Parasitoid Wasp Infection, Eclosion, and Encapsulation Assay

Leptopilina boulardi parasitoid wasps were obtained from Dr. Jan Hrček (Biology Center CAS) and maintained by infecting wild-type *Drosophila* larvae. For the wasp infection assay, forty larvae (second instar) were transferred onto a dish containing cornmeal food, and three female wasps were then placed onto the dish and allowed to attack for 72 h. After infection, 30 infected larvae were collected from the dish and transferred into a vial containing cornmeal for each replicate. Each genotype was tested in at least 10 independent replicates. The total number of eclosed flies and wasps were calculated (26). For the encapsulation assay, the infected larvae were dissected 72 h post-infection and the number of larvae containing intact melanized capsules, broken melanized pieces as well as wasp larvae was recorded.

Nematode Infection

Two nematode species, *Steinernema carpocapsae* and *Heterorhabditis bacteriophora*, were used in this study, under previously described maintenance conditions (58). For the infection assay, nematodes were combined with autoclaved

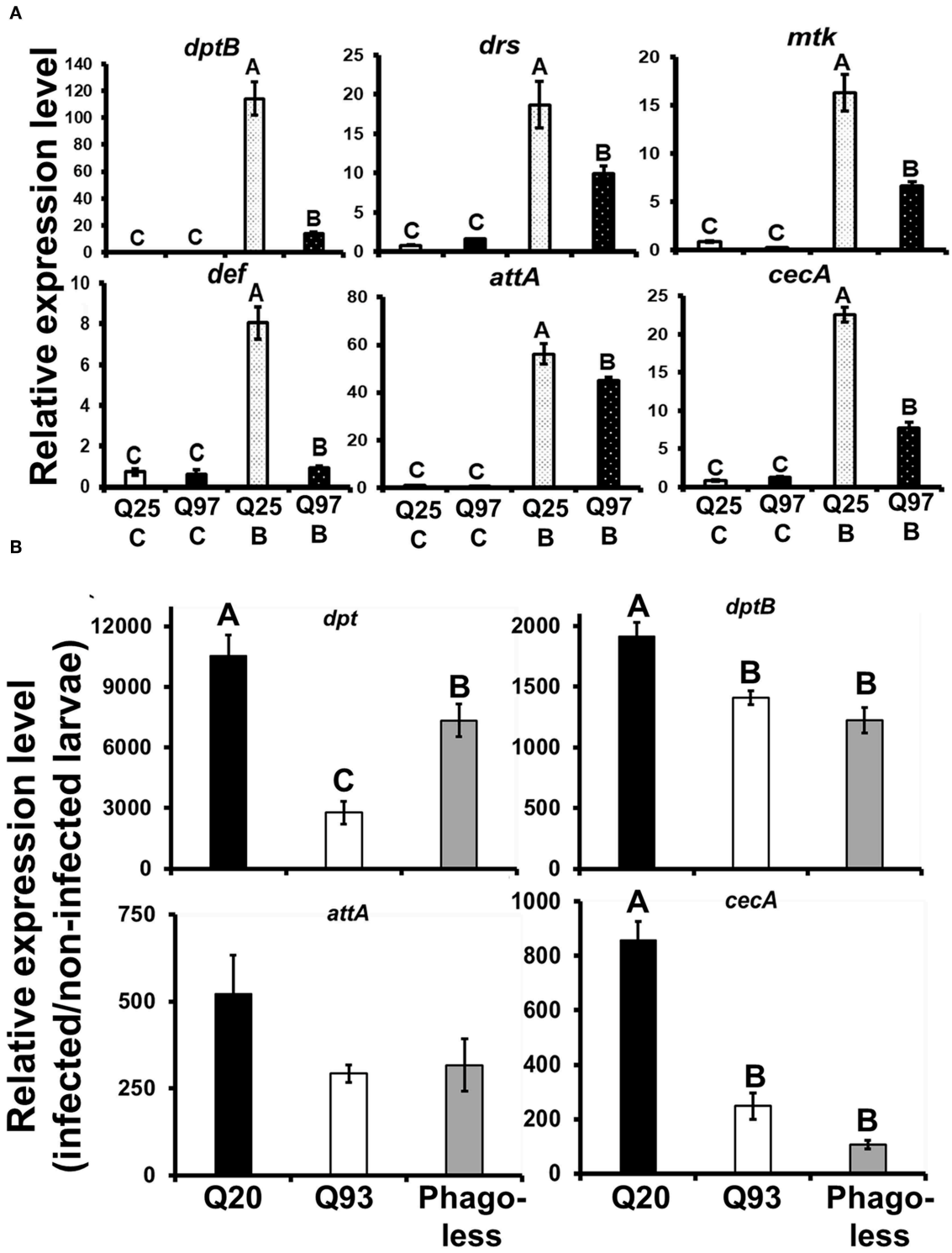

FIGURE 8 | Suppression of antimicrobial peptides (AMPs) induction after bacterial treatment in the mHTT-expressing S2 cells and larvae. **(A)** Q25 and Q97-expressing S2 cells were incubated with *E. coli* and *M. luteus* (Q25_B and Q97_B) or without bacteria (Q25_C and Q97_C) for 8 h, and the expression levels of AMPs was measured. The AMPs expressions were normalized to *rp49* expression and Q25 control. **(B)** Larvae expressing mHTT Q93 or HTT Q20 under *hml-gal4* hemocyte drivers as well as *Phago*^{less} mutants were infected with ECC15-GFP and their expression of AMPs was determined after 8 h. The expressions were normalized to *rp49* transcripts and non-infected controls. The AMPs expression levels of non-infected controls for each genotype were set to one. All the data are presented as average ± SEM from three independent replicates. The significances were analyzed by ANOVA with Fisher LSD *post-hoc* test; different letters on the treatment group indicate significant differences at $P < 0.05$.

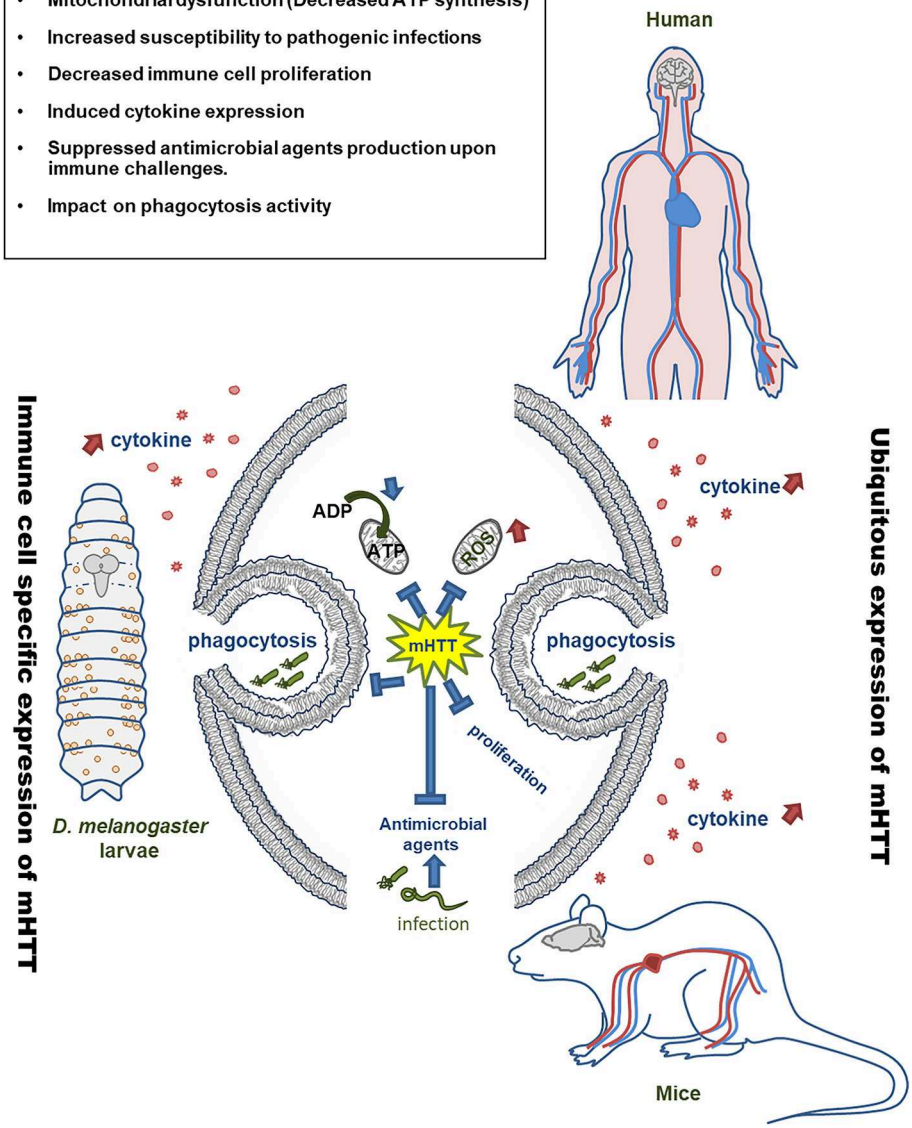

FIGURE 9 | Model of mHTT effects on *Drosophila* and mammalian immune cells. The expression of mHTT in hemocytes of *Drosophila* displays similar effects on the immune cells of HD patients and mice.

water to achieve a concentration of 25 infective juveniles per 10 µl. Then, 10 µl of nematode suspension was applied to paper and placed in each wells of a 96-well plate. Individual larvae were transferred to each well where they stayed in contact with the nematodes, and the plate was covered with Parafilm. The infection was conducted at 25°C in the dark. Each experimental replicate consisted of 32 early third-instar larvae (72 h after egg hatching), and all experiments were done at least in five replicates. The number of dead larvae were counted after 24 and 48 h of infection (23, 24).

Bead Aggregation Assay

The bead aggregation assay was described in our previous study (24). Briefly, 2.5 µl of hemolymph was collected from six late third-instar larvae, mixed with BSA-blocked bead suspension (tosylactivated Dynabeads M-280, Invitrogen), diluted in *Drosophila* Ringer (pH 6.0) in a well of cavity diagnostic slide (Thermo Scientific) and covered with round cover glass. Pictures were taken with a Nikon SMZ-745T stereomicroscope associated with a CANON EOS 550D. The images were analyzed and quantified with the ImageJ graphics software with the "Analyze Particles" module.

Cell Culture

Drosophila Schneider 2 (S2) cells were grown at 25°C in Shields and Sang medium (Sigma) with 0.1% yeast extract, 0.25% peptone, and 10% heat inactivated fetal bovine serum.

To generate stable lines expressing polyglutamine repeats, the S2 cells were transfected with four different Httex1-eGFP pMK33 plasmids (Q25, Q46, Q72, and Q97) containing copper-inducible metallothionein promoter (obtained from Dr. Sheng Zhang) (59).

Phagocytosis Assay

After induction for 5 days (120 h) with 1 mM copper ($CuSO_4$; Sigma), 100 µl of cell suspension (1×10^6 cells/ml) was transferred to each well of a 96-well plate. Then, 100 µl of pHrodo Red *E. coli* (1 mg/ml; Thermo Fisher Scientific) was applied to each well for phagocytosis testing. After 8 h of treatment, the supernatant was removed, the cells were washed two times with 1× PBS, and 100 µl of fresh medium was applied. Cells were observed and photographed with a confocal microscope. From the images, the total number of cells and the number of cells displaying red fluorescence were counted. Three experimental repeats for each treatment were done for statistical analysis.

ATP Measurement

Cells were treated with 1 mM copper for 3 days (72 h) and 5 days (120 h) to induce mHTT expression. Fifty microliter of a 1×10^6 cells/ml solution (5×10^4 cells) was transferred to each well of a 96-well plate. After removing the supernatant, 60 µl of CellTiter-Glo solution (Promega) was applied to each well for 10 min. Then, 50 µl of the mixture was transferred to each well of 96-well white plates and the intensity of luminescence was then measured. Five independent replicates for each treatment were performed for analysis.

Bacterial Infection *in vitro* and *in vivo*

Five milliliter of S2 cells (1×10^6 cells/ml) carrying copper-inducible Q25 HTT or Q97 mHTT transgenes were incubated in media containing 1 mM $CuSO_4$ for 120 h in 60 mm tissue culture plates. After the induction, the cells were treated for 8 h with 1 ml of bacterial mixture containing *Escherichia coli* and *Micrococcus luteus* at an optical density (600 nm) of 1 ($OD_{600} = 1$) (37). The cells were then harvested for RNA extraction.

For the *in vivo* infection, late third instar larvae (96 h after egg hatching) were collected and transferred into a vial with 0.5 g instant *Drosophila* medium (Formula 4–24, Carolina Biological Supply) supplemented with 200 µl of bacterial suspension ($OD_{600} = 50$) *Erwinia carotovora carotovora 15*-GFP (ECC15-GFP) and 1,300 µl of distilled water. The larvae were collected for RNA extraction 8 h after the infection (19, 38).

RNA Extraction

For *in vitro* experiments, S2 cells were washed with 1× PBS three times and harvested with 800 µl of RiboZol (VWR). Samples were preserved at −80°C until RNA purification. For *in vivo* experiments, 10 larvae were washed by distilled water and homogenized by the pestle motor (Kimble) in 200 µl of RiboZol (VWR Life Science). The sample were then preserved at −80°C for further RNA purification. RNA was isolated using NucleoSpin RNA columns (Macherey-Nagel) following the manufacturer's instructions and cDNA was synthesized from 2 µg of total RNA using a RevertAid H Minus First Strand cDNA Synthesis Kit (Thermo Fisher Scientific).

qPCR and Primers

5× HOT FIREPol® EvaGreen® qPCR Mix Plus with ROX (Solis Biodyne) and an Eco Real-Time PCR System (Illumina®) were used for qPCR. The cDNA was diluted 50 times before use. Each reaction contained 4 µl of EvaGreen qPCR mix, 0.5 µl of forward and reverse primer (10 µM), 5 µl of diluted cDNA and ddH2O to adjust the total volume to 20 µl. The list of primers is shown in **Supplemental Table 1**. The expression level was calculated by using the ($2^{-\Delta\Delta CT}$) method. The CT value of target genes were normalized to reference gene, ribosomal protein 49 (*rp49*).

Statistical Analysis

Error bars show standard error of the mean throughout this paper. Significance was established using Student's *t*-test (N.S., not significant, $^*P < 0.05$, $^{**}P < 0.01$, $^{***}P < 0.001$) or one-way ANOVA analysis with Fisher LSD or Tukey HSD *post-hoc* test. The Mann–Whitney *U*-test was used for examing the significance of the data on wasp larval hatching and the host encapsulation activities (**Figures 4C–F**). For the statistical analysis of longevity curve, we used online tool OASIS 2 to perform the weighted log-rank test for determining significance (60).

DATA AVAILABILITY STATEMENT

The raw data supporting the conclusions of this manuscript will be made available by the authors, without undue reservation, to any qualified researcher.

AUTHOR CONTRIBUTIONS

Y-HL conceived the project, performed the experiments and prepared the manuscript. HM performed the hemocyte counting and imaging. EI performed the nematode infections. LK performed the clotting assay. MZ supervised the project and manuscript preparation.

FUNDING

This work was supported by the grant agency of the University of South Bohemia (065/2017/P to Y-HL), junior grant project GACR (19-13784Y to LK). MZ was a member of the COST action Maximizing impact of research in neurodevelopmental disorders (CA16210).

ACKNOWLEDGMENTS

We thank Dr. Sheng Zhang (UThealth) for the Httex1-eGFP pMK33 plasmids, Prof. L. Marsh (UC Irvine, USA) for Q20 and Q93 flies, Dr. Tomas Dolezal (University of South Bohemia) for the hemocyte driver line, Dr. Pavel Hyrsl, Pavel Dobes (Masaryk University) for the nematodes, and Dr. Hrcek Jan, Dr. Chia-Hua Lue (Biology Centre CAS), and Dr. Adam Bajgar (University

of South Bohemia) for the parasitoid wasps, Dr. Julien Royet (IBDM, France) for bacteria ECC-15.

SUPPLEMENTARY MATERIAL

The Supplementary Material for this article can be found online at: https://www.frontiersin.org/articles/10.3389/fimmu.2019.02405/full#supplementary-material

Supplemental Figure 1 | Expression of four different lengths of HTT-GFP fusion proteins under a fluorescence microscope. mHTT-expressing cells (Q46, Q72, and Q97) showed significant mHTT aggregates after copper induction, while there was no aggregate formation in normal HTT-expressing cells (Q25).

Supplemental Figure 2 | Phagocytosis assay in Q25- and Q97-expressing S2 cells with *E. coli* labeled by DNA-specific dye (Hoechst 33342). Cells expressing mHTT were able to initiate phagocytosis.

Supplemental Table 1 | List of qPCR primers used in this study.

REFERENCES

1. Vonsattel JP, DiFiglia M. Huntington disease. *J Neuropathol Exp Neurol.* (1998) 57:369–84. doi: 10.1097/00005072-199805000-00001
2. Sassone J, Colciago C, Cislaghi G, Silani V, Ciammola A. Huntington's disease: the current state of research with peripheral tissues. *Exp Neurol.* (2009) 219:385–97. doi: 10.1016/j.expneurol.2009.05.012
3. Sathasivam K, Hobbs C, Turmaine M, Mangiarini L, Mahal A, Bertaux F, et al. Formation of polyglutamine inclusions in non-CNS tissue. *Hum Mol Genet.* (1999) 8:813–22. doi: 10.1093/hmg/8.5.813
4. Leblhuber F, Walli J, Jellinger K, Tilz GP, Widner B, Laccone F, et al. Activated immune system in patients with Huntington's disease. *Clin Chem Lab Med.* (1998) 36:747–50. doi: 10.1515/CCLM.1998.132
5. Andre R, Carty L, Tabrizi SJ. Disruption of immune cell function by mutant huntingtin in Huntington's disease pathogenesis. *Curr Opin Pharmacol.* (2016) 26:33–8. doi: 10.1016/j.coph.2015.09.008
6. Kwan W, Trager U, Davalos D, Chou A, Bouchard J, Andre R, et al. Mutant huntingtin impairs immune cell migration in Huntington disease. *J Clin Invest.* (2012) 122:4737–47. doi: 10.1172/JCI64484
7. Donley DW, Olson AR, Raisbeck MF, Fox JH, Gigley JP. Huntingtons disease mice infected with *Toxoplasma gondii* demonstrate early kynurenine pathway activation, altered $CD8^+$ T-cell responses, and premature mortality. *PLoS ONE.* (2016) 11:e0162404. doi: 10.1371/journal.pone.0162404
8. Steffan JS, Bodai L, Pallos J, Poelman M, McCampbell A, Apostol BL, et al. Histone deacetylase inhibitors arrest polyglutamine-dependent neurodegeneration in *Drosophila*. *Nature.* (2001) 413:739–43. doi: 10.1038/35099568
9. Song W, Smith MR, Syed A, Lukacsovich T, Barbaro BA, Purcell J, et al. Morphometric analysis of Huntington's disease neurodegeneration in *Drosophila*. *Methods Mol Biol.* (2013) 1017:41–57. doi: 10.1007/978-1-62703-438-8_3
10. Taylor JP, Taye AA, Campbell C, Kazemi-Esfarjani P, Fischbeck KH, Min KT. Aberrant histone acetylation, altered transcription, and retinal degeneration in a *Drosophila* model of polyglutamine disease are rescued by CREB-binding protein. *Genes Dev.* (2003) 17:1463–8. doi: 10.1101/gad.1087503
11. Li XJ, Orr AL, Li S. Impaired mitochondrial trafficking in Huntington's disease. *Biochim Biophys Acta.* (2010) 1802:62–5. doi: 10.1016/j.bbadis.2009.06.008
12. Warrick JM, Chan HY, Gray-Board GL, Chai Y, Paulson HL, Bonini NM. Suppression of polyglutamine-mediated neurodegeneration in *Drosophila* by the molecular chaperone HSP70. *Nat Genet.* (1999) 23:425–8. doi: 10.1038/70532
13. Steffan JS, Agrawal N, Pallos J, Rockabrand E, Trotman LC, Slepko N, et al. SUMO modification of Huntingtin and Huntington's disease pathology. *Science.* (2004) 304:100–4. doi: 10.1126/science.1092194
14. Marsh JL, Walker H, Theisen H, Zhu YZ, Fielder T, Purcell J, et al. Expanded polyglutamine peptides alone are intrinsically cytotoxic and cause neurodegeneration in *Drosophila*. *Hum Mol Genet.* (2000) 9:13–25. doi: 10.1093/hmg/9.1.13
15. Tamura T, Sone M, Yamashita M, Wanker EE, Okazawa H. Glial cell lineage expression of mutant ataxin-1 and huntingtin induces developmental and late-onset neuronal pathologies in *Drosophila* models. *PLoS ONE.* (2009) 4:e4262. doi: 10.1371/journal.pone.0004262
16. Besson MT, Dupont P, Fridell YW, Lievens JC. Increased energy metabolism rescues glia-induced pathology in a *Drosophila* model of Huntington's disease. *Hum Mol Genet.* (2010) 19:3372–82. doi: 10.1093/hmg/ddq249
17. Weiss KR, Kimura Y, Lee WC, Littleton JT. Huntingtin aggregation kinetics and their pathological role in a *Drosophila* Huntington's disease model. *Genetics.* (2012) 190:581–600. doi: 10.1534/genetics.111.133710
18. Melkani GC, Trujillo AS, Ramos R, Bodmer R, Bernstein SI, Ocorr K. Huntington's disease induced cardiac amyloidosis is reversed by modulating protein folding and oxidative stress pathways in the *Drosophila* heart. *PLoS Genet.* (2013) 9:e1004024. doi: 10.1371/journal.pgen.1004024
19. Charroux B, Royet J. Elimination of plasmatocytes by targeted apoptosis reveals their role in multiple aspects of the *Drosophila* immune response. *Proc Natl Acad Sci USA.* (2009) 106:9797–802. doi: 10.1073/pnas.0903971106
20. Defaye A, Evans I, Crozatier M, Wood W, Lemaitre B, Leulier F. Genetic ablation of *Drosophila* phagocytes reveals their contribution to both development and resistance to bacterial infection. *J Innate Immun.* (2009) 1:322–34. doi: 10.1159/000210264
21. Dobes P, Wang Z, Markus R, Theopold U, Hyrsl P. An improved method for nematode infection assays in *Drosophila* larvae. *Fly.* (2012) 6:75–9. doi: 10.4161/fly.19553
22. Small C, Paddibhatla I, Rajwani R, Govind S. An introduction to parasitic wasps of *Drosophila* and the antiparasite immune response. *J Vis Exp.* (2012) 63:e3347. doi: 10.3791/3347
23. Arefin B, Kucerova L, Dobes P, Markus R, Strnad H, Wang Z, et al. Genome-wide transcriptional analysis of *Drosophila* larvae infected by entomopathogenic nematodes shows involvement of complement, recognition and extracellular matrix proteins. *J Innate Immun.* (2014) 6:192–204. doi: 10.1159/000353734
24. Kucerova L, Broz V, Arefin B, Maaroufi HO, Hurychova J, Strnad H, et al. The *Drosophila* chitinase-like protein IDGF3 is involved in protection against nematodes and in wound healing. *J Innate Immun.* (2016) 8:199–210. doi: 10.1159/000442351
25. Lesch C, Goto A, Lindgren M, Bidla G, Dushay MS, Theopold U. A role for Hemolectin in coagulation and immunity in *Drosophila* melanogaster. *Dev Comp Immunol.* (2007) 31:1255–63. doi: 10.1016/j.dci.2007.03.012
26. Mortimer NT, Kacsoh BZ, Keebaugh ES, Schlenke TA. Mgat1-dependent N-glycosylation of membrane components primes *Drosophila* melanogaster blood cells for the cellular encapsulation response. *PLoS Pathog.* (2012) 8:e1002819. doi: 10.1371/journal.ppat.1002819
27. Ramet M, Manfruelli P, Pearson A, Mathey-Prevot B, Ezekowitz RA. Functional genomic analysis of phagocytosis and identification of a *Drosophila* receptor for *E. coli Nature.* (2002) 416:644–8. doi: 10.1038/nature735
28. West AP, Brodsky IE, Rahner C, Woo DK, Erdjument-Bromage H, Tempst P, et al. TLR signalling augments macrophage bactericidal activity through mitochondrial ROS. *Nature.* (2011) 472:476–80. doi: 10.1038/nature09973
29. Chougnet CA, Thacker RI, Shehata HM, Hennies CM, Lehn MA, Lages CS, et al. Loss of phagocytic and antigen cross-presenting capacity in aging dendritic cells is associated with mitochondrial dysfunction. *J Immunol.* (2015) 195:2624–32. doi: 10.4049/jimmunol.1501006
30. Geng J, Sun X, Wang P, Zhang S, Wang X, Wu H, et al. Kinases Mst1 and Mst2 positively regulate phagocytic induction of reactive oxygen species and bactericidal activity. *Nat Immunol.* (2015) 16:1142–52. doi: 10.1038/ni.3268
31. Ehinger JK, Morota S, Hansson MJ, Paul G, Elmer E. Mitochondrial respiratory function in peripheral blood cells from Huntington's disease patients. *Mov Disord Clin Pract.* (2016) 3:472–82. doi: 10.1002/mdc3.12308

32. Sassone J, Maraschi A, Sassone F, Silani V, Ciammola A. Defining the role of the Bcl-2 family proteins in Huntington's disease. *Cell Death Dis.* (2013) 4:e772. doi: 10.1038/cddis.2013.300
33. Quinn L, Coombe M, Mills K, Daish T, Colussi P, Kumar S, et al. Buffy, a *Drosophila* Bcl-2 protein, has anti-apoptotic and cell cycle inhibitory functions. *EMBO J.* (2003) 22:3568–79. doi: 10.1093/emboj/cdg355
34. Monserrate JP, Chen MY, Brachmann CB. *Drosophila* larvae lacking the bcl-2 gene, buffy, are sensitive to nutrient stress, maintain increased basal target of rapamycin (Tor) signaling and exhibit characteristics of altered basal energy metabolism. *BMC Biol.* (2012) 10:63. doi: 10.1186/1741-7007-10-63
35. Bjorkqvist M, Wild EJ, Thiele J, Silvestroni A, Andre R, Lahiri N, et al. A novel pathogenic pathway of immune activation detectable before clinical onset in Huntington's disease. *J Exp Med.* (2008) 205:1869–77. doi: 10.1084/jem.20080178
36. Trager U, Andre R, Lahiri N, Magnusson-Lind A, Weiss A, Grueninger S, et al. HTT-lowering reverses Huntington's disease immune dysfunction caused by NFkappaB pathway dysregulation. *Brain.* (2014) 137:819–33. doi: 10.1093/brain/awt355
37. Lemaitre B, Hoffmann J. The host defense of *Drosophila melanogaster*. *Annu Rev Immunol.* (2007) 25:697–743. doi: 10.1146/annurev.immunol.25.022106.141615
38. Basset A, Khush RS, Braun A, Gardan L, Boccard F, Hoffmann JA, et al. The phytopathogenic bacteria Erwinia carotovora infects *Drosophila* and activates an immune response. *Proc Natl Acad Sci USA.* (2000) 97:3376–81. doi: 10.1073/pnas.97.7.3376
39. Wild E, Magnusson A, Lahiri N, Krus U, Orth M, Tabrizi SJ, et al. Abnormal peripheral chemokine profile in Huntington's disease. *PLoS Curr.* (2011) 3:Rrn1231. doi: 10.1371/currents.RRN1231
40. Chen CM, Wu YR, Cheng ML, Liu JL, Lee YM, Lee PW, et al. Increased oxidative damage and mitochondrial abnormalities in the peripheral blood of Huntington's disease patients. *Biochem Biophys Res Commun.* (2007) 359:335–40. doi: 10.1016/j.bbrc.2007.05.093
41. Zwilling D, Huang SY, Sathyasaikumar KV, Notarangelo FM, Guidetti P, Wu HQ, et al. Kynurenine 3-monooxygenase inhibition in blood ameliorates neurodegeneration. *Cell.* (2011) 145:863–74. doi: 10.1016/j.cell.2011.05.020
42. Bouchard J, Truong J, Bouchard K, Dunkelberger D, Desrayaud S, Moussaoui S, et al. Cannabinoid receptor 2 signaling in peripheral immune cells modulates disease onset and severity in mouse models of Huntington's disease. *J Neurosci.* (2012) 32:18259–68. doi: 10.1523/JNEUROSCI.4008-12.2012
43. Sawa A, Wiegand GW, Cooper J, Margolis RL, Sharp AH, Lawler JF Jr, et al. Increased apoptosis of Huntington disease lymphoblasts associated with repeat length-dependent mitochondrial depolarization. *Nat Med.* (1999) 5:1194–8. doi: 10.1038/13518
44. Anderl I, Vesala L, Ihalainen TO, Vanha-Aho LM, Ando I, Ramet M, et al. Transdifferentiation and proliferation in two distinct hemocyte lineages in *Drosophila* melanogaster larvae after wasp infection. *PLoS Pathog.* (2016) 12:e1005746. doi: 10.1371/journal.ppat.1005746
45. Keebaugh ES, Schlenke TA. Insights from natural host-parasite interactions: the *Drosophila* model. *Dev Comp Immunol.* (2014) 42:111–23. doi: 10.1016/j.dci.2013.06.001
46. Fauvarque MO, Williams MJ. *Drosophila* cellular immunity: a story of migration and adhesion. *J Cell Sci.* (2011) 124:1373–82. doi: 10.1242/jcs.064592
47. Castillo JC, Shokal U, Eleftherianos I. Immune gene transcription in *Drosophila* adult flies infected by entomopathogenic nematodes and their mutualistic bacteria. *J Insect Physiol.* (2013) 59:179–85. doi: 10.1016/j.jinsphys.2012.08.003
48. Trager U, Andre R, Magnusson-Lind A, Miller JR, Connolly C, Weiss A, et al. Characterisation of immune cell function in fragment and full-length Huntington's disease mouse models. *Neurobiol Dis.* (2015) 73:388–98. doi: 10.1016/j.nbd.2014.10.012
49. Swanson JA. Shaping cups into phagosomes and macropinosomes. *Nat Rev Mol Cell Biol.* (2008) 9:639–49. doi: 10.1038/nrm2447
50. Morin-Poulard I, Vincent A, Crozatier M. The *Drosophila* JAK-STAT pathway in blood cell formation and immunity. *JAKSTAT.* (2013) 2:e25700. doi: 10.4161/jkst.25700
51. Wang G. Human antimicrobial peptides and proteins. *Pharmaceuticals.* (2014) 7:545–94. doi: 10.3390/ph7050545
52. Anderson AN, Roncaroli F, Hodges A, Deprez M, Turkheimer FE. Chromosomal profiles of gene expression in Huntington's disease. *Brain.* (2008) 131:381–8. doi: 10.1093/brain/awm312
53. Lin DM, Goodman CS. Ectopic and increased expression of Fasciclin II alters motoneuron growth cone guidance. *Neuron.* (1994) 13:507–23. doi: 10.1016/0896-6273(94)90022-1
54. Sinenko SA, Mathey-Prevot B. Increased expression of *Drosophila* tetraspanin, Tsp68C, suppresses the abnormal proliferation of ytr-deficient and Ras/Raf-activated hemocytes. *Oncogene.* (2004) 23:9120–8. doi: 10.1038/sj.onc.1208156
55. Zettervall CJ, Anderl I, Williams MJ, Palmer R, Kurucz E, Ando I, et al. A directed screen for genes involved in *Drosophila* blood cell activation. *Proc Natl Acad Sci USA.* (2004) 101:14192–7. doi: 10.1073/pnas.0403789101
56. Zhou L, Schnitzler A, Agapite J, Schwartz LM, Steller H, Nambu JR. Cooperative functions of the reaper and head involution defective genes in the programmed cell death of *Drosophila* central nervous system midline cells. *Proc Natl Acad Sci USA.* (1997) 94:5131–6. doi: 10.1073/pnas.94.10.5131
57. Warrick JM, Paulson HL, Gray-Board GL, Bui QT, Fischbeck KH, Pittman RN, et al. Expanded polyglutamine protein forms nuclear inclusions and causes neural degeneration in *Drosophila*. *Cell.* (1998) 93:939–49. doi: 10.1016/S0092-8674(00)81200-3
58. Ibrahim E, Dobes P, Kunc M, Hyrsl P, Kodrik D. Adipokinetic hormone and adenosine interfere with nematobacterial infection and locomotion in *Drosophila* melanogaster. *J Insect Physiol.* (2018) 107:167–74. doi: 10.1016/j.jinsphys.2018.04.002
59. Zhang S, Binari R, Zhou R, Perrimon N. A genomewide RNA interference screen for modifiers of aggregates formation by mutant Huntingtin in *Drosophila*. *Genetics.* (2010) 184:1165–79. doi: 10.1534/genetics.109.112516
60. Han SK, Lee D, Lee H, Kim D, Son HG, Yang JS, et al. OASIS 2: online application for survival analysis 2 with features for the analysis of maximal lifespan and healthspan in aging research. *Oncotarget.* (2016) 7:56147–52. doi: 10.18632/oncotarget.11269

Conflict of Interest: The authors declare that the research was conducted in the absence of any commercial or financial relationships that could be construed as a potential conflict of interest.

Supplementary Material

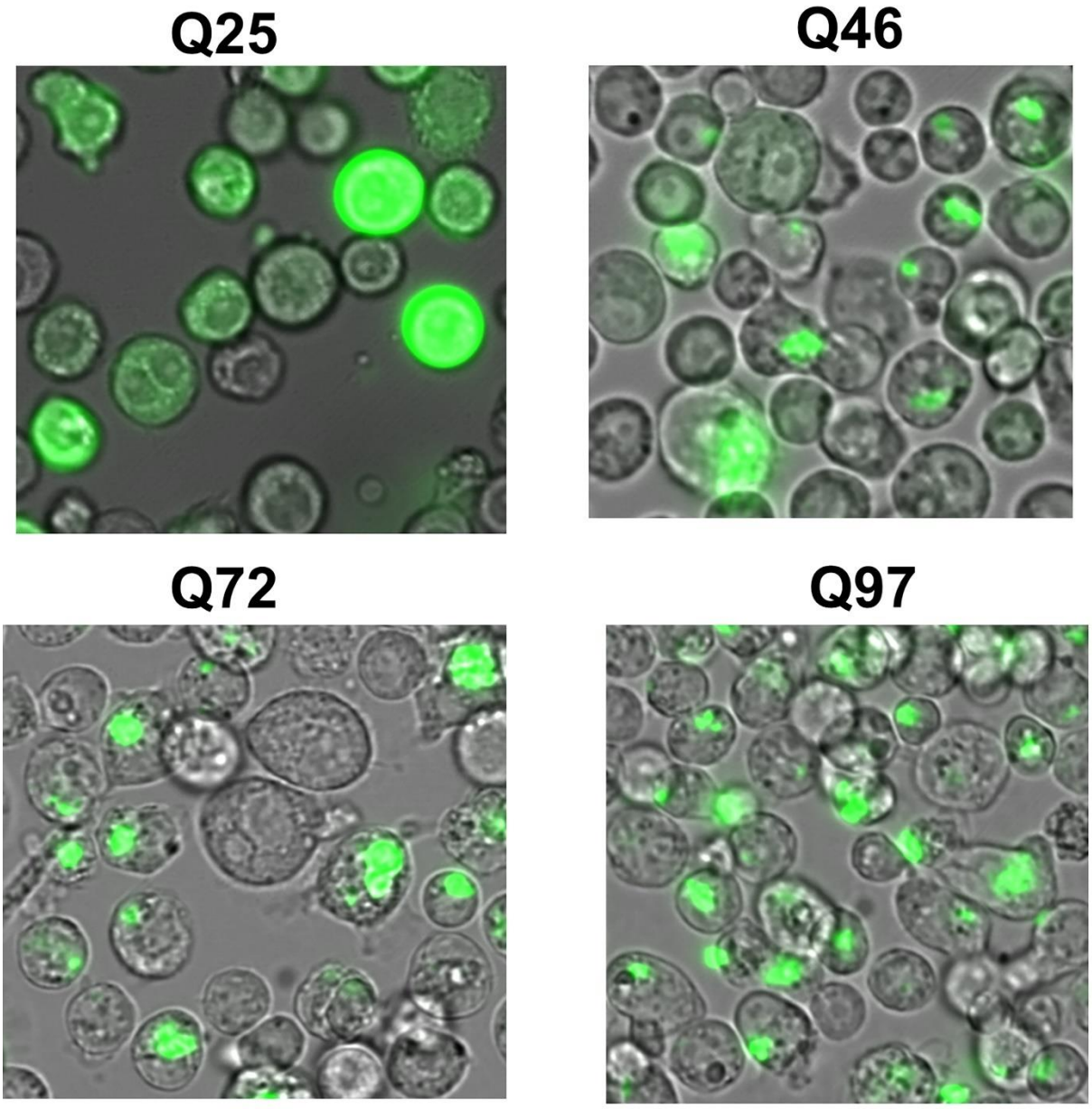

Supplemental Fig. 1. Expression of four different lengths of HTT-GFP fusion proteins under a fluorescence microscope. mHTT-expressing cells (Q46, Q72, and Q97) showed significant mHTT aggregates after copper induction, while there was no aggregate formation in normal HTT-expressing cells (Q25).

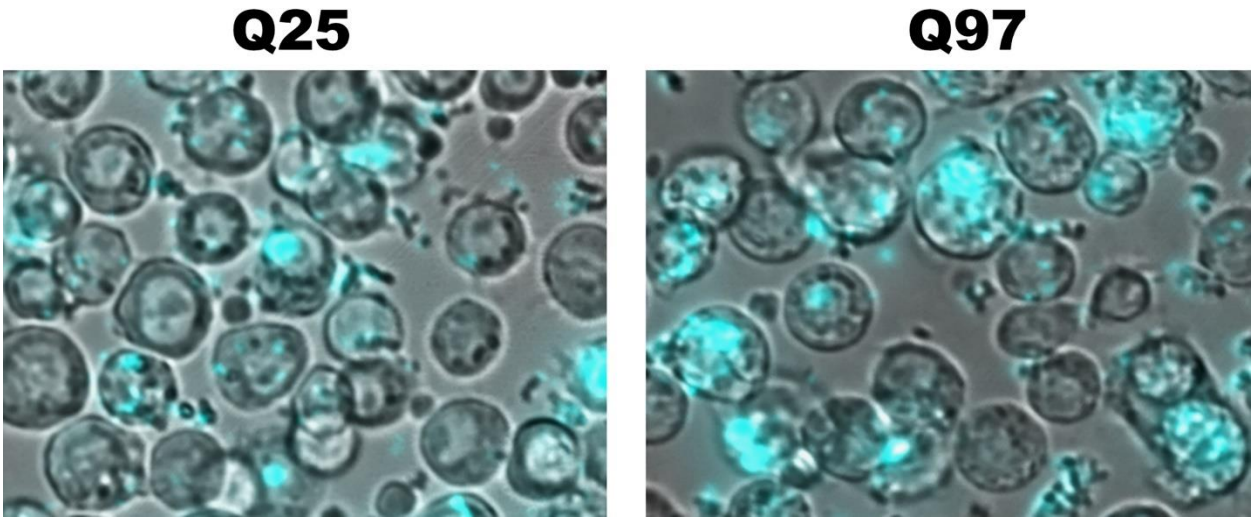

Supplemental Fig. 2. Phagocytosis assay in Q25- and Q97-expressing S2 cells with *E. coli* labeled by DNA-specific dye (Hoechst 33342). Cells expressing mHTT were able to initiate phagocytosis.

genes	left 5'-3'	right 5'-3'
upd1	AATCAGCTGAAGCGCCACG	GGAATTGGGCTTGAGCTTGG
upd2	AAGACTTGGTACCGCCACAT	GGCTCTTCTGCTGATCCTTG
upd3	ATCGCGACCTGCAGATTTAC	TGTACAGCAGGTTGGTCAGG
totA	ATTCTTCAACTGCTCTTATGTGCT	ATCGTCCTGGGCGTTTTT
tep1	GTCCTGCTCGCCCTTCTC	TCAAATGCCAAAACTCTATGTCA
tep2	CGTTCTGCTGGCTTTCTTC	ATACTGGTCGTCCGTCTTGTC
dptB	CTATTCATTGGACTGGCTTGTG	GTCCATTGGGGCTCTGC
drs	CCCTCTTCGCTGTCCTGA	TTAGCATCCTTCGCACCAG
mtk	TGGCCACGGCTACATCA	CCCGGTCTTGGTTGGTTA
def	CGTGGCTATCGCTTTTGCTC	GAGTAGGTCGCATGTGGCTC
attA	TGGTCATGGTGCCTCTTTG	GATTGTGTCTGCCATTGTTGA
cecA	CTTCGTTTTCGTCGCTCTC	TTTTCTTGCCAATTTTCTTCAG
rp49	CTTCATCCGCCACCAGTC	GGCGACGCACTCTGTTGT
debcl	ACGCGCACGATGACTAACTAC	TGTACTGACCACACAGACATTTC
buffy	CGTAGGTTGAGTAATGTCAGCG	GCAACGACCCTGAGAAATGAT
tep3	GCGCTATTCCAGTGCTAATCT	CGCAAAGTATTCGGAGCAATGA
totB	GTTTCGCACTGCTACTGATTGG	TTCAGCAACCCTACGACTGTC
totC	GCCTCCATTTCTCTACTATGCC	TCCCTTTCCTCGTCAGAATAGC
dome	GGCGGCGACTTTAATCTGAG	GGTGTTGTTCAGGATTCGGAT
jak(hop)	AGGATTTCCTCAATCGCCTT	CAGCTGCATCAGGTCGTAAA
dpt	CATTGCCGTCGCCTTACT	CATCGCCGCTCTGGCCA

Supplemental Tab. 1. List of qPCR primers used in this study.

Conclusion

This Ph.D. thesis significantly expands the knowledge of important role of Ado in cell growth and stress response in *Drosophila*. The author of this thesis is the first author on the first publication and a co-author on the other two.

The main conclusions are as follows:

1) **The role of adenosine pathway in cell growth**

- We have localized Cnt2 in the head and tail of *Drosophila* spermatids.
- We demonstrated that *cnt2* affects the mating behavior in *Drosophila*.
- We determined the function of *cnt2* in the maturation process of spermatids in *Drosophila*.
- We show that *cnt2* regulates spermatids mitochondrial morphology, and subsequently energy production for axoneme motorization.

2) **The role of adenosine pathway in the stress response**

- We investigated the role of Ado pathway in the cytotoxic effect of mHTT in *Drosophila*.
- We found that Ado titer is low in response to the cytotoxic effect of mHTT.
- We show that genetically enhanced metabolism of intracellular and extracellular Ado, by overexpression of *adgf-A* and *adenoK* in mHTT flies rescued the phenotype of short lifespan of mHTT mutant flies.
- We show that enhanced Ado signalling, by overexpression of *adoR*, leads to a shortened lifespan of mHTT flies, in contrast to flies in which *adoR* was silenced.
- We identified new downstream targets of the Ado pathway, the modifier of mgd4 (Mod(mdg4)) and heat-shock protein 70 (Hsp70). Finally, we proposed the following cascade for Ado signalling in a stress response: *ent2*, *adoR*, *mod(mdg4)*, and Hsp70.

Bibliography

Bibliography

Acebes, A., Grosjean, Y., Everaerts, C., and Ferveur, J. F. (2004). Cholinergic control of synchronized seminal emissions in Drosophila. *Curr. Biol.* 14, 704–710. doi: 10.1016/j.cub.2004.04.003.

Bader, M., Arama, E., and Steller, H. (2010). A novel F-box protein is required for caspase activation during cellular remodeling in Drosophila. *Development*. doi: 10.1242/dev.050088.

Bajgar, A., Kucerova, K., Jonatova, L., Tomcala, A., Schneedorferova, I., Okrouhlik, J., et al. (2015). Extracellular adenosine mediates a systemic metabolic switch during immune response. *PLoS Biol.* 13, e1002135. doi: 10.1371/journal.pbio.1002135.

Baptissart, M., Vega, A., Martinot, E., and Volle, D. H. (2013). Male fertility: Is spermiogenesis the critical step for answering biomedical issues? *Spermatogenesis* 3, e24114–e24114. doi: 10.4161/spmg.24114.

Becker, P.-H., Demir, Z., Mozer Glassberg, Y., Sevin, C., Habes, D., Imbard, A., et al. (2021). Adenosine kinase deficiency: Three new cases and diagnostic value of hypermethioninemia. *Mol. Genet. Metab.* 132, 38–43. doi: https://doi.org/10.1016/j.ymgme.2020.11.007.

Bellezza, I., and Minelli, A. (2017). Adenosine in sperm physiology. *Mol. Aspects Med.* 55, 102–109. doi: 10.1016/j.mam.2016.11.009.

Benson, D. A., Cavanaugh, M., Clark, K., Karsch-Mizrachi, I., Lipman, D. J., Ostell, J., et al. (2013). GenBank. *Nucleic Acids Res.* 41, D36-42. doi: 10.1093/nar/gks1195.

Borea, P. A., Gessi, S., Merighi, S., and Varani, K. (2016). Adenosine as a Multi-Signalling Guardian Angel in Human Diseases: When, Where and How Does it Exert its Protective Effects? *Trends Pharmacol. Sci.* 37, 419–434. doi: https://doi.org/10.1016/j.tips.2016.02.006.

Borea, P. A., Gessi, S., Merighi, S., Vincenzi, F., and Varani, K. (2017). Pathological overproduction: the bad side of adenosine. *Br. J. Pharmacol.* 174, 1945–1960. doi: 10.1111/bph.13763.

Bryant, P. J., and Simpson, P. (1984). Intrinsic and extrinsic control of growth in developing organs. *Q. Rev. Biol.* 59, 387–415. doi: 10.1086/414040.

Camici, M., Garcia-Gil, M., and Tozzi, M. G. (2018). The Inside Story of Adenosine. *Int. J. Mol. Sci.*

19. doi: 10.3390/ijms19030784.

Clark, K., Karsch-Mizrachi, I., Lipman, D. J., Ostell, J., and Sayers, E. W. (2016). GenBank. *Nucleic Acids Res.* 44, D67–D72. doi: 10.1093/nar/gkv1276.

Coutelis, J. B., Petzoldt, A. G., Spéder, P., Suzanne, M., and Noselli, S. (2008). Left–right asymmetry in Drosophila. *Semin. Cell Dev. Biol.* 19, 252–262. doi: https://doi.org/10.1016/j.semcdb.2008.01.006.

Crickmore, M. A., and Vosshall, L. B. (2013). Opposing Dopaminergic and GABAergic Neurons Control the Duration and Persistence of Copulation in Drosophila. *Cell* 155, 881–893. doi: https://doi.org/10.1016/j.cell.2013.09.055.

Cristalli, G., Costanzi, S., Lambertucci, C., Lupidi, G., Vittori, S., Volpini, R., et al. (2001). Adenosine deaminase: functional implications and different classes of inhibitors. *Med. Res. Rev.* 21, 105–128. doi: 10.1002/1098-1128(200103)21:2<105::aid-med1002>3.0.co;2-u.

Demarco, R. S., Eikenes, Å. H., Haglund, K., and Jones, D. L. (2014). Investigating spermatogenesis in Drosophila melanogaster. *Methods* 68, 218–227. doi: 10.1016/j.ymeth.2014.04.020.

Dobbing, J., and Sands, J. (1973). Quantitative growth and development of human brain. *Arch. Dis. Child.* 48, 757–767. doi: 10.1136/adc.48.10.757.

Dolezal, T., Dolezelova, E., Zurovec, M., and Bryant, P. J. (2005). A role for adenosine deaminase in Drosophila larval development. *PLoS Biol.* 3, e201. doi: 10.1371/journal.pbio.0030201.

Dragan, Y., Valdés, R., Gomez-Angelats, M., Felipe, A., Javier Casado, F., Pitot, H., et al. (2000). Selective loss of nucleoside carrier expression in rat hepatocarcinomas. *Hepatology* 32, 239–246. doi: 10.1053/jhep.2000.9546.

Enesco, M., and Leblond, C. P. (1962). Increase in Cell Number as a Factor in the Growth of the Organs and Tissues of the Young Male Rat. *Development* 10, 530–562. doi: 10.1242/dev.10.4.530.

Fabian, L., and Brill, J. A. (2012). Drosophila spermiogenesis. *Spermatogenesis*. doi: 10.4161/spmg.21798.

Falconer, D. S., Gauld, I. K., and Roberts, R. C. (1978). Cell numbers and cell sizes in organs of mice selected for large and small body size. *Genet. Res.* 31, 287–301. doi:

10.1017/s0016672300018061.

Fleischmannova, J., Kucerova, L., Sandova, K., Steinbauerova, V., Broz, V., Simek, P., et al. (2012). Differential response of Drosophila cell lines to extracellular adenosine. *Insect Biochem. Mol. Biol.* 42, 321–331. doi: https://doi.org/10.1016/j.ibmb.2012.01.002.

Franco, R., Cordomí, A., Llinas Del Torrent, C., Lillo, A., Serrano-Marín, J., Navarro, G., et al. (2021). Structure and function of adenosine receptor heteromers. *Cell. Mol. Life Sci.* 78, 3957–3968. doi: 10.1007/s00018-021-03761-6.

Fredholm, B. B., Abbracchio, M. P., Burnstock, G., Daly, J. W., Harden, T. K., Jacobson, K. A., et al. (1994). Nomenclature and classification of purinoceptors. *Pharmacol. Rev.* 46, 143–156.

Gemignani, A. S., and Abbott, B. G. (2010). The emerging role of the selective A2A agonist in pharmacologic stress testing. *J. Nucl. Cardiol. Off. Publ. Am. Soc. Nucl. Cardiol.* 17, 494–497. doi: 10.1007/s12350-010-9211-9.

Gilchrist, A. S., and Partridge, L. (2000). WHY IT IS DIFFICULT TO MODEL SPERM DISPLACEMENT IN *DROSOPHILA MELANOGASTER*: THE RELATION BETWEEN SPERM TRANSFER AND COPULATION DURATION. *Evolution (N. Y).* 54, 534–542. doi: 10.1554/0014-3820(2000)054[0534:WIIDTM]2.0.CO;2.

Gray, J. H., Owen, R. P., and Giacomini, K. M. (2004). The concentrative nucleoside transporter family, SLC28. *Pflugers Arch.* 447, 728–734. doi: 10.1007/s00424-003-1107-y.

Hsu, C.-L., Lin, W., Seshasayee, D., Chen, Y.-H., Ding, X., Lin, Z., et al. (2012). Equilibrative nucleoside transporter 3 deficiency perturbs lysosome function and macrophage homeostasis. *Science* 335, 89–92. doi: 10.1126/science.1213682.

Huh, J. R., Vernooy, S. Y., Yu, H., Yan, N., Shi, Y., Guo, M., et al. (2004). Multiple apoptotic caspase cascades are required in nonapoptotic roles for Drosophila spermatid individualization. *PLoS Biol.* 2, E15. doi: 10.1371/journal.pbio.0020015.

Kang, N., Jun, A. H., Bhutia, Y. D., Kannan, N., Unadkat, J. D., and Govindarajan, R. (2010). Human equilibrative nucleoside transporter-3 (hENT3) spectrum disorder mutations impair nucleoside transport, protein localization, and stability. *J. Biol. Chem.* 285, 28343–28352. doi: 10.1074/jbc.M110.109199.

Klein, D. M., Harding, M. C., Crowther, M. K., and Cherrington, N. J. (2017). Localization of nucleoside transporters in rat epididymis. *J. Biochem. Mol. Toxicol.* 31. doi: 10.1002/jbt.21911.

Knight, D., Harvey, P. J., Iliadi, K. G., Klose, M. K., Iliadi, N., Dolezelova, E., et al. (2010). Equilibrative nucleoside transporter 2 regulates associative learning and synaptic function in Drosophila. *J. Neurosci.* doi: 10.1523/JNEUROSCI.6241-09.2010.

Lee, G., and Hall, J. C. (2001). Abnormalities of male-specific FRU protein and serotonin expression in the CNS of fruitless mutants in Drosophila. *J. Neurosci. Off. J. Soc. Neurosci.* 21, 513–526. doi: 10.1523/JNEUROSCI.21-02-00513.2001.

Lee, N., Russell, N., Ganeshaguru, K., Jackson, B. F., Piga, A., Prentice, H. G., et al. (1984). Mechanisms of deoxyadenosine toxicity in human lymphoid cells in vitro: relevance to the therapeutic use of inhibitors of adenosine deaminase. *Br. J. Haematol.* 56, 107–119. doi: 10.1111/j.1365-2141.1984.tb01276.x.

Leung, G. P., Ward, J. L., Wong, P. Y., and Tse, C. M. (2001). Characterization of nucleoside transport systems in cultured rat epididymal epithelium. *Am. J. Physiol. Cell Physiol.* 280, C1076-82. doi: 10.1152/ajpcell.2001.280.5.C1076.

Lin, Y.-H., Maaroufi, H. O., Ibrahim, E., Kucerova, L., and Zurovec, M. (2019). Expression of Human Mutant Huntingtin Protein in Drosophila Hemocytes Impairs Immune Responses. *Front. Immunol.* 10, 2405. doi: 10.3389/fimmu.2019.02405.

Lin, Y.-H., Maaroufi, H. O., Kucerova, L., Rouhova, L., Filip, T., and Zurovec, M. (2021). Adenosine receptor and its downstream targets, mod(mdg4) and Hsp70, work as a signaling pathway modulating cytotoxic damage in Drosophila *bioRxiv*, 2019.12.22.886143. doi: 10.1101/2019.12.22.886143.

Linden, J. (1994). Cloned adenosine A3 receptors: pharmacological properties, species differences and receptor functions. *Trends Pharmacol. Sci.* 15, 298–306. doi: 10.1016/0165-6147(94)90011-6.

Lotti, F., and Maggi, M. (2018). Sexual dysfunction and male infertility. *Nat. Rev. Urol.* 15, 287–307. doi: 10.1038/nrurol.2018.20.

Maaroufi, H. O., Pauchova, L., Lin, Y.-H., Wu, B. C.-H., Rouhova, L., Kucerova, L., et al. (2022). Mutation in Drosophila concentrative nucleoside transporter 1 alters spermatid maturation and mating behavior. *Front. Cell Dev. Biol.* 10. doi: 10.3389/fcell.2022.945572.

MacBean, I. T., and Parsons, P. A. (1967). Directional selection for duration of copulation in Drosophila melanogaster. *Genetics* 56, 233–239. doi: 10.1093/genetics/56.2.233.

Maier, S. A., Galellis, J. R., and McDermid, H. E. (2005). Phylogenetic Analysis Reveals a Novel Protein Family Closely Related to Adenosine Deaminase. *J. Mol. Evol.* 61, 776–794. doi: 10.1007/s00239-005-0046-y.

Mandaravally Madhavan, M., and Schneiderman, H. A. (1977). Histological analysis of the dynamics of growth of imaginal discs and histoblast nests during the larval development ofDrosophila melanogaster. *Wilhelm Roux's Arch. Dev. Biol.* 183, 269–305. doi: 10.1007/BF00848459.

Masino, S., and Boison, D. (2013). *Adenosine: A key link between metabolism and brain activity*. doi: 10.1007/978-1-4614-3903-5.

Merighi, S., Mirandola, P., Milani, D., Varani, K., Gessi, S., Klotz, K.-N., et al. (2002). Adenosine receptors as mediators of both cell proliferation and cell death of cultured human melanoma cells. *J. Invest. Dermatol.* 119, 923–933. doi: 10.1046/j.1523-1747.2002.00111.x.

Mondal, B. C., Mukherjee, T., Mandal, L., Evans, C. J., Sinenko, S. A., Martinez-Agosto, J. A., et al. (2011). Interaction between differentiating cell- and niche-derived signals in hematopoietic progenitor maintenance. *Cell* 147, 1589–1600. doi: 10.1016/j.cell.2011.11.041.

Mukhopadhya, I., Murray, G. I., Berry, S., Thomson, J., Frank, B., Gwozdz, G., et al. (2016). Drug transporter gene expression in human colorectal tissue and cell lines: modulation with antiretrovirals for microbicide optimization. *J. Antimicrob. Chemother.* 71, 372–386. doi: 10.1093/jac/dkv335.

Noguchi, T., and Miller, K. G. (2003). A role of actin dynamics in individualization during spermatogenesis in Drosophila melanogaster. *Development*. doi: 10.1242/dev.00406.

Pavlou, H. J., and Goodwin, S. F. (2013). Courtship behavior in Drosophila melanogaster: towards a 'courtship connectome.' *Curr. Opin. Neurobiol.* 23, 76–83. doi:

https://doi.org/10.1016/j.conb.2012.09.002.

Pérez-Torras, S., Mata-Ventosa, A., Drögemöller, B., Tarailo-Graovac, M., Meijer, J., Meinsma, R., et al. (2019). Deficiency of perforin and hCNT1, a novel inborn error of pyrimidine metabolism, associated with a rapidly developing lethal phenotype due to multi-organ failure. *Biochim. Biophys. Acta - Mol. Basis Dis.* 1865, 1182–1191. doi: https://doi.org/10.1016/j.bbadis.2019.01.013.

Richani, D., Lavea, C. F., Kanakkaparambil, R., Riepsamen, A. H., Bertoldo, M. J., Bustamante, S., et al. (2019). Participation of the adenosine salvage pathway and cyclic AMP modulation in oocyte energy metabolism. *Sci. Rep.* 9, 18395. doi: 10.1038/s41598-019-54693-y.

Sanchez, J. J., Monaghan, G., Børsting, C., Norbury, G., Morling, N., and Gaspar, H. B. (2007). Carrier frequency of a nonsense mutation in the adenosine deaminase (ADA) gene implies a high incidence of ADA-deficient severe combined immunodeficiency (SCID) in Somalia and a single, common haplotype indicates common ancestry. *Ann. Hum. Genet.* 71, 336–347. doi: 10.1111/j.1469-1809.2006.00338.x.

Sayers, E. W., Barrett, T., Benson, D. A., Bolton, E., Bryant, S. H., Canese, K., et al. (2012). Database resources of the National Center for Biotechnology Information. *Nucleic Acids Res.* doi: 10.1093/nar/gkr1184.

Steinhauer, J. (2015). Separating from the pack: Molecular mechanisms of Drosophila spermatid individualization. *Spermatogenesis* 5, e1041345–e1041345. doi: 10.1080/21565562.2015.1041345.

Steller, H. (2008). Regulation of apoptosis in Drosophila. *Cell Death Differ.* 15, 1132–1138. doi: 10.1038/cdd.2008.50.

Stenesen, D., Suh, J. M., Seo, J., Yu, K., Lee, K.-S., Kim, J.-S., et al. (2013). Adenosine Nucleotide Biosynthesis and AMPK Regulate Adult Life Span and Mediate the Longevity Benefit of Caloric Restriction in Flies. *Cell Metab.* 17, 101–112. doi: https://doi.org/10.1016/j.cmet.2012.12.006.

Summerbell, D. (1976). A descriptive study of the rate of elongation and differentiation of the skeleton of the developing chick wing. *J. Embryol. Exp. Morphol.* 35, 241–260.

Sun, Y., and Huang, P. (2016). Adenosine A2B Receptor: From Cell Biology to Human Diseases. *Front. Chem.* 4, 37. doi: 10.3389/fchem.2016.00037.

Tokuyasu, K. T. (1975). Dynamics of spermiogenesis in Drosophila melanogaster. VI. Significance of “onion” nebenkern formation. *J. Ultrasructure Res.* doi: 10.1016/S0022-5320(75)80089-X.

Wojtal, K. A., Cee, A., Lang, S., Götze, O., Frühauf, H., Geier, A., et al. (2014). Downregulation of duodenal SLC transporters and activation of proinflammatory signaling constitute the early response to high altitude in humans. *Am. J. Physiol. Gastrointest. Liver Physiol.* 307, G673-88. doi: 10.1152/ajpgi.00353.2013.

Xie, P., Dou, S.-X., and Wang, P.-Y. (2006). Model for unidirectional movement of axonemal and cytoplasmic dynein molecules. *Acta Biochim. Biophys. Sin. (Shanghai).* 38, 711–724. doi: 10.1111/j.1745-7270.2006.00223.x.

Xu, C., Franklin, B., Tang, H.-W., Regimbald-Dumas, Y., Hu, Y., Ramos, J., et al. (2020). An in vivo RNAi screen uncovers the role of AdoR signaling and adenosine deaminase in controlling intestinal stem cell activity. *Proc. Natl. Acad. Sci. U. S. A.* 117, 464–471. doi: 10.1073/pnas.1900103117.

Young, J. D. (2016). The SLC28 (CNT) and SLC29 (ENT) nucleoside transporter families: a 30-year collaborative odyssey. *Biochem. Soc. Trans.* 44, 869–876. doi: 10.1042/BST20160038.

Yu, J., Chen, B., Zheng, B., Qiao, C., Chen, X., Yan, Y., et al. (2019). ATP synthase is required for male fertility and germ cell maturation in Drosophila testes. *Mol. Med. Rep.* 19, 1561–1570. doi: 10.3892/mmr.2019.9834.

Zhang, J., Visser, F., King, K. M., Baldwin, S. A., Young, J. D., and Cass, C. E. (2007). The role of nucleoside transporters in cancer chemotherapy with nucleoside drugs. *Cancer Metastasis Rev.* doi: 10.1007/s10555-007-9044-4.

Ziegler, A. B., Berthelot-Grosjean, M., and Grosjean, Y. (2013). The smell of love in Drosophila. *Front. Physiol.* 4. doi: 10.3389/fphys.2013.00072.

Curriculum Vitae

Houda Ouns Maaroufi, Ph.D.

Curriculum Vitae

University of South Bohemia, Czech Republic

houda.ouns.maaroufi@gmail.com

www.linkedin.com/in/houda-ouns-maaroufi

Education

PhD in Physiology and Developmental Biology| **2015 – 2022**
Department of Animal Physiology, University of South Bohemia, Czech Republic
Thesis: Role of adenosine pathway on cell growth and stress response in *Drosophila*, Institute of Entomology, Biology Centre CAS, Czech Republic

MSc in Molecular life sciences | **2013 - 2015**
Department of Molecular Biosciences, The Wenner-Gren Institute, Stockholm University, Sweden
Thesis: 1) Ethanol sensitivity in 10 *Drosophila* species
2) Role of Imaginal Disc Growth Factors (IDGFs) in *Drosophila* Immunity

BSc in Food quality control | **2006 - 2009**
Higher Institute of Biotechnology of Monastir, University of Monastir, Tunisia
Thesis: Microbiological analysis of milk and its derivatives.

Fellowships

PhD fellowship from University of South Bohemia (2015 – 2022)

BC grant Program (IBERA) (2022) (for a conference in San Diego, USA)

International Mobility grant (2019) (For internship in Taipei, Taiwan)

BC grant Program (IBERA) (2018) (for a conference in Philadelphia, USA)

BC Program (2018) (For internship in Taipei, Taiwan)

International travel grant (2017) (for a conference, Germany)

Professional Affiliations

Doctoral researcher | **2015 – Present (Defense in October)**
Molecular genetics laboratory, Institute of Entomology, Biology Centre CAS, Academy of Sciences, Czech Republic

Research Projects

1. Role of adenosine pathway on cell growth and stress response in *Drosophila*. (Molecular genetics laboratory, Biology Centre CAS, Academy of Sciences, **2015-**):

a. *Functional characterization of cnt1 in Drosophila spermatogenesis.*

b. *Functional characterization of cnt2 in Drosophila gut homeostasis.*

2. Pathological mechanisms of polyglutamine disorder in *Drosophila* model of Huntington disease (Molecular genetics laboratory, Biology Centre CAS, Academy of Sciences, **2015-2020**)

3. Insect silk and glue (Molecular genetics laboratory, Biology Centre CAS, Academy of Sciences, **2022-2022**)

4. Identification of immune regulatory genes in Apis mellifera through caffeine treatment. (Department of Entomology, National Taiwan University, Taipei, Taiwan, **2020-2020**)

5. Investigations on neuropeptide-producing neurons and their distribution in the nervous system of the water flea *Daphnia magna* (Department of Zoology, Stockholm University, Sweden, **2015-2015**)

6. Ethanol sensitivity in 10 *Drosophila* species (Department of Molecular Biosciences, The Wenner-Gren Institute, Stockholm University, Sweden, **2013-2015**)

7. Role of Imaginal Disc Growth Factors (IDGFs) in Drosophila Immunity (Department of Molecular Biosciences, The Wenner-Gren Institute, Stockholm University, Sweden, **2013-2015**)

8. Microbiological analysis of milk and its derivatives. (Higher Institute of Biotechnology of Monastir, University of Monastir, Tunisia, **2009**).

Workshop and Training

1. Training course: Leadership for early carrier researchers. Czech Republic | 2021.

2. Training course: Personality training | 2021

3. Training course: R studio for beginners | 2021

4. Training course: Technology How to publish in peer-reviewed journals | 2020.

Research Skills

- PCR/qRT-PCR operation and relevant techniques
- RNAseq data analysis
- Immunohistochemical staining
- Fluorescence and confocal microscope imaging
- Dissection (Daphnia, *Drosophila*, mouse)
- Genetic crossing (*Drosophila*)
- Presentation (oral and poster)
- Grant writing
- Scientific illustration

Research Articles Published (Or In preparation)

Bulah Chia-hsiang Wu, Ivo Sauman, **Houda Ouns Maaroufi**, Anna Žaloudíková, Martina Žurovcová, Barbara Kludkiewicz, Miluše Hradilová and Michal Zurovec (2022, under review process). The impact of omics data on the characterization and classification of silk genes in the Mediterranean flour moth (Ephestia kuehniella Zeller). Front. Mol. Biosciences

Houda Ouns Maaroufi, Lucie Pauchova, Yu-Hsien Lin, Bulah Chia-hsiang Wu, Lenka Rouhova, Lucie Kucerova, Ligia Cota Vieira, Marek Renner, Hana Sehadova, Miluse Hradilova, Michal Zurovec (2022). Mutation in *Drosophila* concentrative nucleoside transporter 1 alters spermatid maturation and mating behavior. Front. Cell Dev. Biol. DOI: 10.3389/fcell.2022.945572

Yu-Hsien Lin, **Houda Ouns Maaroufi**, Lucie Kucerova, Lenka Rouhova, Tomas Filip, Michal Zurovec (2021). Adenosine signaling and its downstream target mod(mdg4) modify the pathogenic effects of polyglutamine in a Drosophila model of Huntington's disease. Front. Cell Dev. Biol. DOI: doi.org/10.3389/fcell.2021.651367

Yu-Hsien Lin, **Houda Ouns Maaroufi**, Emad Ibrahim, Lucie Kucerova, Michal Zurovec (2019). Expression of human mutant huntingtin protein in Drosophila hemocytes impairs immune responses. Frontiers in immunology. DOI: 10.3389/fimmu.2019.02405

Yun-Heng Lu1, Carol-P Wu, Cheng-Kang Tang, Yu-Hsien Lin, **Houda Ouns Maaroufi**, Yi-Chi Chuang, Yueh-Lung Wu (2020). Identification of Immune Regulatory Genes in Apis mellifera through Caffeine Treatment. Insects DOI: 10.3390/insects11080516

Lucie Kucerova, Vaclav Broz, Badrul Arefin, **Houda Ouns Maaroufi**, Jana Hurychova, Hynek Strnad and Michal Zurovec, Ulrich Theopold (2016). The Drosophila Chitinase-Like Protein IDGF3 Is Involved in Protection against Nematodes and in Wound Healing. J. Innate Immun. 8:199–210, DOI: 10.1159/000442351

Conference Presentation

Maaroufi H.O., Zurovec M., "Mutation in *Drosophila* concentrative nucleoside transporter 1 alters spermatid maturation and mating behavior", 21st Symposium of the International Society of Endocytobiology (ISE), Ceske Budejovice, Czech Republic (2022, Talk)

Maaroufi H.O., Zurovec M., "Mutation in *Drosophila* concentrative nucleoside transporter 1 alters spermatid maturation and mating behavior", 63rd Annual *Drosophila* Research Conference, San Diego, CA, USA (2022, Poster presentation)

Maaroufi H.O., Zurovec M., "Role of concentrative nucleoside transporters 2 (cnt2) in *Drosophila* gut homeostasis", 39th Annual Meeting of Taiwan Entomological Society, Tainan, Taiwan (2018, Talk)

Maaroufi H.O., Zurovec M. "Functional characterization of concentrative nucleoside transporters (CNTs) in Drosophila melanogaster", 59th Annual *Drosophila* Research Conference, Philadelphia, USA (2018, Poster presentation)

Maaroufi H.O., Zurovec M. "Functional characterization of *cnt2* in *Drosophila*", Physiological days conference, Pilzen, Czech Republic (2018, Talk)

Maaroufi H.O., Zurovec M. "Functional characterization of *cnt2* in *Drosophila*", Heidelberg Forum for Young Life Scientists (HFYLS), Heidelberg, Germany (Poster presentation)

Awards

21st Symposium of the International Society of Endocytobiology (ISE) (2022): 1st prize of the excellent scientific achievement.
39th Annual Meeting of Taiwan Entomological Society (2018): Award for the second-best scientific project and presentation in the English oral session
Ph.D. conference (2018): Award for the second-best scientific project and presentation among PhD students
Ph.D. conference (2017): Award for the second-best scientific project and presentation among PhD students
99designs contest (2016): Award for the best illustration and graphic drawing "Abstract Theme"

Leadership experience

2019-present: Co-advisor of two students at South Bohemia University_ Czech Republic
2022: Frontier in Physiology and Disease_ Team leader of the international workshop FPD_ Czech Republic
2019: Frontiers in Insect Physiology_ Team leader of the international workshop FIIP_ Czech Republic

Volunteer/community engagement experience:

Night of scientists 2022: teaching about fluorescent microscope, fluorescence, genetics, *Drosophila*.
Night of scientists 2021: teaching about fluorescent microscope, drawing microscope and *Drosophila*.
Week of science 2019: teaching about *Drosophila* and *Bombyx*
Week of science 2018: teaching about *Drosophila*
Open science days 2017: teaching about *Drosophila*

Visit my LinkedIn online CV from any device to learn more about my experiences, success cases and more.

houda.ouns.maaroufi@gmail.com

Role of adenosine pathway on cell growth and stress response in *Drosophila*

Ph.D. Thesis